Bedrock Geology of The Monroe Quadrangle, Orange County, New York

Howard W. Jaffe and Elizabeth B. Jaffe

MAP AND CHART SERIES NUMBER 20
NEW YORK STATE MUSEUM AND SCIENCE SERVICE

The University of the State of New York/The State Education Department/Albany 1973

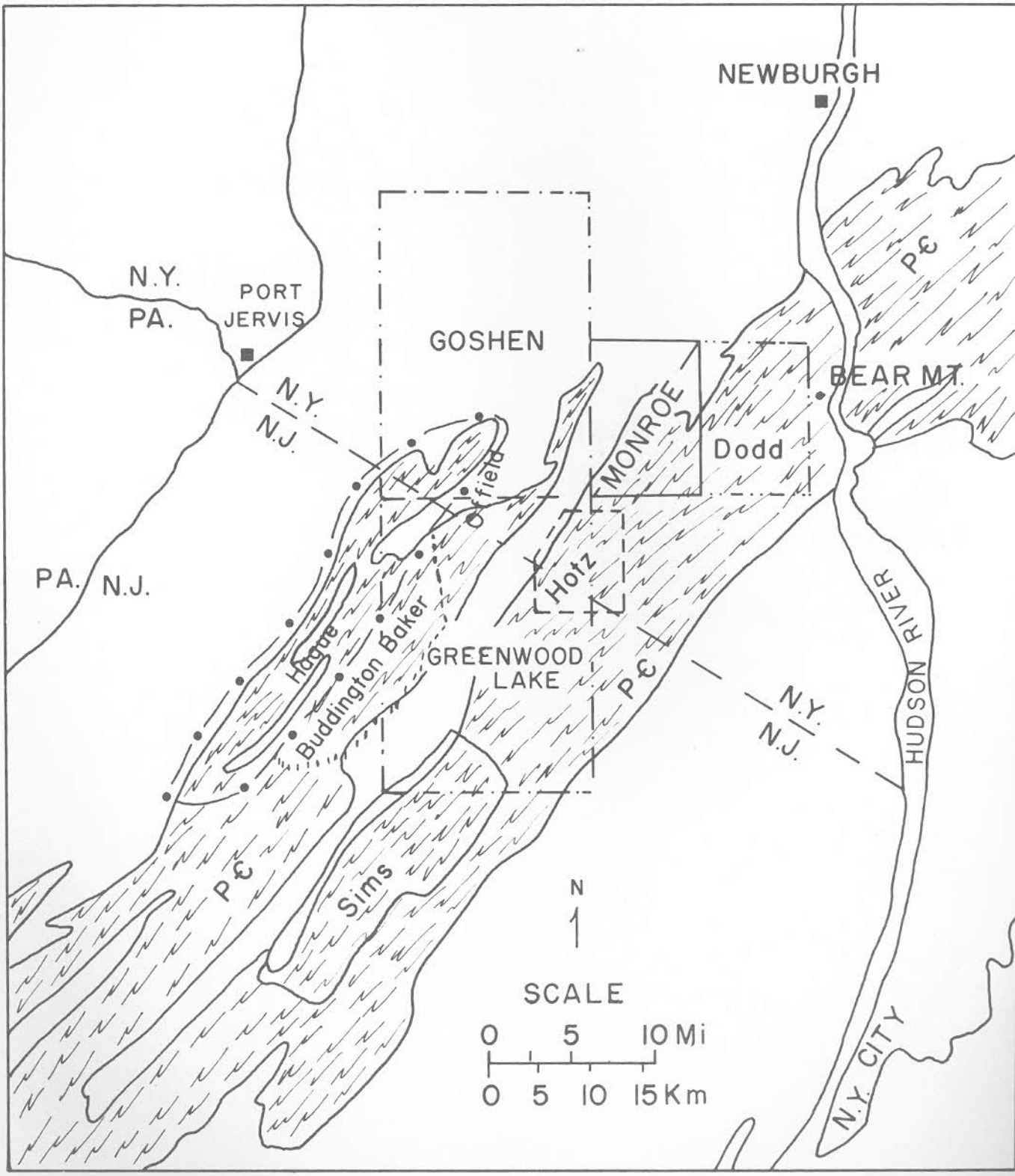

FIGURE 1. Index map showing location of the Monroe quadrangle in the Precambrian Highlands of the Reading Prong of the New York-New Jersey area. Also outlined are pertinent areas of the Highlands mapped in recent years by Hotz, Sims, Hague et. al., Dodd Offield, and Buddington and Baker.

THE UNIVERSITY OF THE STATE OF NEW YORK

Regents of the University *(with years when terms expire)*

1984 JOSEPH W. MCGOVERN, A.B., J.D., L.H.D., LL.D., D.C.L.,
Chancellor - New York

1985 EVERETT J. PENNY, B.C.S., D.C.S.,
Vice Chancellor - - - - - - - - - - - - - - - - White Plains

1978 ALEXANDER J. ALLAN, JR., LL.D., Litt.D. - - - - - - - - Troy

1973 CHARLES W. MILLARD, JR., A.B., LL.D., L.H.D. - - - - - Buffalo

1987 CARL H. PFORZHEIMER, JR., A.B., M.B.A., D.C.S., H.H.D. - Purchase

1975 EDWARD M. M. WARBURG, B.S., L.H.D. - - - - - - - - - New York

1977 JOSEPH T. KING, LL.B. - - - - - - - - - - - - - - - - Queens

1974 JOSEPH C. INDELICATO, M.D. - - - - - - - - - - - - Brooklyn

1976 MRS. HELEN B. POWER, A.B., Litt.D., L.H.D., LL.D. - - - Rochester

1979 FRANCIS W. MCGINLEY, B.S., J.D., LL.D. - - - - - - - - Glens Falls

1980 MAX J. RUBIN, LL.B., L.H.D. - - - - - - - - - - - - New York

1986 KENNETH B. CLARK, A.B., M.S., Ph.D., LL.D., L.H.D., D.Sc. Hastings on Hudson

1982 STEPHEN K. BAILEY, A.B., B.A., M.A., Ph.D., LL.D. - - - Syracuse

1983 HAROLD E. NEWCOMB, B.A. - - - - - - - - - - - - - Owego

1981 THEODORE M. BLACK, A.B., Litt.D. - - - - - - - - - - Sands Point

President of the University and Commissioner of Education
EWALD B. NYQUIST

Executive Deputy Commissioner of Education
GORDON M. AMBACH

Associate Commissioner for Cultural Education
JOHN G. BROUGHTON

Director, State Science Service
HUGO JAMNBACK

State Geologist
JAMES F. DAVIS

State Paleontologist
DONALD W. FISHER

Contents

PAGE

ABSTRACT 1

INTRODUCTION 3
- Location and geography 3
- Acknowledgments 3
- Previous Study 3
- Purpose, Scope, and Methods of Study 4

PRECAMBRIAN ROCKS 6
- General Statement 6
- Stratigraphy 6
- Rocks of the Monroe and Ramapo Blocks 7
- Allochthonous Precambrian Gneisses 35
- Metamorphic History 37

PALEOZOIC ROCKS 42
- Cambrian System 42
- Cambrian-Ordovician System 43
- Lamprophyre Dikes 44
- Leucophyre Dikes 48
- Ordovician System 48
- Silurian System 49
- Devonian System 51

STRUCTURAL GEOLOGY 54
- Introduction 54
- Precambrian Rocks 54
- Paleozoic Rocks 58
  - Fractures 60
  - Structural History 61

ECONOMIC GEOLOGY 64

REFERENCES CITED 65

APPENDIX 70

Illustrations

PLATES

1. Bedrock geology of the Monroe quadrangle, New York.....(In envelope)
2. Anorthite content of plagioclase in Precambrian gneisses.....(In envelope)

FIGURES PAGE

1. Index map showing the location of the Monroe quadrangle.....Cover 2
2. Working curve for estimating iron-magnesium ratios of clinopyroxenes.. 4
3. Index and reference map..... 6
4. Microperthite in hornblende (ferrohastingsite) granite gneiss..... 9
5. Modal quartz, plagioclase, and alkali feldspar in hornblende granite gneiss 11
6. Pyribolite 12
7. Influence of crystal structure on rock frbric in amphibolites..... 15
8. Biotite-hypersthene-quartz-antiperthitic plagioclase gneiss..... 16
9. Textures and compositions of replacement antiperthite and exsolution mesoperthite 18
10. Distribution of Mg and Fe^{+2} in coexisting orthopyroxene and calcic clinopyroxene 20
11. Sympathetic variation of Na in plagioclase with Fe in biotite and hornblende 20
12. Prograde reaction in amphibolite..... 22
13. Anorthite (An_{93}) microline and quartz in calc-silicate gneiss..... 22
14. ACF diagram for hornblende granulite facies gneisses of the Monroe quadrangle 25
15. Biotite and mesoperthite in biotite-mesoperthite gneiss..... 27
16. Optic orientation diagram of mesoperthite..... 27
17. Biotite-hypersthene-K-feldspar-quartz-plagioclase gneiss (charnockite).. 28
18. Sillimanite-cordierite-almandine-biotite-quartz-feldspar gneiss 29
19. Polysynthetic twinning in cordierite grain showing marginal pinitization. 31
20. AFM diagram showing assemblages in pelitic paragneisses..... 31
21. Augite ($Ca_{42}Mg_{36}Fe_{22}$) host grain containing three sets of exsolution lamellae of clinopyroxene (pigeonite and/or clinohypersthene)..... 34
22. Exsolution lamellae in and optic orientation diagram for coexisting augite and ferrohypersthene..... 35
23. Prehnite replacing albite in retrograded calc-silicate gneiss..... 35
24. Albite-leucogneiss, Goose Pond Mountain klippe..... 36
25. Diagram showing the estimated T and P of formation of the gneisses of the Monroe quadrangle..... 40
26. Poughquag conglomerate, Lower Cambrian..... 42
27. Wappinger dolostone, Cambrian-Ordovician 43
28. Zoned kaersutite phenocryst in albite-mela-camptonite dike..... 47
29. Oligoclase phenocrysts and microphenocrysts in granodiorite leucophyre dike 48

FIGURES PAGE

30. Calcareous quartzite (subarkose) unit of Ramseyburg Member of Martinsburg Formation, Middle Ordovician 49
31. Shawangunk orthoquartzite, Lower to Middle Silurian 50
32. *Coronura myrmecophorus* from basal Esopus beds 52
33. Bellvale graywacke, Middle Devonian 53
34. Principal fault blocks of the Monroe quadrangle 54
35. A,B,C,D fold axes and poles of foliation of Precambrian gneisses 55
35E. North and south plunges of fold axes aligned in northwest-trending belts 56
36. Fold in amphibolite (am) and hypersthene-quartz-plagioclase gneiss 57
37. Precambrian gneiss of Museum Village klippe thrust over Cambrian-Ordovician Wappinger dolostone 58
38. Fold in Ramseyburg shale 59
39. Structures in Shawangunk quartzite and conglomerate 59
40. Poles of joints and dikes 61
41. Geologic map of parts of the Monroe and Warwick quadrangles before the rotation of blocks 8, 9, and 10 63

TABLES

1. Composition of hornblende (ferrohastingsite) granite gneiss (hg) 8
2. Optical properties and iron-magnesium ratios of ferrohastingsite from hornblende granite gneiss 9
3. Optically determined iron-magnesium ratios of coexisting ferrohastingsite and biotite and anorthite content of coexisting plagioclase from hornblende granite gneiss 10
4. Composition of amphibloite and pyribolite (hornblende- and pyroxene-plagioclase gneiss), (am) 13
5. Composition of biotite-hypersthene-quartz-plagioclase gneiss (hqp) 14
6. Optically determined iron-magnesium ratios of coexisting hypersthene, clinopyroxene, hornblende, and biotite and anorthite content of coexisting plagioclase from amphibolite, and pyribolite 17
7. Optically determined iron-magnesium ratios of coexisting hypersthene, clinopyroxene, hornblende, and biotite and anorthite content of coexisting plagioclase from biotite-hypersthene-quartz-placioclase gneiss 19
8. Electron microprobe analysis of hornblende (ferrohastingsite) from amphibolite, sample 345, Monroe quadrangle, New York 21
9. Composition of calc-silicate gneiss (cs) 24
10. Composition of biotite-mesoperthite gneiss and albite-oligoclase leucogranodiorite (bmp), biotite gneiss (bg), and biotite-hypersthene-microperthite quartz-plagioclase gneiss (charnockite) (hk) 26
11. Composition of sillimanite-cordierite-almandine-biotite-quartz-feldspar gneiss (pelitic paragneiss) (sgb) 30
12. Modes of microcline alaskite (leucogranite) (al) and magnetite-garnet-andesine-microperthite leucogneiss (mag) 33
13. Modes of pyroxene and hornblende granulite 34
14. Modes of allochthonous gneisses from Goose Pond Mountain and Museum Village klippen (gcs, alg, acs) 36

TABLES PAGE

15. Mode of a totally retrograded amphibolite 40
16. Mode of Lower Cambrian Poughquag conglomeratic arkose 41
17. Composition of camptonitic lamprophyre dikes 45
18. Electron microprobe analysis, optical properties, and K-Ar age determination of kaersutite from camptonite dike (Sample No. J-50) 46
19. Mode of Bushkill shale of the Martinsburg Formation (Ob), Middle Ordovician 48
20. Modes of Ramseyburg Member of Middle Ordovician Martinsburg Formation (Org) 49
21. Modes of Shawangunk orthoquartzite (Silurian) (Ssk) and Bellvale graywacke (Devonian) (Dbv) 50

Bedrock Geology of The Monroe Quadrangle, Orange County, New York[1]

by Howard W. Jaffe [2] and Elizabeth B. Jaffe

ABSTRACT

The Monroe quadrangle is located in southeastern New York in the Hudson Highlands area of the Reading Prong, about 65 kilometers northwest of New York City, and due west of the Hudson River at Bear Mountain. Approximately one-half of the quadrangle is underlain by highly metamorphosed Precambrian rocks, and the remainder by relatively unmetamorphosed Paleozoic sedimentary rocks ranging in age from Early Cambrian to Medial Devonian. Post-Wappinger (Cambrian-Ordovician) lamprophyre dikes are abundant and occupy northwest-trending transverse joints.

Precambrian rocks are divided into three stratigraphic sequences. As inferred from oldest to youngest, these are: 1) cordierite-sillimanite-almandine-biotite-quartz-feldspar gneiss, magnetite-garnet-andesine leucogneiss, and biotite-mesoperthite gneiss, believed to have originated from marine shales and zeolitized graywackes or tuffs; 2) amphibolite, pyribolite, biotite-hypersthene-quartz-plagioclase gneiss, amphibolite-granodiorite, and calc-silicate gneiss, believed to be derived principally from volcanics (basalt and dacite) along with minor interlayered sediments (calcareous quartzite, marl, and subgraywacke); and 3) hornblende (ferrohastingsite) granite gneiss believed to have originated from a thick pile of rhyolitic volcanics analogous to those (> 15,000 feet thick) from the Lower Devonian of north-central Maine. This sequence of pelitic and calc-siliceous sediments and interlayered volcanics was totally recrystallized, and partly melted when the region underwent hornblende granulite facies metamorphism approximately 1150 million years (my) ago. Temperatures and pressures during this event were about 700–800° C. and 4–2 kb (kilobars), with water pressure lower than load pressure in many parts of the terrane. Many of the rocks are migmatitic due to partial anatexis.

Typical assemblages include: cordierite-sillimanite-almandine-biotite-intermediate plagioclase-K-feldspar-quartz-tourmaline; quartz-biotite-mesoperthite; hornblende-orthopyroxene-clinopyroxene-plagioclase; salite-scapolite - calcic plagioclase - sphene - quartz - microcline; magnetite-ferroan biotite-ferrohastingsite-oligoclase-microperthite-quartz; biotite-hypersthene-andesine antiperthite-quartz; and hypersthene–K-feldspar-biotite-quartz-plagioclase.

Hypersthene has originated from 1) the breakdown of ferroan biotite + quartz to produce charnockitic gneiss, and 2) the breakdown of hornblende to produce hypersthene-quartz-antiperthitic plagioclase gneiss (enderbitic gneiss) and hypersthene-clinopyroxene-andesine pyribolite (basic granulite or basic charnockite). In these rocks, hypersthene is richer in iron than coexisting clinopyroxene, while hornblende and biotite coexisting in the same rocks are richer in iron than both pyroxenes.

Exsolution lamellae in coexisting ortho- and clinopyroxene increase in abundance and size with increasing iron content in accordance with the inferred shape of the pyroxene solvus. Clinopyroxene (Fe_{38}), coexisting with ferrohypersthene (Fe_{52}), contains 3 unique sets of exsolution lamellae. These are parallel to (*100*), (*h0l*), and to a direction that makes an angle of 116° rather than 105° (crystallographic angle β) with the c-crystallographic axis of the host. The lamellae may be pigeonite and/or clinohypersthene as suggested from

[1] Manuscript submitted for publication September 2, 1969. Accepted for publication May 16, 1972.

[2] Professor, Department of Geology, University of Massachusetts, Amherst, Massachusetts 01002.

extinction angles. Lamellae in coexisting ferrohypersthene are twinned clinopyroxene (augite?) oriented parallel to (*100*) of the host.

In hornblende (ferrohastingsite) granite gneiss, ferroan biotite or annite (Fe_{80-100}) coexists with ferrohastingsite (Fe_{80-100}) and oligoclase (An_{22}) along with microperthite, quartz, and magnetite.

A marked angular unconformity separates the vertically-dipping Precambrian gneisses from the overlying, essentially flat-lying Lower Cambrian Poughquag Quartzite. The Poughquag contains quartzite, conglomerate, and arkosic members overlain by fine-grained Wappinger dolostone. Lamprophyre dikes, mostly camptonitic types, intrude the Poughquag and the Wappinger but not the overlying Middle Ordovician Martinsburg Formation or any younger rocks. A K-Ar age of 398 my was recently obtained on amphibole from one of these dikes. The Wappinger dolostone is unconformably overlain by the Ramseyburg calcareous quartzite and shale member of the Martinsburg rather than by the older Bushkill shale member of this formation. The Ramseyburg member of the Martinsburg is unconformably overlain by coarse vein-quartz-pebble conglomerate and orthoquartzite of the Shawangunk Formation which is exposed only on the west side of the down-dropped Schunemunk Mountain syncline of the Green Pond-Schunemunk outlier. Helderberg limestones are absent from the quadrangle although they could occur in a covered interval between Silurian and other Lower Devonian (Connelly Conglomerate) rocks. Connelly Conglomerate is represented by three small outcrops and is overlain apparently conformably by a thick section of the Esopus Formation that is highly fossiliferous at its base. The Esopus Formation is exposed only on the east side of the Schunemunk Mountain syncline. It is overlain by a very thick section of Bellvale graywacke and shale estimated at upwards of 400 meters in the Schunemunk Mountain area.

The regional strike is about N33°E, and dips are predominantly east, from shallow to nearly vertical. Plunges are gentle to the north with a few exceptions. Block faulting along and across the regional strike has been repeated at frequent intervals during and since the Precambrian and has had a major influence on the topography and culture of the region. Lamprophyre and other dikes occupy northwest-trending tension joints which are found in the Precambrian and Cambrian-Ordovician, but not in the Devonian. The apparently anomalous joint pattern of the Devonian rocks is explained as the possible result of a lateral shear component of the block faulting that produced the rotation of Museum Village klippe and part of the Schunemunk Mountain syncline.

Introduction

LOCATION AND GEOGRAPHY

The Monroe quadrangle is located in Orange County, New York, about 65 kilometers northwest of New York City and about 16 kilometers due west of Bear Mountain and the Hudson River (fig. 1). The southern half of the quadrangle consists entirely of Precambrian crystalline rocks, largely gneisses, that form part of the Hudson Highlands, a part of the larger Reading Prong which extends northeasterly from Pennsylvania, through western New Jersey and southeastern New York, into Connecticut. By contrast, the northern and northwestern half of the quadrangle consists of relatively unmetamorphosed Paleozoic (Lower Cambrian to Middle Devonian) strata that form part of the Green Pond-Schunemunk Mountain outlier. This is a narrow, down-dropped synclinal block lying to the east of the principal area of Paleozoic strata of the Appalachian Valley and Ridge physiographic province.

The topography in the Monroe quadrangle is controlled primarily by structure, modified by lithology. The dominant physiographic feature is a series of northeasterly trending ridges separated by narrow valleys, many of which are occupied by lakes. Elevations of the principal ridges range from about 250 to 430 meters. Maximum relief in the quadrangle is 315 meters. The highest point occurs in the northeastern part of the quadrangle at 475 meters on Schunemunk Mountain, and the lowest, at 136 meters near Camp LaGuardia in the northwestern part of the area. These topographic features are modified by those of Pleistocene glaciation and are represented by northerly, and northwesterly-trending drumlins and drumlinoid hills, along with some kame and kettle features. Many of these, in turn, also follow older structural lineaments. Hence drainage is controlled fundamentally by structure and lithology, rather than by glaciation.

Perhaps the most striking example of structural control of the geography is afforded by the location of all of the major highways and many of the minor roads in fault zones. The New York State Thruway, N.Y. 17-M, Lakes Road, and Lazy Hill Road all lie in fault zones that follow the prevailing-northeasterly grain of the region. West Mombasha Road and N.Y. 208 follow north-trending faults and New York 17-U.S. 6, locally known as the Quickway, follows a major transverse fault striking approximately east-west.

Climate is moderate and pleasant with summer daytime maximum temperatures averaging in the 75–85° F. range and winter daytime maximum temperatures averaging in the low 20° F. range. Most of the population of the area is centered around the village of Monroe (population 5,000) and outlying smaller residential developments. A large number of these residents commute daily to New York City by bus, train, or automobile. Conversely, a large influx of residents from the metropolitan New York area expands the summer population of the Monroe region by about threefold.

ACKNOWLEDGMENTS

We thank John G. Broughton, Donald W. Fisher, Yngvar W. Isachsen, and James F. Davis of the Geological Survey, New York State Museum and Science Service, for providing encouragement, critical review, and thin section support for this project, and Fisher for identification of the large trilobite, *Coronura myrmecophorus*.

We are also grateful to Dr. Brian Mason, Smithsonian Institution, U.S. National Museum for making electron microprobe analyses of two amphiboles.

Special thanks are due to Professor Wilbur G. Valentine, Department of Geology, Brooklyn College. In addition to encouragement, he visited our field area for several consultations and provided technical criticisms and editorial assistance.

PREVIOUS STUDY

The geological literature on the Hudson Highlands has been summarized by Colony (1923), Sims (1958), Offield (1968), and it appears unnecessary and wasteful to repeat these descriptions here. In the New York area of the Highlands, work by Darton (1894), Ries (1895), Colony (1933), and Lowe (1950) has contributed to our knowledge of this region. More recently, detailed mapping in this region has been carried out in the Precambrian by Hotz (1953), Dodd (1965), Offield (1968), Helenek (in progress), Frimpter (in progress), and in the Paleozoic by Boucot (1959), Southard (1960), Kothe (1960). Field guidebook

articles on the geology of parts of the Monroe area were prepared by Jaffe and Jaffe (1962, 1967). Other than the guidebook articles, no detailed geologic mapping of significance has been reported for the Monroe area since the excellent earlier work of Ries (1895) and Colony (1933).

PURPOSE, SCOPE, AND METHODS OF STUDY

During the years 1958–65, Howard worked for the Union Carbide Ore and Nuclear Companies at their research laboratories in Sterling Forest, south of the Monroe area. At this time we resided in Monroe, became interested in the geology and metamorphic petrology of the rocks in the area, and began systematic mapping when we learned that no detailed work had been done in the area in many years. Work was carried out on weekends, evenings, and during other periods of free time from 1960 through 1965. The authors led field trips in the area for the New York State Geological Association in 1962 in conjunction with Brooklyn College, and again in 1967, in conjunction with New Paltz State University College. During the entire period of study, a large number of optical determinations were made to aid in guiding the mapping and interpreting the petrology. It was determined early in the mapping that most of the different lithologic units could be distinguished on the basis of the anorthite content of their plagioclase. As a result, the An contents of a large number of specimens accrued, and the results are given in the text as well as in plate 2, an overlay showing plagioclase compositions throughout the area.

In a similar, but much less extensive project, the iron : magnesium ratios were determined for a considerable number of orthopyroxenes, clinopyroxenes, hornblendes, and biotites. Thin section modes were determined by 1,000 point counts of a large number of specimens, and on occasion grain counting techniques (Chayes, 1944) were used to supplement these data. Shand (1947) has emphasized that if the mineralogical composition of a rock is accurately known, it is possible to arrive at its chemical composition by simple computation. He concluded that one can calculate this chemical composition from modes and mineralogical data much more accurately than one can do the reverse; e.g., determine the mineralogy and modes from the chemical analysis. In order to learn more about the bulk chemical composition of potential isochemical parent rocks for the Highlands gneisses, a fair number of such chemical compositions were calculated from the modes of gneisses and optical properties of constituents. It is believed that these do represent reasonably reliable estimates of the true chemical composition of the rocks and as such are useful in petrologic calculations and interpretations.

The accuracy of the optically determined anorthite content of plagioclase is believed to be $\pm$ An_2 by measurement of the alpha index of refraction in oils checked at measurement with an Abbe type refractometer and the use of Chayes (1952) curves. Measurements of Fe/(Fe + Mg) ratios of orthopyroxenes from the gamma index of refraction are perhaps accurate to $\pm$ Fe_5 because the curves do not correct for variation due to small amounts of Fe^{+3}, Ca, and Al. Nevertheless, the curves for the composition of orthopyroxene (Hess, 1952; Deer, Howie, and Zussman, 1963) can be considered quite reliable. Compositions were estimated for clinopyroxenes by measurement of the gamma index of refraction after a working curve (fig. 2) was con-

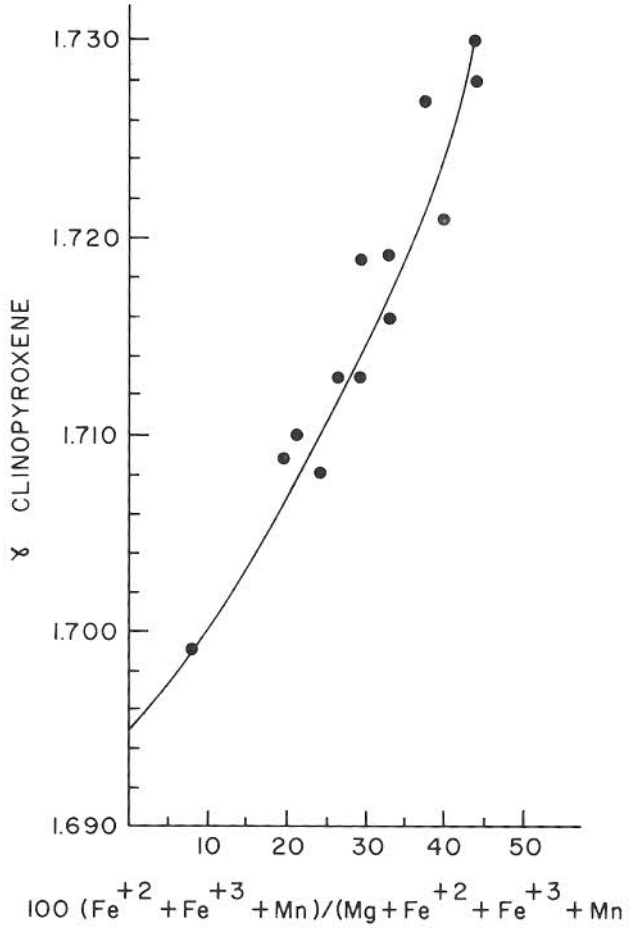

FIGURE 2. Working curve developed for estimatin iron-magnesium ratios of clinopyroxenes from the gamma index of refraction, in Highlands gneisses.

structed for several specimens by measuring all three indices of refraction, calculating 2V, and using the curves of Hess (1949) and Muir (1951). These are subject to many compositional variables and the compositions deduced in this way are to be considered reasonable estimates of unknown accuracy. The fact that these measurements consistently show the well-known proper Fe fractionation and enrichment in orthopyroxene with respect to clinopyroxene suggests that the compositions deduced from optical properties are "in the ball park." In a similar way, Fe/(Fe + Mg) ratios were determined for hornblendes using the curves for pargasite-ferrohastingsite of Deer, Howie, and Zussman (1963). Hornblendes are, of course, subject to variation in optical properties due to many constituents; notable among these are Ti^{+4} and Fe^{+3}. As a result, these estimated compositions are also best estimates. The optical-composition curves for biotites of Wones (1963) are much better because these were obtained by Wones under controlled conditions of oxygen fugacity, and use of the curves for the buffer most closely representing the mineralogy of a given rock will eliminate the variation due to Fe^{+3}. In the case of the biotites of this area, Ti ions are expected to be the principal cause of variation and error in determining biotite compositions, Fe/(Fe + Mg).

With a similar approach, Binns (1962) used optical properties to determine iron : magnesium ratios for a large number of coexisting orthopyroxenes and clinopyroxenes from New South Wales granulite terrane to demonstrate that mutual solid solution and iron contents increase with metamorphic grade.

Precambrian Rocks

GENERAL STATEMENT

Detailed geologic mapping in the Hudson Highlands is complicated by the lack of established stratigraphic control. This has been and will continue to be difficult to establish because the high grade of metamorphism to which the region was subjected in Precambrian time has obliterated much of the original record of sedimentation and volcanic activity. All of the sedimentary and volcanic rocks originally deposited in an ancient Precambrian eugeosyncline in this area have been totally recrystallized, and some have been partly to completely melted so that only vestiges of an early record of deposition and folding remain. Further complications are introduced by the resulting migmatitic nature of many of the gneisses and by the presence of amphibolite and leucogranitic members in most of these. Be that as it may, because the gneisses were only negligibly affected by retrograde alteration since their formation in the Precambrian, and because the metamorphism was largely isochemical, it is possible to distinguish gneisses of sedimentary from those of volcanic or plutonic parentage, and in so doing, attempt to set up a stratigraphy.

STRATIGRAPHY

The results of this study suggest the establishment of a tripartite stratigraphy for the Precambrian metamorphic rocks of the Monroe block (fig. 3) and their extension, on strike, to the southwest. This division is in no way intended to relate to the original three-fold division of Spencer (1908) into Pochuck, Losee, and Byram gneisses, and any similarities are fortuitous.

A framework of reference to the stratigraphic, structural, mineralogical-petrological features of the Monroe quadrangle is provided by figure 3, an outline map subdividing the northeast-trending belts of Precambrian rock. The tripartite stratigraphic division of the authors, given below, refers to the Monroe block (fig. 3) and may or may not be valid for the Ramapo block (fig. 3). The stratigraphic position of the allochthonous Precambrian gneisses of Belts 23–26 (fig. 3) is uncertain.

The Monroe block is stratigraphically subdivided below. Location numbers in parentheses refer to similar map units in the Ramapo block. Mineral names are listed in order of increasing volume percent. Relative ages are based on our structural interpretation of the Monroe block.

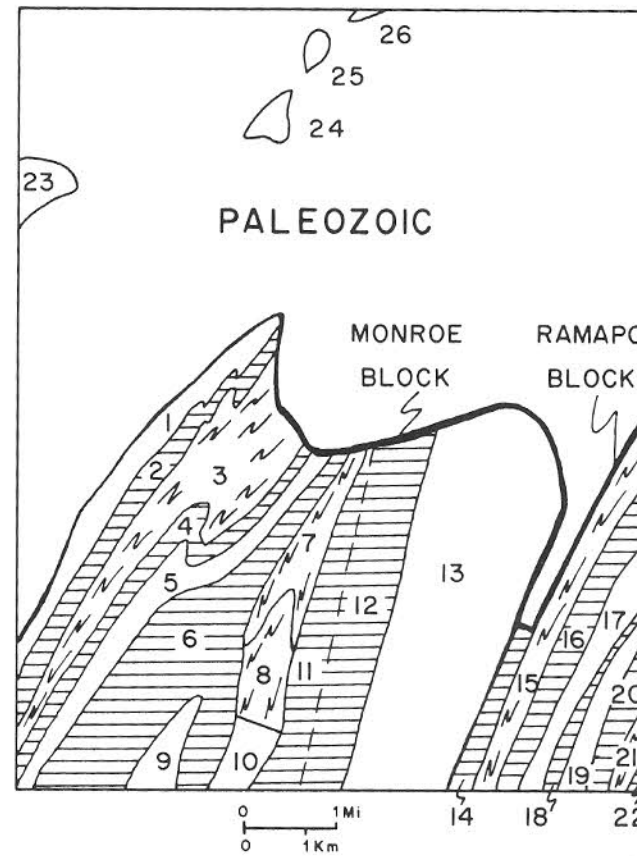

FIGURE 3. Index and reference map showing subdivision of Precambrian rocks of the Monroe quadrangle into belts.

Although gneisses of much the same lithology occur in the Ramapo block, which includes Belts 15 through 22, the details of their mineralogy and petrology suggest that they may be of a higher grade of metamorphism. The mineralogical names used for the gneisses in the Ramapo block are essentially the same as those used for similar rocks in the Monroe block but this does not necessarily imply stratigraphic equivalence.

The following additional lithologic units have been recognized in the definitely allochthonous Precambrian slices of Belts 23 through 26. Relative age is based upon structural interpretation.

Location	Lithology	Probable Parentage
YOUNGEST		
Belts: 1, 5, 13 (17, 19)	Hornblende (ferrohastingsite) granite gneiss and associated leucogranitic rocks (hg)	Volcanic
INTERMEDIATE		
Belts: 2, 4, 6, 11, 12, 14 (16, 18, 20, 22)	Amphibolite-granodiorite gneiss (amg)	Volcanic
	Calc-silicate gneiss, (cs)	Sedimentary
	Amphibolite and pyribolite (am)	Volcanic
	Hypersthene-quartz-plagioclase gneiss (hqp)	Volcanic
OLDEST		
Belts: 3, 7, 8, 9, 10 (15, 21)	Microcline alaskite (al)	Volcanic or sedimentary
	Biotite gneiss (bg)	Sedimentary
	Biotite-mesoperthite gneiss (bmp)	Sedimentary
	Albite-oligoclase leucogranodiorite (bmp)	Igneous
	Hypersthene-K-feldspar-plagioclase (charnockitic) gneiss (hk)	Sedimentary
	Sillimanite-cordierite-almandine-biotite-quartz-feldspar gneiss (sgb)	Sedimentary
	Magnetite-garnet-andesine leucogneiss (mag)	Sedimentary
	Pyroxene granulite	Sedimentary

Location	Lithology	Parentage
Belts 23–26		
Youngest	Calc-silicate/amphibolite (acs)	Sedimentary
	Albite leucogneiss (alg)	Igneous
Oldest	Graphitic sillimanite gneiss / Graphitic calc-silicate gneiss and quartzite (gcs)	Sedimentary

If these allochthonous slices represent separate blocks that have slid over or tumbled onto the Paleozoic strata rather than klippen, they need have no stratigraphic relation to one another. The sections exposed at Goose Pond Mountain (Belt 23) and at Museum Village (Belt 24) suggest the stratigraphic sequence shown above.

ROCKS OF THE MONROE AND RAMAPO BLOCKS

Hornblende (ferrohastingsite) granite gneiss

Hornblende (ferrohastingsite) granite gneiss occurs in five belts which occupy 30 percent of the Precambrian crystalline rock area of the Monroe quadrangle. These are belts or zones numbered 1, 5, and 13 in the Monroe block, and 17 and 19 in the Ramapo block (fig. 3). The most extensive area of outcrop occurs in Belt 13 where the granite gneiss occupies a syncline averaging about $1\frac{1}{4}$ miles in width. Granite gneiss of Belt 5 is mineralogically, texturally, and chemically identical to that of Belt 13, whereas that of Belt 1 differs principally in being coarser-grained and lower in color index. Mineralogical and petrological evidence suggest that the Ramapo block has been metamorphosed at a higher grade than the Monroe block, so that gneisses of Belts 17 and 19 are not necessarily equivalent to rock of Belts 1, 5, and 13. (See discussion under Metamorphic History.)

In hand specimen the hornblende granite gneiss is a fine- to medium-grained salmon pink, buff, or gray rock discontinuously streaked with black ferrohastingsite and biotite along with minor magnetite. The color index of the average specimen, frequently overestimated in the field, is only 3 to 12 (table 1). Outcrops are commonly rounded with smooth to corrugated surfaces which weather to a light ochre or a dark brown. Several specimens of granite gneiss collected along the Orange Turnpike near the western contact of Belt 13 contain dark red-brownish black allanite in grains up to about 8 mm. These are surrounded by pink-stained granite and commonly show radiating expansion cracks

TABLE 1. Composition of hornblende (ferrohastingsite) granite gneiss (hg).

A. Modes

	Belt 13						Belt 1				Belt 5	Belts 17, 19		
Sample No.*	22	46	356	360	723	751	263	699	521	724	407	745	718	750
Quartz	24.6	35.4	36.0	31.2	34.6	31.0	27.8	29.0	29.8	30.4	26.0	33.3	34.7	23.5
Microperthite	42.5	49.1	52.7	47.2	42.1	51.8	43.6	49.7	37.8	56.2	42.7	41.0	30.2	40.4
Plagioclase [1]	20.4	12.8	5.4	14.0	14.3	10.7	20.8	18.0	29.6	8.7	24.2	21.1	25.1	29.7
Hornblende	5.3	2.1	4.6	2.9	4.0	6.0	5.8	2.0	1.0	2.5	6.2	2.7	5.2	4.2
Biotite	6.5	0.4	0.6	4.5	4.8	0.4	1.6	1.2	1.8	1.5	0.3	0.2	+	0.1
Magnetite	0.3	0.2	0.4	0.1	+	0.1	0.4	0.1	+	0.5	0.6	1.7	2.8	2.0
Apatite	0.4	+	+	+	+	+	+	+	+	0.2	+	+	+	+
Zircon	+	+	0.3	0.1	0.2	+	+	+	+	+	+	+	+	0.1
[1] Mol. % An	23	21	21	17	22	21	14	17	17	15	15	28	30	25
Color Index	12	3	6	8	9	6	8	3	3	5	7	5	8	6
Avg. grain (mm)	1.2	0.6	0.8	1.0	0.5	0.7	1.0	1.5	1.5	2.5	1.2	1.3	1.2	1.0

resulting from alpha particle bombardment generated by decay of thorium. Foliation and/or lineation are conspicuous in most outcrops and all constituents tend to be elongated parallel to either the b- or a-fabric axis or to both. Compositional layering is poorly to moderately well developed as are gradations in color and texture which appear to result from slight variations in color index, quartz (dark gray)-microperthite (pink)-oligoclase (gray-white) ratios, degree of weathering of mafic minerals and resultant hematitic staining; to variations in grain size, the degree of foliation, and the development of porphyroblasts and augen of microperthite. Textural variations notwithstanding, the granite gneiss is compositionally homogeneous (table 1). Occasional simple pegmatites of microcline (or microperthite) quartz-ferrohastingstite-oligoclase occur as both concordant pods and discordant dikes or veins, but the gneiss unit is only locally migmatitic. Although remnants and schlieren of other rocks are uncommon in the granite gneiss, both biotite-rich gneiss and amphibolite have been observed as concordant lenses and pods both in the interior of the large Belt 13 unit and along its contacts. One such exposure occurs near the western contact of this unit in a road-cut on the eastern side of the Orange Turnpike about 900 feet north of its intersection with Bramertown Road. Here, 1-5-inch wide pods of amphibolite are concordantly folded in the granite gneiss. The amphibolite pods alternate with coarse pegmatite and fine- and medium-coarse grained granite gneiss imparting a conspicuous layered appearance to the outcrop. Contacts between granite gneiss and amphibolite pods are sharp.

B. Chemical composition calculated from the modes and optical properties of constituent minerals[2]

	22	46	360	S-156-48 [3]
SiO_2	68.79	76.66	73.39	74.89
TiO_2	0.43	0.10	0.27	0.21
Al_2O_3	14.17	12.35	12.89	12.53
Fe_2O_3	0.93	0.35	0.51	0.69
FeO	3.82	0.85	2.40	1.50
MgO	0.55	0.11	0.35	0.16
CaO	1.94	0.81	1.00	0.91
Na_2O	3.36	2.97	3.04	2.95
K_2O	5.52	5.74	5.89	5.38
H_2O	0.17	0.03	0.10	0.45
F	0.13	0.02	0.09	—
Cl	0.05	0.02	0.03	—
P_2O_5	0.21	—	0.08	0.04
Total	100.07	100.01	100.04	99.74

[2] Calculation assumes an estimated 30 percent albite is held in solid solution in microperthite.

[3] Chemical analysis of hornblende granite from near Splitrock Pond, Boonton quadrangle, Dover district, New Jersey, Sims (1953), also contains MnO=0.03.

* Sample locations in appendix.

In thin section the hornblende (ferrohastingsite granite gneiss is seen to be medium-grained for the most part, with average grain diameters on the order of 1 mm. Gneiss of the largest belt, 13, tends to be finer grained, averaging about 0.7 mm., whereas gneiss of Belt 1 is twice as coarse, averaging about 1.6 mm (table 1). The average grain diameters cited in table (and in the other tables of modes) represent the fie

diameter in mm. divided by the number of grains lying along the horizontal cross-hair of the microscope ocular. In foliated rocks the measurements are made across the shortest dimension or with the horizontal cross-hair parallel to the c-fabric axis of the specimen. Most specimens of the granite gneiss show an inequigranular granoblastic texture, in which alkali feldspars, plagioclase, and quartz are consistently anhedral. Only hornblende, biotite, and the accessory minerals show any tendency towards euhedral development. A typical specimen shows abundant elongated porphyroblasts or augen of microperthite (7 x 3.5 mm.) lying in a fine-granular aggregate of quartz, plagioclase, microperthite, and the mafic minerals (0.2–0.3 mm.). Most grains of all minerals tend to be elongated parallel to both the a- and b-fabric axes, imparting a good foliation to the rock. Biotite lies with its c-axis parallel to the c-fabric axis of the rock and, in addition, often shows stretching parallel to the b-fabric axis imparting both foliation and lineation, respectively, to the rock. Hornblende may lie with its c-axis parallel to either the b-fabric axis or to the a-fabric axis producing a lineated gneiss, and very often has its c-axis at random angles in the a-b fabric plane imparting a foliation to many specimens. In general, a compositional layering exists (although it is not readily noted) whereby the biotite and hornblende tend to be concentrated in those finer grained layers also rich in plagioclase and quartz. These darker layers are in turn interspersed with coarser alaskitic layers rich in microperthite and quartz.

Quartz is commonly elongated and intensely strained in all five belts, and in some of the gneisses shows, under crossed nicols, a strain pattern resembling a microcline grid pattern. In all five belts, the alkali feldspar is predominantly microperthite or microcline microperthite with relatively minor amounts of microcline. All of the alkali feldspar crystallized for a melt, initially as a microperthite, and eventually unmixed partially to a microcline microperthite. Albite-oligoclase exsolution blebs are uniformly distributed in microperthite grains and as further unmixing takes place the cores of the grains remain microperthite, the marginal or outer zones clear up and show slight microcline twinning, and the exsolution blebs move out to form narrow (40μ) rims of albite-oligoclase (An_{0-10}) on microcline microperthite (fig. 4). In addition to these narrow exsolution rims, free plagioclase grains occur in all five belts of granite gneiss. Because of their significant anorthite content, these crystallized contemporaneously with microperthite in a two-feldspar granite. In the Monroe block the free plagioclase is all intermediate oligoclase, averaging An_{22} in Belt 13, An_{16} in Belt 5 and An_{17} in Belt 1. In Belts 17 and 19 rock of the Ramapo block, the plagioclase is calcic oligoclase or/and andesine, ranging from An_{25-31} (table 1 and plate 2). An occasional grain of myrmekite occurs in most thin sections.

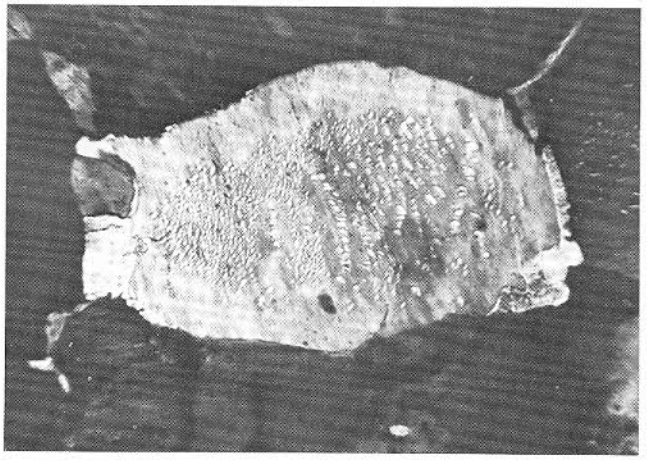

FIGURE 4. Microperthite in hornblende (ferrohastingsite) granite gneiss. Plagioclase blebs remain in center of grain, but have been cleared from outer zone by unmixing, and have moved outward to form a marginal strip of albite-oligoclase (right side of grain). Microperthite grain is 1 mm. in length. Sample 356. Crossed nicols.

TABLE 2. Optical properties and iron-magnesium ratios of ferrohastingsite from hornblende granite gneiss.*

	46	22	168	723	494	B–189[2]
	1.719	1.720	1.722	1.726	1.735	1.7235
β	1.715	1.714	1.718	1.722	1.729	1.7170
	1.693	1.694	1.697	1.701	1.703	1.6940
—	0.026	0.026	0.025	0.025	0.032	0.0295
$2V_x$ (calc.)	48°	57°	48°	46°	50°	55°
Disp.	r<v	r<v	r<v	r<v	r<v	r<v
Z c	15°	—	12°	13°	10°	12–13°
%Fe[1]	86	87	88	89	98	89.7[2]

Absorption is Y=Z>>X in all specimens.

[1] 100 $(Fe^{+2}+Fe^{+3}+Mn)/(Mg+Fe^{+2}+Fe^{+3}+Mn)$ from optical curves for pargasite-ferrohastingsite (Deer, Howie, and Zussman, 1963).

[2] 100$(Fe^{+2}+Fe^{+3}+Mn)$ / $(Mg+Fe^{+2}+Fe^{+3}+Mn)$ from chemical analysis of ferrohastingsite from ferrohastingsite granite, Cranberry Lake quadrangle, Adirondacks, New York (Buddington and Leonard, 1953).

* Sample locations in appendix.

TABLE 3. Optically determined iron-magnesium ratios of coexisting ferrohastingsite and biotite and anorthite content of coexisting plagioclase from hornblende granite gneiss.

Sample No.*	Ferrohastingsite		Biotite		Plagioclase	
	%Fe[1]		%Fe[2]		%An[3]	
Belt 1						
692	1.719	86	—		—	
263	1.723	89	1.682	85	1.535	14
517	—		1.681	84	1.537	17
Belt 5						
281	1.718	85	—		1.539	21
270	1.725	90	1.690	92	1.537	17
499	1.730	96	None		1.536	15
Belt 13						
46	1.719	86	1.688	90	1.539	21
22	1.720	87	1.686	88	1.540	23
309	1.721	87	1.689	89	1.541	25
168	1.722	88	1.691	93	1.536	15
37	1.722	88	1.684	87	1.540	23
360	1.722	88	1.688	90	1.537	17
320	—		1.691	93	1.540	23
359	—		1.688	90	1.537	17
793	1.726	91	—		—	
723	1.726	91	1.690	92	1.540	23
132	1.729	94	—		1.538	19
Belt 17						
740	1.700	60	1.656	65	1.542	27
768	1.712	75	1.661	68	1.544	31
Belt 19						
718	1.745	100	None		1.544	31
743	1.711	72	1.665	70	1.542	27

[1] $100(Fe^{+2}+Fe^{+3}+Mn) / (Mg+Fe^{+2}+Fe^{+3}+Mn)$ from curves of Deer, Howie, and Zussman (1963).

[2] 100 Fe/(FE+Mg) from curves of Wones (1963 for synthetic biotites, Fe_2SiO_4–SiO_2–Fe_3O_4 buffer.

[3] Mole % anorthite, from curves of Chayes (1952), which are given in weight % anorthite.

* Sample locations in appendix.

Optical properties and supporting qualitative spectroscopic analysis indicate that the principal mafic mineral is a titanium-rich ferrohastingsite rather than a common hornblende. Complete optical data are given in table 2 for representative samples of this amphibole and are compared with a similar, chemically analyzed specimen from the younger hornblende granite in the Cranberry Lake quadrangle of the Adirondacks (Buddington and Leonard, 1953). These data serve to verify and emphasize the extremely high total iron, ferric iron, and titanium contents of ferrohastingsite that may be expected in rocks classed as hornblende granite and hornblende granite gneiss. Buddington and Leonard (1953) suggest that this iron enrichment in ferrohastingsite may be correlated with quartz- and potash-rich granite that represents a younger differentiate of the same magma that produced the normal hornblende granite. Using these data and the optical-composition curves given in Deer, Howie, and Zussman (1963), the iron-magnesium ratios of a number of ferrohastingsites were determined approximately by measuring their gamma index of refraction (table 3). It should be noted that some of the specimens in tables 2 and 3 have gamma indices of refraction exceeding the ferrohastingsite end-member ($\gamma = 1.730$) listed in Deer, Howie, and Zussman (1963) and may represent extreme enrichment in titanium as suggested by our spectroscopic data or, less likely, possible enrichment in chlorine as indicated by Krutov (1936) who reported a ferrohastingsite containing 7.24 percent Cl with a gamma index of refraction of 1.751. These exceptions notwithstanding, it is believed that the cited optical-composition curves are sufficiently reliable to yield reasonable estimates of iron-magnesium ratios in the ferrohastingsites, and as will now be shown, in the biotites, as well. Biotite accompanies hornblende (ferrohastingsite) in subordinate to equal amounts in granite gneiss of Belts 1, 5, and 13 and in some specimens may be more abundant than hornblende. Biotite-rich hornblende granite gneiss occurs along the western contact of the Belt 13 synclinal limb which is gradational to calc-silicate gneiss and in another zone near the center of this belt which may also be a contact zone near the synclinal axis. Gneiss of Belts 17 and 19 (Ramapo block) once again differs from the 1, 5, 13 (Monroe block) group in having only very minor biotite. Although the optical-composition curves for biotite are subject to many compositional variables, estimates of their iron-magnesium ratios were also made by measuring their gamma index of refraction (a difficult task in itself) and using the buffer-controlled curves of Wones (1963) to minimize the ferrous-ferric iron variable. These curves were obtained by Wones on a series of biotites (phlogopite-annite) which he synthesized at a variety of temperatures, pressures, and oxygen fugacities. The curve used to estimate the composition of the Monroe biotites is that defined by the Fe_2SiO_4—SiO_2—Fe_3O_4 buffer. The results of the optical measurements on biotite are shown in table 3 where they are compared with similar data for coexisting ferrohastingsite and plagioclase. The results clearly show that: 1) biotite and ferrohastingsite vary sym-

pathetically in their iron-magnesium ratios in all five belts of granite gneiss; 2) these ratios, expressed as atom percent Fe $= 100(Fe^{2+}+Fe^{3+}+Mn)/(Mg+Fe^{2+}+Fe^{3+}+Mn)$ do not depart significantly from Fe_{90} in Belts 1, 5, and 13 of the Monroe crystalline block; 3) they tend to be much lower in Belts 17 and 19 of the Ramapo crystalline block; 4) the Fe ratios of ferrohastingsite and biotite vary antipathetically with the An content of plagioclase where all three minerals coexist; 5) where biotite is absent the Fe ratio of the ferrohastingsite, and/or the Ti content as well, increase markedly. Although the optical curves for minerals as complex as hornblende and biotite cannot be considered as reliable as those for plagioclase and orthopyroxene, the data presented in tables 2 and 3 are internally consistent.

The remaining mafic constituent of importance is magnetite which occurs in all specimens. In the Monroe block the magnetite content is in the tenths of a percent whereas in Belts 17 and 19 of the Ramapo block it ranges from 1 to 3 percent.

Persistent accessory minerals are apatite and zircon, and more rarely, the allanite mentioned earlier. Zircon is commonly dark red in hand specimen and pink-orange under the microscope; it is commonly zoned and euhedral as noted for the Bear Mountain granite by Eckelmann (1963) and Dodd (1965). Not a single grain of either ortho- or clinopyroxene was observed in thin section or in index oils in the many samples of granite gneiss studied, except where remnants of included amphibolite were recognizable. These contain both pyroxenes. Perhaps the pyroxene reported in this map unit by most other investigators in the Highlands is, as implied here and earlier suggested by Buddington (1939), consistently inherited from amphibolite remnants in granite.

Modes of the hornblende (ferrohastingsite) granite gneiss representative of all five belts along with chemical compositions calculated from the modes are presented in table 1. As would be expected these are similar to those reported by Hotz (1953) for the same map unit in the Sterling-Ringwood District to the south of the Monroe quadrangle, Dodd (1965) for the Popolopen Lake quadrangle immediately to the east, Lowe (1950) for Storm King granite at Bear Mountain, and by Offield (1967) for the Goshen and Greenwood Lake quadrangles, and Sims (1953) for the Dover district, New Jersey to the west and south of this map area. They also show petrographic and mineralogical similarities to hornblende granite and granite gneiss from the younger granitic rocks of the Adirondacks described by Buddington (1939) and Buddington and Leonard (1953 and 1962), particularly those from the Alexandria, Lowville, and St. Regis types. All of these are compared modally in figure 5 which serves to emphasize some of the differences and similarities. Although there is considerable overlap, the largest bodies of this map unit both in the Adirondacks and the Highlands (Bear Mountain) contain the most microperthite and the least free plagioclase. For all examples, quartz shows considerable variation, ranging from about 23–40 percent. Enrichment in quartz cannot be shown, in the Highlands, to be the result of magmatic differentiation.

All units mapped in the Hudson Highlands and Adirondacks as hornblende granite and hornblende granite gneiss need not have originated in the same way. Many features in common include their composition, some textural features; their occurrence in high-grade metamorphic terranes; and their Precam-

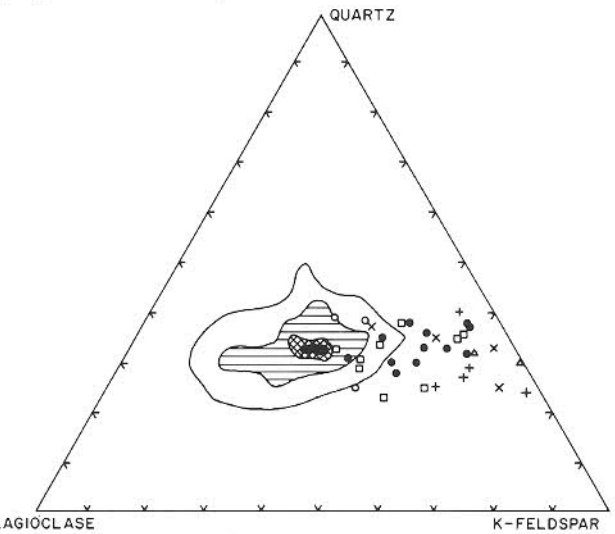

FIGURE 5. Distribution of modal quartz, plagioclase, and alkali feldspar in hornblende granite gneiss of the Monroe quadrangle and other related areas. ● — Belts 1, 5, and 13, Monroe Block; ○ — Belts 17 and 19, Ramapo Block, both of the Monroe quadrangle: × — Popolopen Lake quadrangle (Dodd, 1965): □ — Goshen-Greenwood Lake quadrangles (Offield, 1967); △ — Sterling-Ringwood magnetite district (Hotz, 1953); + — Adirondacks ("younger granites" of Buddington, 1939, Buddington and Leonard, 1962). Contoured area shows modal analyses of 260 granites from eastern U.S.; contour values are > 0, 2, 5, and 7 percent (Chayes cited in Tuttle and Bowen, 1958). Plot shows the relatively large amounts of Na-plagioclase held in solid solution in K-feldspar from granitic rocks of the Highlands and Adirondack areas.

brian age of major recrystallization dated at about 1150 my, by Tilton, et al. (1960) from lead-uranium isotopes on zircon. Virtually all investigators of the subject in the Highlands interpreted the hornblende granite gneiss as having crystallized from a melt, and Hotz (1953), Sims (1953), and Dodd (1965) follow Buddington's lead in adopting a syntectonic intrusive origin as the mode of emplacement of the magmas, in the form of phacoliths or sheets. Offield (1967) adopted this view, as well, but with some reservations, noting that in the Dover, New Jersey district (Sims, 1953) most of the area is underlain by granite gneiss and granitic rocks and if these are removed, there remains but little of an older sedimentary terrane into which syntectonic magmas could intrude. In short, the old room problem remains with us. Although the present authors also interpret the hornblende granite gneiss as having crystallized from a melt, they favor an alternative view for the origin of the melt. It is well-known that volcanic rocks form an important, if not dominant, part of many eugeosynclines. Particularly significant is the very thick pile of rhyolitic volcanics (>15,000 feet) described by Rankin (1968) from the Lower Devonian of Maine, and by Aubouin (1965) from the Lower Carboniferous of the Vosges. Metamorphism of such a rhyolitic volcanic pile in a eugeosyncline at temperatures of 700–800° C and pressures on the order of 3000–4000 bars P_{H_2O} at a depth of perhaps 7 miles, would readily result in the production of an anatectic granite magma which on crystallization would be largely conformable with the enclosing or intercalated sediments of the eugeosyncline. The gneissic structure would then develop in the granite gneiss at the same time as in the other gneisses. The uncommon, small-scale cross-cutting relationships described by Hotz (1953), and Dodd (1965), are not inconsistent with this hypothesis because of probable later anatexis accompanying metamorphism. Large-scale crosscutting relationships are not common, if they occur at all in the Highlands. In the Monroe quadrangle, the hornblende granite gneiss was not seen to transect the foliation of any of the units with which it is in contact, specifically calc-silicate gneiss, amphibolite, and hypersthene-quartz-plagioclase-gneiss. Discordant relations are shown by small bodies of late essentially isotropic alaskite and pegmatite veins and dikes which cut most of the units including the hornblende granite gneiss, but never by the gneiss itself. It seems reasonable to conclude, therefore, that the hornblende granite gneiss of the Monroe block, with its extensions southward and westward into the Sloatsburg, Greenwood Lake, and Warwick quadrangles, has stratigraphic significance and has not reached its present level by haphazard intrusion.

Hornblende-pyroxene-plagioclase gneiss (amphibolite and pyribolite)
Biotite-hypersthene-quartz-plagioclase gneiss
Amphibolite-granodiorite gneiss.

These three map units, hornblende-pyroxene-plagioclase gneiss (amphibolite and pyribolite), biotite-hypersthene-quartz-plagioclase gneiss (intermediate charnockite or enderbite), and amphibolite-granodiorite are so consistently closely associated in the field that to discuss them separately would mask this relationship. Modal analyses of the amphibolites, pyribolites, and quartz-plagioclase gneisses are, however, presented separately in tables 4 and 5 for comparative purposes. Amphibolite, sensu stricto, is the name given to rocks that consist essentially of hornblende and plagioclase. Hotz (1953) used the name, pyroxene amphibolite, for the relatively common Highlands rocks in which pyroxenes are present in amounts exceeding hornblende. Offield (1967) adopted this usage, justifying it by stating that in such rocks "the percentage of hornblende is large and because of the intimate association with amphibolite." Although these rocks are indeed intimately associated in the field, both the modes of Hotz (1953) and those presented here (table 4) refute this quotation and show that pyroxene-plagioclase gneiss with little or even no hornblende does occur in both the Monroe quadrangle (fig. 6) and in the Sloatsburg and Greenwood Lake quadrangles (Hotz, 1953)

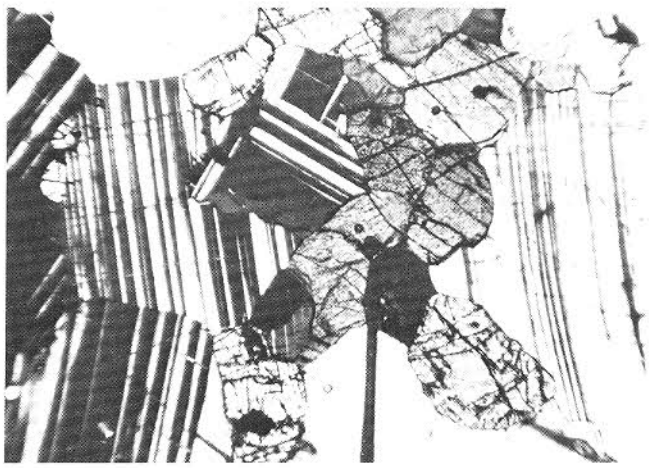

FIGURE 6. Pyribolite showing granular hypersthene and clinopyroxene (gray) and albite and pericline twinning in andesine; hornblende is absent. Sample 406. Crossed nicols. Length of photograph = 3.5 mm.

TABLE 4. Composition of amphibolite and pyribolite (hornblende- and pyroxene-plagioclase gneiss), (am).

A. Modes

	Amphibolite						Pyribolite				
Belt	8	2	6	18	11	4	4	2	6	6	6
Sample No.*	345	659A	71A	744	515A	437A	437P	700	372	178	406
Plagioclase[1]	39.6	50.4	55.9	51.3	70.0	57.3	65.1	51.4	58.7	66.7	70.2
Hornblende	44.4	24.0	25.5	25.0	29.5	34.3	1.4	15.0	9.6	8.5	+
Orthopyroxene	5.8	10.4	+	14.7	+	3.0	16.3	—	10.4	18.4	14.0
Clinopyroxene	5.4	8.8	10.5	5.1	—	2.3	11.8	22.2	10.6	5.0	13.8
Biotite	2.0	—	2.2	—	0.5	+	+	—	3.1	+	—
Magnetite	2.6	5.2	3.7	3.9	+	2.5	3.0	7.2	7.3	1.0	2.0
Apatite	0.2	1.2	0.1	+	+	0.6	0.1	1.6	0.3	0.4	+
Orthoclase	—	—	—	—	—	—	1.7	2.6	—	—	—
Quartz	—	—	—	—	—	—	0.6	—	—	—	—
Chlorite, serp.	+	+	2.1	+	+	+	+	+	+	+	+
* Sample locations in appendix.											
[1] Mol. % An	41	65	29	47	41	35	32	16	35	41	46
Color Index	60	51	44	49	30	43	33	46	41	33	30
Avg. grain (mm)	0.3	0.2	0.3	1.0	0.7	0.5	0.9	0.5	0.4	0.6	1.1

B. Chemical composition calculated from the modes and optical properties of constituent minerals.

	Amphibolite [1]	Spilite [2]	744	515A	437A	437P	178	406
SiO_2	50.3	51.22	47.85	52.57	51.49	53.90	52.79	52.19
TiO_2	1.6	3.32	0.70	0.71	0.94	0.13	0.30	0.16
Al_2O_3	15.7	13.66	15.72	21.43	18.05	15.93	18.10	18.66
Fe_2O_3	3.6	2.84	5.38	0.85	1.37	3.61	2.29	3.22
FeO	8.0	9.45	11.54	5.38	9.54	9.46	8.39	7.32
MgO	7.0	4.55	6.38	3.51	3.97	4.26	5.58	4.72
CaO	9.5	6.89	8.65	9.44	8.97	7.53	7.88	9.73
Na_2O	2.9	4.93	3.12	4.99	4.57	4.60	4.25	4.00
K_2O	1.1	0.75	0.24	0.62	0.38	0.28	0.09	—
H_2O		1.88	0.42	0.42	0.64	0.02	0.15	—
P_2O_5	0.3	0.29	—	—	0.04	0.26	0.17	—
F			—	—	0.04	0.02	0.01	—
CO_2		0.94	—	—	—	—	—	—
Total	100.01	100.72	100.00	100.00	100.00	100.00	100.00	100.00

[1] Average of 200 amphibolites from Poldervaart (1955).
[2] Average of 19 spilites from Turner and Verhoogen (1960).

to the south and west of Monroe. Obviously, a rock carrying little or no hornblende or other amphibole cannot be classed as an amphibolite. In this report the name pyribolite (Jaffe and Jaffe, 1962) will be used in place of the ambiguous "pyroxene amphibolite" for those mesocratic pyribole-plagioclase metamorphic rocks in which the content of orthopyroxene + clinopyroxene exceeds that of hornblende.

Amphibolite and pyribolite occur throughout the Monroe quadrangle in more or less discontinuous layers and pods intercalated with rock of all other map units. These rocks are consistently very intimately associated with biotite-hypersthene-quartz-plagioclase gneiss (an intermediate charnockite or enderbite) and in many areas it is difficult to distinguish these two rock-types in the field. An additional map unit, amphibolite-

TABLE 5. Composition of biotite-hypersthene-quartz-plagioclase gneiss (hqp).

A. Modes

Belt	2	6	6	6	2	16	6	6	16
Sample No.*	515	258	297	425	648	481	71	402	713W
Quartz	32.6	27.8	26.4	21.7	19.9	18.2	16.2	11.3	6.6
K-feldspar [1]	1.2	1.8	5.1	2.0	1.5	3.6	5.2	6.0	4.0
Plagioclase [2]	55.5	56.8	60.8	68.8	60.7	60.6	62.1	63.3	74.8
Hypersthene	7.7	2.5	4.7	3.0	7.4	7.3	11.9	2.1	5.0
Talc, cl., serp.	+	0.8	+	0.2	2.0	0.6	1.0	0.9	+
Biotite	0.7	1.0	1.9	1.3	0.2	—	2.8	7.6	—
Clinopyroxene	1.3	—	—	—	—	0.3	+	6.0	8.2
Hornblende	—	—	—	1.0	4.4	8.4	—	—	0.6
Magnetite	0.7	2.5	0.9	1.3	3.7	0.8	0.6	2.4	0.8
Apatite	0.3	+	0.2	0.7	0.2	0.2	0.2	0.4	+
Zircon	—	—	+	—	—	—	+	+	—

* Sample locations in appendix.

[1] Occurs principally as exsolution blebs in antiperthitic plagioclase; may be microcline or orthoclase; less commonly as interstitial grains.

[2] Mol. % An	39	33	24	31	33	33	29	33	31
Color Index	11	7	8	7	18	18	15	19	15
Avg. grain (mm)	2.2	2.4	1.0	1.2	0.5	1.0	2.0	2.3	2.0

B. Chemical composition calculated from the modes and optical properties of constituent minerals.

	515	297	Average dacite [3]	71	Graywacke [4]
SiO_2	69.32	69.48	63.58	63.76	64.7
TiO_2	0.04	0.06	0.64	0.11	0.5
Al_2O_3	14.95	15.71	16.67	16.71	14.8
Fe_2O_3	1.26	1.37	2.24	1.23	1.5
FeO	2.94	2.41	3.11	4.47	4.0
MgO	2.15	1.36	2.12	3.57	2.2
CaO	5.08	3.25	5.35	3.90	3.1
Na_2O	3.73	5.20	3.98	4.87	3.1
K_2O	0.25	0.99	1.40	1.07	1.9
H_2O	0.02	0.08	0.56	0.22	3.1
P_2O_5	0.15	0.08	0.17	0.08	0.2
F	0.01	0.01	—	0.01	
Total	100.00	100.00	99.82	100.00	99.1

[3] Average effusive dacite, after Nockolds (1954).

[4] Average of 23 graywackes from Pettijohn (1957).

granodiorite gneiss, consisting of mafic and felsic gneiss interlayered on a 1–25 mm. scale is also closely associated with hornblende-pyroxene-plagioclase gneiss and biotite-hypersthene-quartz-plagioclase gneiss. All of these, along with the calc-silicate gneiss and ubiquitous alaskite, make up the middle stratigraphic unit of the Monroe crystalline block. Belt 2 consists of amphibolite-granodiorite with smaller discontinuous layers of amphibolite and quartz-plagioclase gneiss. In places amphibolite is boudinaged in elliptical pods (10–100 cm. in length) in alaskite, and in other areas, it grades, on strike, into medium- to coarse-grained, poorly foliated hornblende granodiorite. Unusual quartz-plagioclase gneisses in which hornblende, rather than hypersthene, is the principal mafic mineral occur in Belt 2 but are rare elsewhere in the quadrangle. Belt 2, which

is mapped largely as amphibolite-granodiorite, grades to the southwest into a zone in which quartz-plagioclase gneiss predominates over amphibolite. The rock of Belt 4 is very similar to that of Belt 2 but is relatively richer in amphibolite.

Belts 6 and 11, which form the west and east limbs, respectively, of a northeast-plunging anticline consist largely of medium-grained gray, green, or pink biotite-hypersthene-quartz-plagioclase gneiss bounded on both margins by pyribolite and less commonly by amphibolite. In many localities the biotite-hypersthene-quartz-plagioclase gneiss is massive and foliation readings can only be obtained by measuring the attitude of the enclosed concordant amphibolite-pyribolite pods and layers. An excellent exposure of amphibolite boudinaged in mobilized biotite-hypersthene-quartz-plagioclase gneiss occurs in Belt 6 along the western edge of Mombasha Lake at the end of the circular drive due east of the 918 foot elevation on West Mombasha Road. Another similar occurrence is at the 1,000 foot contour on the Appalachian Trail west of East Mombasha Road. Still another in Belt 6 is just west of the Appalachian Trail at the outlet of Kloibers Pond where the quartz-plagioclase gneiss discordantly transects and appears to be replacing the amphibolite. In Belt 11, on an eastward traverse from the h in East Mombasha Road to the summit of a ridge marked 1035, one encounters about 300 feet of a migmatitic biotitic calc-silicate gneiss, followed by a dark greenish black rock consisting of interlayered millimeter to inches-wide fine-grained (0.5 mm.) amphibolite and medium-grained (1.0 mm.) pyribolite. In a col at about the 1,000 foot contour, a beautiful exposure of this rock (samples 515A and 515) clearly shows biotite-hypersthene-quartz plagioclase gneiss in cross-cutting relationship to the amphibolite-pyribolite layers (modes in tables 4 and 5). The quartz-plagioclase gneiss is greenish and in the field it closely resembles the green pyribolite layers intercalated with amphibolite.

In thin section the amphibolite tends to be slightly finer-grained than the pyribolite, although this is not always so (table 4). Both rocks show a granoblastic fabric and either a strong lineation or foliation, depending upon the orientation of hornblende and pyroxene, which is not always the same (fig. 7). In some specimens with a stronger lineation than a foliation, hornblendes lie with their c-crystallographic axes parallel to the b-fabric axis of the rock and often with the b-crystallographic axes parallel to the a-fabric axis of the rock. In such specimens, a typical thin section cut parallel to the a-c fabric plane shows a large number of end-sections of strongly pleochroic hornblendes oriented with their dark brownish-green absorption direction, Y (Y=b), parallel to the a-fabric axis and the polarizer of the microscope. In other specimens, a foliation is developed with the c-crystallographic axes of hornblendes rotated at various angles in the a-b fabric plane of the rock. In response to rock deformation, the octahedral layers in hornblende, which are parallel to their b-c crystallographic plane, orient in an analogous manner to the octahedral and tetrahedral layers in biotite, which are parallel to the a-b crystallographic plane; in both cases the crystallographic layers lie parallel to the metamorphic foliation (fig. 7). Pyroxenes tend to orient themselves in a similar manner to hornblende because their crystal structures are similar. Because of their good (*100*) crystallographic parting, pyroxenes, in response to deformation, produce an a-lineation in these rocks because slippage occurs with the c-crystallographic axes parallel to the a-fabric axis (fig. 7).

Biotite-hypersthene-quartz-plagioclase gneiss is relatively unfoliated, and coarser-grained than the amphibolite and pyribolite. Most specimens have an average grain size of about 2 mm. as contrasted with about 0.3 mm. for amphibolite and 0.8 mm. for pyribolite (tables 4 and 5). There is a similar range in color index, with quartz plagioclase gneiss averaging about 18 percent

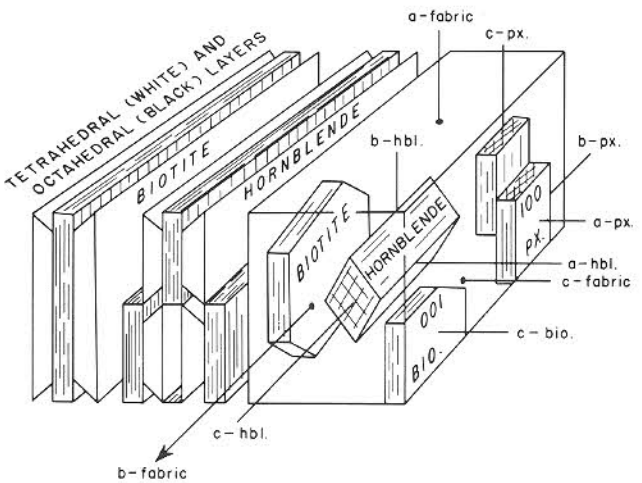

FIGURE 7. Influence of crystal structure on rock fabric in foliated and/or lineated amphibolites. Both biotite and hornblende tend to lie with their tetrahedral and octahedral crystallographic layers parallel to the a-b-fabric plane of foliation. Prismatic hornblende and stretched biotite produce b-fabric lineations; (*100*) parting in pyroxenes may produce an a-fabric lineation.

of mafic minerals; pyribolite, about 35; and amphibolite, about 45. Quartz-plagioclase gneiss is commonly granoblastic, and occasionally the texture may approach hypautomorphic-granular habit with some of the plagioclase grains showing a tendency to develop euhedral shape. Quartz and plagioclase are only slightly elongated, and foliation, although poor, tends to increase directly with color index due to preferred orientation of the mafic minerals. As has been noted by Hotz (1953) and others, the quartz content of the hypersthene-quartz-plagioclase gneiss is variable over quite a large range. The modes in table 5 show a range of from 7 to 33 percent quartz. Specimens low in quartz are extremely difficult to distinguish from rocks mapped as pyribolite, and, in the field, there is every gradation from one to the other. Under the microscope, quartz is not uniformly distributed in the quartz-plagioclase gneiss, and large areas of a given thin section may be devoid of this mineral. Plagioclase in the average specimen is andesine, showing an alpha index of refraction of 1.544 equivalent to An_{31} mole percent based upon Chayes' curves (1952) which yield slightly higher values because they are in weight percent. Anorthite contents range from a low of 24 to a high of 39, and a value of An_{31} is representative for the unit. Plagioclase is consistently antiperthitic, representative modes showing from 1 to 6 percent of potassic feldspar (both microcline and orthoclase in different (specimens) most of which occurs as rectangular strips enclosed in plagioclase. A few specimens contain some small interstitial grains of free potassic feldspar which have probably unmixed from antiperthite. The rectangular strips of potassic feldspar enclosed in plagioclase range from micron dimensions up to a length of 0.24 mm., and vary widely in size both in the same grain and in adjoining grains of the host. It is not uncommon to find a plagioclase grain completely free of included K-feldspar next to other grains veritably loaded with these inclusions (fig. 8). Examinations made of numerous grains in oil immersion mounts show that this variation is not due to orientation or the way a given thin section was cut; the variation in distribution and size is real. Some of the larger strips of included K-feldspar themselves contain telescoped inclusions of apatite, tourmaline, or quartz. Some of the plagioclase grains, in addition to being antiperthitic, are also sagenitic, containing needles of rutile, while others may contain euhedral, hexagonal plates of a dark brown mineral which has not been identified. Was the antiperthite produced by exsolution from an originally homogeneous solid solution or was it formed by a replacement process? Hubbard (1965) suggests an exsolution origin for the antiperthites from very similar intermediate charnockite (enderbite) from Nigeria for plagioclase compositions of $Or_{13}Ab_{46}An_{41}$, noting that this composition falls within the high temperature limits of solid solution shown by Tuttle and Bowen (1958). Sen (1959), who made a detailed study of the subject, showed average Or contents of plagioclase to increase with temperature of formation, averaging $Or_{0.5}$ in amphibolites, $Or_{1.2}$ in granites, $Or_{2.2}$ in granulite facies rocks, and $Or_{3.6}$ in volcanic rocks. He favored an exsolution origin for most of these but noted that replacement origin was also common in metamorphic rocks and showed as examples plagioclases containing abundant rectangular inclusions in amounts greater than could have been dissolved in plagioclase. Although some of the antiperthites in the Highlands quartz-plagioclase gneiss may be of exsolution origin, the authors believe that the texture, amount, erratic size, variable distribution and large strips of included K-feldspar favor a replacement origin perhaps resulting from the breakdown of small amounts of biotite found in almost all specimens. Calculations from grain count of the antiperthitic plagioclase shown in figure 9 yielded a bulk feldspar composition of $Or_{26}Ab_{52}An_{22}$. As this amount of K-feldspar appears too much to be held in solid solution, the antiperthite is believed to be of a replacement origin.

FIGURE 8. Biotite-hypersthene-quartz-antiperthitic plagioclase gneiss. Andesine antiperthite in contact with nonperthitic twinned andesine, hypersthene (upper right), biotite (lower center) and quartz (black and white). Sample 71. Crossed nicols. Length of photograph is 4.0 mm.

A large number of optical determinations were made of the constituent minerals of amphibolite, pyribolite,

TABLE 6. Optically determined iron-magnesium ratios of coexisting hypersthene, clinopyroxene, hornblende and biotite, and anorthite content of coexisting plagioclase, from amphibolite, and pyribolite.

Sample*	Hypersthene	%Fe[1]	Clinopyroxene	%Fe[2]	Hornblende	%Fe[3]	Biotite	%Fe[4]	Plagioclase	%An[5]
Belt 2										
700	—		1.719	35	1.694	54	—		1.535	16
729	—		1.718	34	1.697	57	1.660	68	1.547	37
143N	1.730	53	1.720	36	—		—		1.544	31
659	—		—		1.693	53	—		1.562	65
778	—		—		1.713	76	1.657	66	1.543	29
148	—		1.719	35	1.719	86	1.674	78	1.542	27
Belt 4										
653	1.718	43	—		1.692	51	1.641	47	1.568	77
437A	1.731	54	1.720	36	1.700	60	—		1.546	35
455	1.724	48	—		1.701	61	—		1.544	31
150	1.723	47	—		1.697	57	—		1.544	31
Belt 6										
372	1.713	38	1.713	28	1.687	45	1.654	64	1.546	35
241S	1.717	42	1.714	29	—		1.655	65	1.546	35
178	1.719	44	1.714	29	—		—		1.549	41
406	1.723	47	1.719	35	—		—		1.552	46
495	—		—		1.665	25	—		1.557	54
Belt 7										
127	1.717	42	—		1.685	43	1.644	52	1.554	49
Belt 8										
345	1.727	51	1.722	38	1.701	61	1.681	83	1.549	41
Belt 11										
515A	—		—		1.691	50	—		1.549	41
155	1.721	46	1.719	35	1.686	44	—		1.550	42
232	1.721	46	1.719	35	1.691	50	—		1.546	35
53	1.725	49	1.717	33	1.688	47	1.655	64	1.546	35
Belt 12										
61	1.718	43	1.713	28	1.689	48	1.656	65	1.548	39
Belt 18										
480	1.719	44	—		1.695	55	—		1.546	35
766	1.723	47	—		+		—		1.548	39
716	1.724	48	1.722	38	1.710	71	—		1.553	47
Average		46		34		55		65		40

[1] $100(Fe^{2+}+Fe^{3+}+Mn)/(Mg+Fe^{2+}+Fe^{3+}+Mn)$ using curves of Hess (1952), and Deer, Howie, and Zussman (1963).

[2] Same ratio using curve shown in figure 2 and derived data of Hess (1949), Muir (1951) and Deer, Howie, and Zussman (1963). These can only be considered estimates as the gamma index of refraction alone is not satisfactory.

[3] Same ratio, using the curves of Deer, Howie, and Zussman (1963) for the pargasite-ferrohastingsite series. A probe analysis of amphibole from one of these amphibolites, 345, by Brian Mason, indicates that the amphibole has little or no octahedral Al and a high alkali content along with high iron content indicating it to be a member of this series.

[4] Same ratio using the Fe_2SiO_4–SiO_2–Fe_3O_4–buffered curves for synthetic biotites (Wones, 1963).

[5] Mol. % An converted from the weight % An curves of Chayes (1952).

* Sample locations in appendix.

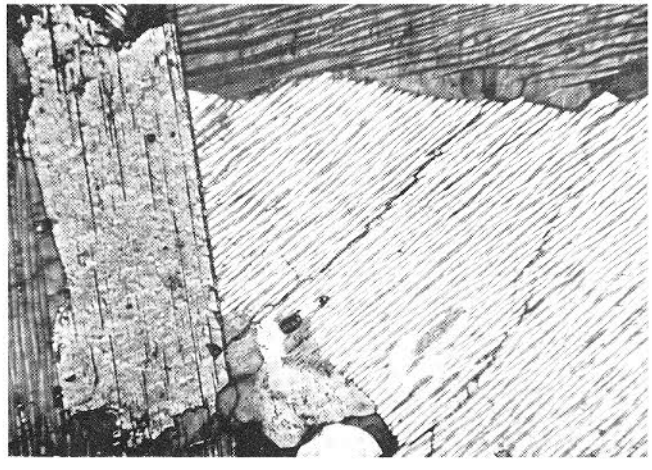

FIGURE 9. Textures and compositions of:

(1) Replacement antiperthite in biotite-hypersthene-quartz-plagioclase gneiss. Photograph is 0.85 mm. x 0.6 mm. Crossed nicols.

(2) Exsolution mesoperthite in biotite mesoperthite gneiss (two samples). Mesoperthite lamellae are 5–6μ in width. Crossed nicols.

1 2

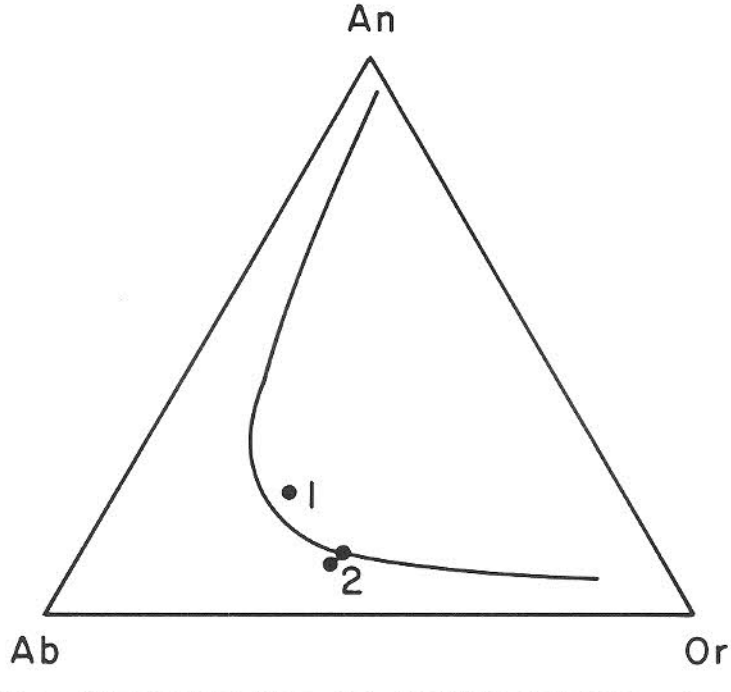

1. REPLACEMENT ANTIPERTHITE IN HYPERSTHENE – QUARTZ–PLAGIOCLASE GNEISS.
2. EXSOLUTION MESOPERTHITE IN BIOTITE–MESOPERTHITE GNEISS

TABLE 7. Optically determined iron-magnesium ratios of coexisting hypersthene, clinopyroxene, hornblende, and biotite and anorthite content of coexisting plagioclase from biotite-hypersthene-quartz-plagioclase gneiss.

Sample*	Hypersthene	%Fe[1]	Clinopyroxene	%Fe[2]	Hornblende	%Fe[3]	Biotite	%Fe[4]	Plagioclase	%An[5]
Belt 2										
262	1.733	55	1.722	38	—		—		1.545	33
691	1.739	60	1.725	41	1.719	86	1.675	78	1.544	31
725	1.740	61	1.728	43	—		—		1.544	31
Belt 6										
798	1.713	38	—		1.686	44	1.654	64	1.544	31
297	1.716	41	—		—		—		1.540	24
71	1.717	42	—		—		—		1.543	29
394	1.718	43	—		—		1.655	64	1.546	35
286	1.719	44	—		—		1.656	65	1.545	33
402	1.720	45	—		—		1.649	59	1.545	33
238	1.728	51	—		—		1.675	78	1.543	29
258	1.716	41	—		—		1.658	67	1.545	33
Belt 11										
515	1.717	42	1.712	27	—		1.651	61	1.548	39
318W	1.720	45	—		—		—		1.544	31
41	1.724	48	—		—		—		1.543	29
Belt 16										
479	1.719	44	—		—		—		1.546	35
742	1.721	46	1.719	35	1.702	62	—		1.544	31
481	1.722	47	—		—		—		1.545	33
Average		47		37		64		67		32

[1], [2], [3], [4] and [5] see footnotes to table 6.
* Sample locations in appendix.

and biotite-hypersthene-quartz-plagioclase gneiss. Indices of refraction and compositions deduced from these for plagioclase coexisting with hypersthene, clinopyroxene, hornblende, or biotite, and in some cases, all of these, are presented in tables 6 and 7. Plagioclase compositions range from An_{16} to An_{77} in amphibolites as contrasted with the limited range of An_{24} to An_{39} in quartz-plagioclase gneiss. Iron-magnesium ratios, $100\ (Fe^{2+}+Fe^{3+}+Mn)\ /\ (Mg+Fe^{2+}+Fe^{3+}+Mn)$, show approximately the same range of compositions for each mafic mineral, hypersthene, clinopyroxene, hornblende, and biotite, in the amphibolite-pyribolite group as compared with the biotite-hypersthene-quartz-plagioclase gneiss. These data, tabulated in tables 6 and 7 and plotted in figures 10 and 11, show the following important relations: 1) As is well-known, and shown here, orthopyroxenes are enriched in iron with respect to coexisting clinopyroxenes. Although the optical curves for clinopyroxene (using $n\gamma$) can only be considered an estimate, whereas those for hypersthene should be reliable, the results shown here (tables 6 and 7 and fig. 10) are internally consistent and in general agreement with the distribution found by Kretz (1963). 2) Where hornblende, and/or biotite coexist with hypersthene and/or clinopyroxene, both hornblende and biotite are selectively enriched in iron. 3) Where hornblende and biotite coexist, the latter tends to be slightly enriched in iron. However, allowing for variability in the existing optical curves for composition of both minerals, iron may prove to be about equally distributed in both. 4) For coexisting biotite-plagioclase pairs Fe and Na (or annite and albite) vary sympathetically (fig. 11-a) in all rocks believed to have an igneous parentage. The same trend is suggested for hornblende-plagioclase pairs (fig. 11-b) and the greater spread of the data perhaps reflects a somewhat greater thermal stability of biotite with respect to hornblende under the metamorphic conditions that prevailed in this area.

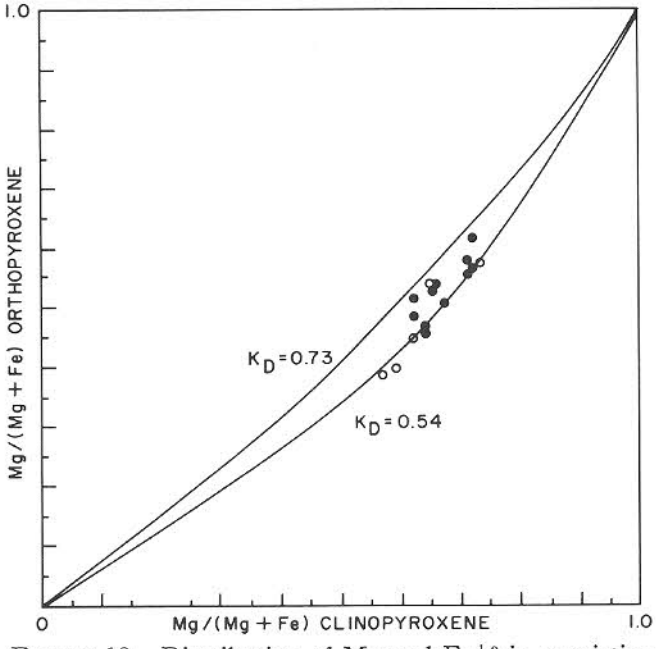

FIGURE 10. Distribution of Mg and Fe^{+2} in coexisting orthopyroxene and calcic clinopyroxene from amphibolite and pyribolite — ● ; and for biotite-hypersthene-quartz-plagioclase gneiss — ○. Curves, $K_D = 0.73$ and 0.54 correspond to igneous and metamorphic distribution coefficients, respectively, suggested by Kretz (1963) for ideal solution relations.

5) The Fe/(Fe + Mg) ratios of orthopyroxene and clinopyroxene show no particular relationship to the albite-anorthite content of the coexisting plagioclases.

In both the amphibolites and hypersthene-quartz-plagioclase gneiss, clinopyroxenes richest in iron contain exsolutions of clinopyroxene parallel to (*100*) of the host and to two additional directions making angles of 116° and 6° with (*100*). Coexisting hypersthene host grains show diopside exsolution lamellae parallel to (*100*) of the host (Hess, 1960). A more detailed discussion of these exsolution phenomena given under the section on pyroxene granulite is equally pertinent to the amphibolite and hypersthene-quartz-plagioclase gneiss.

In Belt 4, about 700 feet due east of the a in Berry Road, amphibolite and pyribolite are interlayered on a millimeter to 25 mm. scale in a greenish to black rock. The modes of each layer and the calculated chemical composition from modes 437A and 437P are presented in table 4. Although the modes and grain sizes of individual layers are strikingly different, the calculated chemical compositions are remarkably similar. With the exception of small but perhaps significant differences in the alumina, ferric iron, and water contents, the compositions are close enough to approach what might normally be accepted as duplicate analyses of the same rock. Either the amphibolite is being converted to pyribolite with water moving out in channels parallel to the layering, or else the two layers represent intercalated volcanics with slightly different bulk compositions. If the latter were true it is difficult to account

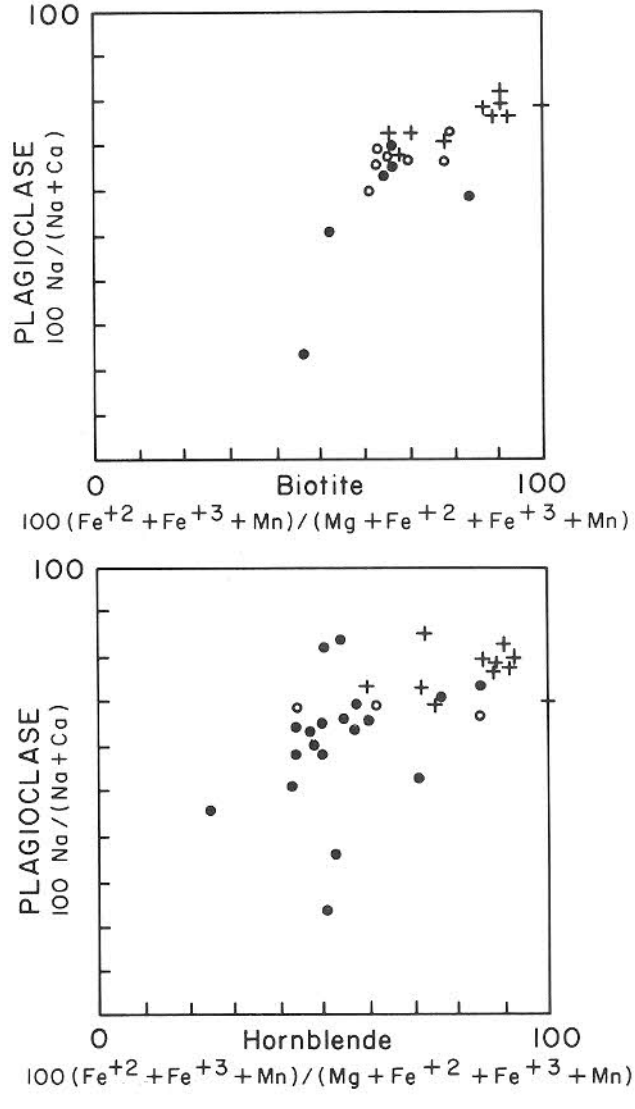

FIGURE 11.

A. Sympathetic variation of Na in plagioclase with Fe in biotite (albite with annite) in gneisses of probably igneous parentage. ● — amphibolite and pyribolite; ○ — biotite-hypersthene-quartz-plagioclase gneiss; + — hornblende (ferrohastingsite) granite gneiss.

B. Similar plot showing variation of Na in plagioclase with Fe in hornblende for the same rock units. Code as in A.

for the grain size of each unit varying by a factor of two. An inspection of the modes suggests that the hornblende, a ferrohastingsite, is breaking down in the amphibolite layers to yield hypersthene + clinopyroxene + additional plagioclase, resulting in a 10 percent decrease in color index of the pyribolite. This is similar to the prograde reaction suggested by Binns (1965) for amphibolite-granulite terrane in New South Wales which marks the orthopyroxene isograd bounding the amphibolite with the granulite facies. Binns notes that

TABLE 8. Electron microprobe analysis of hornblende (ferrohastingsite) from amphibolite, sample 345*, Monroe quadrangle, New York.

Analysis				Ionic ratios			
	A	B[2]		23 O from A		24[O, (OH)] from B	
SiO	40.1	40.1	Si	6.219	8.000	6.054	8.000
TiO_2	2.7	2.7	Al	1.781		1.887	
Al_2O_3	10.6	10.6	Ti^{4+}	.000		.059	
FeO[1]	17.6	11.7[2]	Ti^{4+}	.315	5.066	.248	4.685
Fe_2O_3[2]		6.5[2]	Al	.157		.000	
MnO	0.24	0.24	Fe^{2+}	2.283		1.449	
MgO	10.0	10.0	Fe^{3+}			.738	
CaO	12.0	12.0	Mg	2.311		2.250	
Na_2O	1.7	1.7	Mn	.032	2.001	.031	2.000
K_2O	1.4	1.4	Fe^{2+}	.000		.028	
H_2O[3]	——	2.5[3]	Ca	1.969		1.941	
Total	96.34	"99.44"	Na	.511	0.789	.497	0.767
			K	.278		.270	
Brian Mason, analyst			H			2.517	2.517

[1] Total Fe calculated as FeO.

[2] Analysis A after total Fe is recalculated as 1/3 Fe_2O_3, 2/3 FeO.

[3] H_2O assumed at 2.5%, an average value reported in hornblende analyses; result is essentially H_2O by difference.

* Sample locations in appendix.

the tschermakitic molecule of hornblende breaks down and reacts with plagioclase to yield orthopyroxene + clinopyroxene + a more calcic plagioclase according to the reaction:

$$Ca_2(Mg,Fe)_4Al(AlSi_7O_{22})(OH)_2 \rightarrow CaAl_2Si_2O_8 + 3(Mg,Fe)SiO_3 + Ca(Mg,Fe)Si_2O_6 + H_2O$$

At the same time, the nontschermakitic part of the original hornblende would recrystallize as a more edenitic hornblende depleted in octahedral aluminum and enriched in titanium and ferric iron. A probe analysis made by Brian Mason of a hornblende from a pyroxene-bearing amphibolite (345, table 8) shows the amphibole to be enriched in edenitic alkalies, low in to devoid of octahedral aluminum, and enriched in titanium. Whether the probe analysis is calculated on a basis of 23 oxygens (ignoring water and ferric iron) or by assuming that one-third of the total iron is actually ferric (a much more reasonable assumption based on numerous analyses in the literature; e.g., Deer, Howie, and Zussman, 1963; Leake, 1968) and taking the difference to represent H_2O, the results are not very different and tend to support Binns' suggestions. Binns also noted that the reaction may be more complex and that soda from the original hornblende may also participate. In the example shown (sample 437, table 4), the optical data do not show the expected increase in anorthite content of the plagioclas of the pyribolite (An_{32}) over that in the amphibolite (An_{35}), but a slight decrease. This may indicate that the original plagioclase of the amphibolite was more sodic than it is now. Note also that the 1.7 percent of modal orthoclase in the pyribolite layer has come from potassium held in hornblende. Evidence that something approaching Binns' postulated reaction may occur is beautifully shown in pyribolite 155 (optical data in table 6) which crops out in Belt 11 about 200 feet west of the Orange Turnpike and 1,200 feet northwest of elevation 927 (directly across the road from the single building on the map, which is an old one-room red brick schoolhouse). Here wisps and remnants of fine-grained black amphibolite are sporadically distributed in medium- to coarse-grained dark green pyribolite so massive that it is difficult to obtain a foliation reading. Up to 5 percent of quartz occurs in some parts of the outcrop suggesting a gradation to hypersthene-quartz-plagioclase gneiss into which this unit does indeed grade to the west and the south. In thin section, many of the hornblende grains of the amphibolite remnant in the pyribolite show beautiful prograde fine-grained reaction rims of hypersthene with some clinopyroxene (fig. 12). Hypersthene everywhere mantles hornblende, and clinopyroxene in some places mantles hypersthene, suggesting that the calcium and magnesium ions tend to move further from the reaction site than do the iron ions which become enriched in hypersthene relative to clinopyroxene. Inclusions of hornblende in both pyroxenes also can be observed in this section but the rims are more abundant. Concomitant with this conversion of fine-grained amphibolite to coarser grained pyribolite is the usual marked decrease in color index resulting from the significant amount of the original plagioclase of the amphibolite entering the newly formed plagioclase in the reaction described

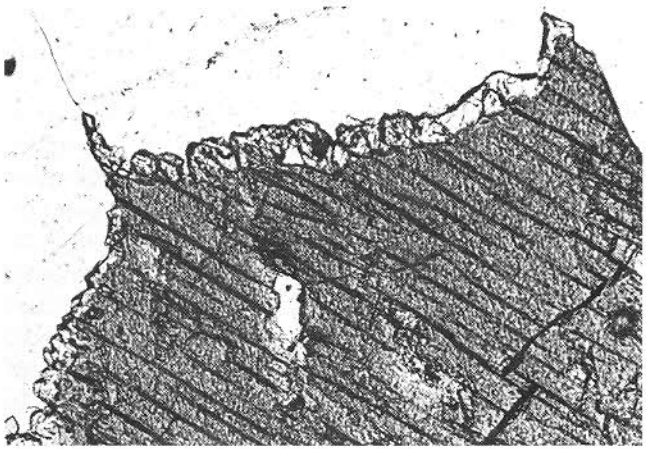

FIGURE 12. Prograde reaction in amphibolite showing hypersthene and minor clinopyroxene (light gray granules) growing at the expense of and rimming brown hornblende (dark gray-black). Breakdown of tschermakitic hornblende molecule in quartz-free amphibolites yields hypersthene + clinopyroxene + plagioclase. Sample 155. Plane polarized light. Length of photograph = 0.6 mm.

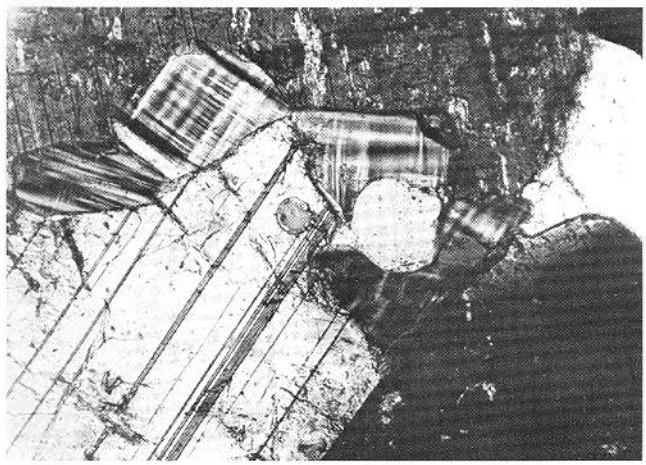

FIGURE 13. Polysynthetically twinned anorthite (An_{93}) in contact with smaller, twinned microcline and quartz grains (clear) in calc-silicate gneiss. Sample 287. Crossed nicols. Length of photograph is 1.3 mm.

above, essentially that suggested by Binns. An examination of the modes of amphibolite and pyribolite and of the chemical compositions calculated from the modes suggests that amphibolite originated as volcanic rock of basaltic composition (table 4). The relatively high soda content of the amphibolite compared with the average amphibolite suggests suboceanic eruption accompanied by alteration associated with sea water. The composition of the average spilite (Turner and Verhoogen, 1960) agrees more favorably with that of the amphibolites than does that of the average basalt. As has been implied earlier, the pyribolite represents a more highly metamorphosed, or dried out, amphibolite featured by the breakdown of hornblende to pyroxenes and additional plagioclase. Although the isochemical purist would argue for a difference in bulk composition of amphibolite and pyribolite, the very similar compositions of sample 437A and P cited in table 4 speak against this. This implies that these intimately interlayered rocks are of transitional metamorphic grade. Much has been written about the origin of the enigmatic biotite-hypersthene-quartz-plagioclase gneiss. Buddington (1939) suggested that similar rocks in the Adirondacks may be a facies of amphibolite modified by thermal solutions given off by granitic magma, and also noted that the quartz-plagioclase gneiss appears to have formed from material that moved locally as magma. Hotz (1953) suggested that it formed from material that was emplaced as a magma and that may have been derived from the partial fusion of sediments. Because of an inferred very high soda/potash ratio of several of these rocks, Dodd (1965) suggested that they represent diagenetically altered volcanics, possibly quartz keratophyres. The compositions calculated from the modes of rocks of the Monroe crystalline block indicate a somewhat higher antiperthite, biotite, and hence total potash content than that found by Dodd to the east. More chemical analyses are needed to better establish the alkali ratios of this unit over a large area, and point-counting antiperthitic K-feldspar exsolutions or inclusions as both Dodd and the present writers have had to do is a poor substitute for the real thing. Based upon the results shown in table 5, the authors believe that the compositions calculated from the modes of this rock agree reasonably well with that of the average effusive dacite (Nockolds, 1954) and not quite so well with that of the average graywacke of Pettijohn (1957) which has too low an alumina content. The intimate association of this rock with amphibolite suggests a volcanic origin for both rocks. They may well have originated as interlayered basaltic and porphyritic dacitic volcanics now metamorphosed at high grade to amphibolite and biotite-hypersthene-quartz-plagioclase gneiss. It is suggested that the metamorphic grade was high enough to melt the quartz-rich dacites but not the basalts, resulting in the field relations and relatively coarse grain size of the quartz-plagioclase gneiss as contrasted with more refractory amphibolite and calc-silicate gneiss.

The distribution coefficients, $K_{(Mg-Fe)}$, for coexisting orthopyroxene and calcic clinopyroxene (fig. 10, based on tables 6 and 7), are higher for amphibolites (mean = 0.64) than for hypersthene quartz plagioclase gneiss (mean = 0.54). This reinforces the suggestion that these two rock types originated from isochemical metamorphism of basalt and dacite, respectively, retaining their original Mg-Fe ratios. Although the temperature-dependence (at P) of these distribution coefficients has been questioned by Binns (1962) and others, it should be noted that basalt would crystallize at a higher temperature than dacite and should have had an initial bulk composition higher in Mg. It may be that the distribution coefficients for Mg-Fe in coexisting pyroxenes of amphibolite and quartz-plagioclase gneiss reflect bulk compositional differences of the parent volcanics rather than temperature of metamorphic equilibration. In this regard, Binns (1962) suggests that " the stability fields of coexisting pyroxenes appear to depend on the iron: magnesium ratios of the parent rock; that is, under given temperature and pressure conditions only those coexisting pyroxene pairs within a relatively limited iron-magnesium compositional field are stable." If the K values were largely temperature-dependent as indicated by Kretz (1963), it would be difficult to explain why the amphibolites should crystallize at higher temperatures than the intimately associated, often interlayered, hypersthene-quartz-plagioclase gneiss. Inasmuch as the data plotted in figure 10 do show considerable overlap, the differences in mean K values between these two map units may not be too significant.

Calc-silicate gneiss

Calc-silicate gneiss occupies all of Belt 12 and a small part of Belt 11. It is always in contact with either amphibolite-pyribolite, or hypersthene-quartz-plagioclase gneiss, all three units making up one stratigraphic horizon. The contact of the eastern edge of Belt 12 with the western edge of Belt 13 hornblende granite gneiss is exposed at several localities east of the Orange Turnpike and has been found to be completely gradational. In many localities along this contact the calc-silicate rock is a biotite-quartz-plagioclase-microcline gneiss which can be mistaken for a border facies of the granite gneiss, and distinction between the two may require microscopic examination. In many places, small grains of red-brown sphene or yellow-green epidote can be observed with a hand lens, and serve to identify this unit. In their absence, microscopic examination for the presence of intermediate to highly calcic plagioclase and magnesian biotite in addition to the ubiquitous sphene serve to distinguish the biotitic phase (samples 39 and 166, table 9) from granite gneiss which everywhere carries high-iron biotite.

The most typical lithology of this map unit is a fine- to medium-grained, white to light gray inconspicuously foliated rock speckled with black diopside-hedenbergite and yellow-green epidote and small, round, red grains of sphene (table 9). Next in abundance is the fine-grained, gray or pink and black biotitic and hornblendic phase described above. Green and white epidotic quartzite is moderately abundant in the Monroe quadrangle and becomes very abundant to the south in the Sloatsburg quadrangle. The map unit is highly migmatitic throughout, in some places being composed of a 50:50 mixture of layers of fine-grained greenish white calc-silicate rock interlayered with coarse pods of alaskite or pegmatite composed entirely of potassium feldspar and quartz. Narrow lenses of hypersthene-bearing amphibolite occur sporadically within the principal calc-silicate Belt 12.

In thin section the calc-silicate unit is consistently fine-grained, most specimens showing average grain diameters of about 0.5 mm. (table 9). Compositional layering on a fine scale, strong deformation and elongation of quartz grains, a rude parallelism of the c-axes of clinopyroxenes, and a strong parallelism of the biotite foliae with the b-fabric impart a pronounced gneissic texture to most specimens. All minerals, with the exception of microcline, show some degree of elongation parallel to the b-fabric axis. Microcline is sugary in habit, and in contrast to its occurrence in granitic rocks, is not perthitic in this map unit. Calcic or intermediate plagioclase is characteristic of this unit and anorthite percentages commonly range between 50 and 95. Bytownite is common (plate 2), and one sample (287, fig. 13, and table 9) contains anorthite with optical properties of = 1.574, β = 1.581, = 1.586 indicating a composition of An_{93} on the determinative curves of Chayes (1952). Scapolite commonly contains about 60 percent of the meionite molecule and a representative example (324, table 9) has optical properties of ω = 1.579 and ϵ = 1.550. Its composition may be determined from the approximately linear variation of $(\epsilon + \omega)/2$, both values increasing with the calcium or meionite content (Deer, Howie, and Zussman, 1963). Clinopyroxene, very characteristic of these rocks, is blue-green in transmitted light, weakly to moderately pleochroic, and shows gamma indices of refraction ranging from 1.712–1.733, indicating iron ratios of approximately 28–61 percent, where % Fe =

TABLE 9. Composition of calc-silicate gneiss(cs).

A. Modes

	Belt 12										
Sample No.†	287	58	332A	324	204	328	327	348	351	39	166
Quartz	27.9	59.7	46.5	59.0	41.7	45.2	61.0	20.2	75.7	38.6	43.8
Microcline	40.1	—	31.7	1.1	18.2	42.0	—	64.0	—	15.4	12.4
Plagioclase[1]	6.2	13.8	5.5	—	—	4.7	28.2	—	—	25.3	36.4
Scapolite[2]	—	1.2	3.6	22.9	8.8	—	+	—	—	—	—
Clinopyroxene[3]	18.7	3.5	4.6	10.9	9.7	1.2	—	—	12.2	2.1	—
Sphene	3.1	0.5	0.9	2.6	3.0	+	0.4	4.6	+	+	0.1
Epidote	0.2	13.4	6.0	2.3	11.9	—	6.8	—	+	+	—
Clinozoisite	—	—	—	—	+	—	—	—	—	—	—
Actinolite	—	—	+	—	+	4.3	1.4	11.2	—	—	—
Hornblende	+	+	—	—	—	—	—	+	—	5.2	—
Biotite[4]	—	—	—	—	—	1.2	—	—	—	10.2	6.0
Chlorite	—	—	0.1	—	+	0.9	0.4	—	2.0	+	+
Andradite	—	—	—	0.8	2.0[5]	—	—	—	10.1	—	—
Prehnite	—	1.5	—	—	—	—	—	—	—	—	—
Sericite	+	6.2	+	—	4.7	+	0.6	—	—	—	+
Magnetite	1.9	—	0.9	0.2	—	0.5	1.0	—	—	—	0.2
Ilmenite	1.9	+	—	0.2	—	—	—	+	—	3.2	0.8
Hematite	—	—	—	—	+	—	—	—	+	—	—
Apatite	+	0.2	0.2	+	+	+	0.2	+	—	+	0.2
Zircon	+	+	+	+	+	+	+	+	+	+	0.1
† Sample locations in appendix.											
[1] Mol. % An	93	72	62	—	—	46	71	—	—	53	37
[2] Mol. % Me				62	67						
[3] $\%Fe^{2+}+Fe^{3+}+Mn$*	40	43		61					60	28	
[4] $\%Fe^{2+}+Fe^{3+}+Mn$**										46	56
[5] Mol. % And. (a_o=11.99A)					75						
Color Index	25	20	12	17	27	8	10	16	12	21	7
Avg. grain (mm)	0.6	1.0	0.5	0.8	0.8	0.5	0.5	0.4	0.6	0.4	0.5

* From curves for diopside-hedenbergite (Deer, Howie, and Zussman, 1963).
** From curves for tremolite-ferroactinolite (Deer, Howie, and Zussman, 1963).

$100(Fe^{2+} + Fe^{3+} + Mn)/(Fe^{2+} + Fe^{3+} + Mn + Mg)$. It is classed as salite or ferrosalite after Poldervaart and Hess (1951). Red-brown sphene is an essential constituent of almost all specimens and its presence in abundance serves to identify this map unit. Epidote shows a strong greenish yellow color in transmitted light, a large optically negative axial angle, and strong birefringence indicating it to be relatively enriched in ferric iron. Its composition may vary, however, as indicated by zoning in some specimens. Optically positive clinozoisite with anomalous blue interference colors is uncommon. Pale blue-green actinolite and olive-green hornblende occur in those specimens rich in microcline and/or biotite. It is commonly a magnesian actinolite, a typical example (328, table 9) showing = 1.620, β = 1.636, = 1.645 equivalent to approximately Fe_{23}. Deep brownish red andradite garnet occurs in a few specimens, generally those rich in quartz and scapolite. X-ray powder diffraction data on the garnet indicate a unit cell dimension of a_o = 11.99A and optical studies, an index of refraction of 1.855, indicating a composition of andradite–75, grossularite–25. Both magnetite and ilmenite are common accessory minerals.

Modes of representative examples of calc-silicate gneiss are presented in table 9 and mineral assemblages are shown on an ACF diagram (fig. 14). It should be noted that the calc-silicate rocks originated as cal-

B. Chemical composition calculated from modes and optical properties of constituent minerals.

	287	324	204	Ofs[6]
SiO_2	63.88	76.72	68.75	65.0
TiO_2	3.18	1.71	1.51	—
Al_2O_3	8.78	6.76	10.68	9.6
Fe_2O_3	2.38	0.59	2.39	1.6
FeO	6.98	2.29	2.33	1.1
MgO	1.23	1.24	0.67	0.4
CaO	7.48	8.30	9.29	10.1
Na_2O	0.05	1.27	0.77	2.1
K_2O	6.03	0.17	2.75	1.4
H_2O	0.01	0.05	0.50	1.0
Cl	—	0.36	0.13	—
CO_2	—	0.61	0.26	6.9
P_2O_5	—	—	—	0.1
S	—	—	—	0.2
Total	100.00	100.07	100.03	99.5

[6] Subgraywacke, Frio "sandstone," Oligocene of Texas, average of ten chemical analyses, Nanz (1954).

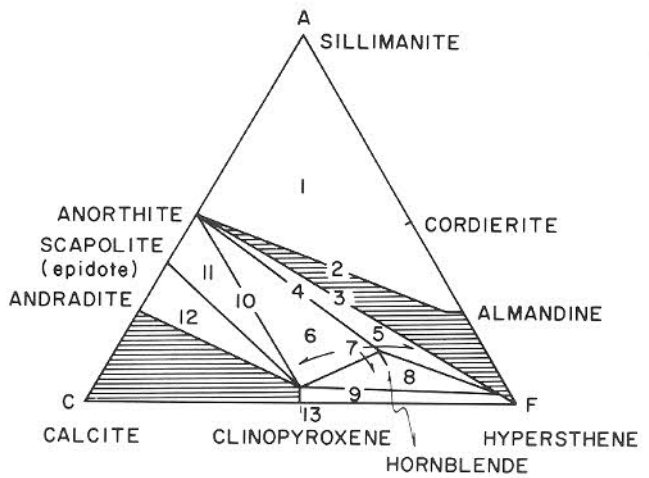

FIGURE 14. ACF diagram for hornblende granulite facies gneisses of the Monroe quadrangle. SiO_2 and K_2O are present in excess. Shaded fields are not represented in the quadrangle.

careous subgraywackes, marls or limy muds, subarkoses, and calcareous quartzites. None of them were rich enough in calcite to have been limestones or dolomites. As a matter of fact, the alternating sequence of limy mudstone or shale and calcareous subarkose that characterize the Ramseyburg member of the Martinsburg Formation of the Monroe quadrangle (table 20) should, if subjected to conditions of high grade regional metamorphism, be converted to calc-silicate rocks similar to those just described. Chemical compositions calculated from the modal analyses and optical properties of constituent minerals are also presented in table 9, with actual chemical analyses of rock of similar chemistry. No marble was found in the Monroe quadrangle although small exposures of marble and silicated marble were found by Hotz (1953) to the south, by Dodd (1965), and Offield (1967) to the west. Wollastonite has never been reported in any of the rocks of the Hudson Highlands suggesting that pressures were too high to permit the escape of substantial amounts of CO_2. Although the chemistry of the scapolites in these rocks has not been studied in detail, it is very likely that this phase does carry some CO_2. Delineation of mineral assemblages on ACF diagrams (fig. 14) as representing a given metamorphic facies is complicated by retrograde metamorphic changes to which the calc-silicate gneiss was more susceptible than the other rocks because of the brittle nature of this quartz-rich rock and the instability of highly calcic plagioclase. Minerals such as actinolite, some or all of the epidote, and sericite (paragonite), and clinozoisite are clearly retrograde products of salite and highly calcic plagioclase. The origin of the andradite, scapolite, and ferrosalite in these rocks is uncertain. Buddington (1939), Hotz (1953), Sims (1953), and others would consider these to be clear-cut examples of metasomatic introduction of ferric iron, chlorine, and other constituents into limestones and they may be correct. The three occurrences of andradite-bearing rocks in this unit all occur close to and on strike with a northeast-trending fault at the west edge of Belt 12 and liquids of granitic or alaskitic composition were present in abundance. On the other hand, it is equally likely that andradite, scapolite, and ferrosalite in the rocks of this unit originated during prograde metamorphism of an isochemical nature. The analysis of the subgraywacke shown in table 9 indicates that ferric iron, sodium, and other requisite constituents are present in amounts comparable to those shown in some of the andradite-bearing calc-silicate rocks of the Monroe quadrangle.

Biotite-mesoperthite gneiss
Albite-oligoclase leucogranodiorite
Biotite-hypersthene-microperthite-quartz-plagioclase gneiss (charnockite)

Almost of all Belt 3 in the Monroe block and Belts 15 and 21 in the Ramapo block consist of rocks rich in biotite and mesoperthitic feldspar in which albite or oligoclase is the host. Because Belt 3 is of a lower

metamorphic grade than Belts 15 and 21, they will be discussed separately and then related.

Belt 3 — The typical biotite-mesoperthite gneiss is a fine- to medium-grained (0.5–2.0 mm.) flesh pink to light gray rock mottled with abundant biotite (table 10). Many specimens show a pepper and salt appearance and darker gray varieties rich in biotite can easily be mistaken for amphibolite at first glance. This rock, along with the omnipresent amphibolite, is intruded by pink, medium to coarse-grained (1–10 mm.) massive leucogranodiorite (samples 84 and 441, table 10), gray and pink biotite granite, and granite pegmatite, all of which carry very sodic plagioclase in the albite-oligoclase range. A very small amount of hornblende occurs in some of the massive intrusive granitic rocks and may be inherited from amphibolite. Concordant lenses and pods of amphibolite are in some areas abundantly interlayered with biotite-mesoperthite gneiss, and both rocks can be found boudinaged, broken, and rotated in the more massive granitic rocks. The unit is bounded on the east and west by amphibolite or amphibolite-granodiorite and represents a tightly folded, anticlinal core of remobilized and partly remelted rock.

Belts 15 and 21 — The rocks of this area (immediately east of the New York Thruway) carry much less biotite than those in Belt 3. Their appearance has also been modified by cataclastic deformation and hydrothermal alteration associated with Triassic, and perhaps older faults which are abundant in this part of the map area. Discontinuous amphibolites are again very much in evidence and some of these have been recrystallized to medium coarse-grained rocks which resemble diorite. Biotite-mesoperthitic gneiss occurs in the southern third of Belt 15, leucogranitic rocks dominate the central third, and biotite-microperthite-albite-quartz gneiss the northern third, near Arden House.

In thin section, the biotite mesoperthite gneiss shows a granular, anhedral, mosaic texture with only biotite showing euhedral development and consistent orientation. Many specimens are syenitic (table 10) in that they carry less than 10 percent quartz. It is perhaps the most interesting of all of the rocks under the micro-

TABLE 10. Composition of biotite-mesoperthite gneiss and albite-oligoclase leucogranodiorite (bmp), biotite gneiss (bg), and biotite-hypersthene-microperthite-quartz-plagioclase gneiss (charnockite) (hk).

A. Modes

	biotite-mesoperthite gneiss (bmp)						albite-oligoclase leuco-granodiorite (bmp)		(bg)	(bmp)	charnockite (hk)		
	Belt 3								Belt 15				Belt 21
Sample No.*	83	438	640	680	265	409	84	441	472	477A	477NEA	673	757
Quartz	8.2	14.2	8.4	7.0	8.2	37.4	20.7	25.4	19.0	3.5	9.4	29.8	28.8
Mesoperthite	62.0	50.0	52.0	40.3	71.0	53.2	+	—	—	24.0	—	31.4	—
Microcline	—	—	4.0	+	—	—	19.9	20.1	31.8[1]	12.5	42.1[1]	7.1	22.2
Plagioclase [2]	5.0	7.8	12.8	26.9	5.1	5.4	58.3	50.3	34.2	41.0	30.1	26.5	35.6
Biotite	23.6	26.8	21.0	25.8	15.7	1.8	1.0	—	11.0	17.5	10.1	1.2	7.2
Hypersthene	—	—	—	—	—	—	—	—	—	—	6.9	1.7	4.2
Hornblende	—	—	0.4	—	—	1.8	—	—	—	—	—	—	—
Magnetite	+	0.6	0.2	+	+	0.2	+	3.0	0.6	1.0	1.3	0.6	1.0
Apatite	1.2	0.4	1.2	+	+	+	+	+	—	—	0.1	0.4	0.4
Zircon	+	+	+	+	+	0.2	0.1	+	+	—	—	—	—
Monazite	+	0.2	—	—	—	—	—	—	—	—	—	—	—
Calcite	—	—	—	—	—	—	—	—	0.2	0.2	—	—	—
Chlorite, talc, serp.	—	—	—	—	—	—	—	1.2	3.2	0.3	+	1.3	+
[1] Microcline microperthite.													
[2] Mol. % An	8	10	11	15	10	7	9	10	4	14	22	14	28
Color Index	24	28	24	26	16	4	1	4	15	19	17	5	14
Avg. grain (mm)	2.0	0.7	1.0	1.0	1.2	0.5	4.0	4.0	1.0	1.5	0.9	2.1	1.1

* Sample locations in appendix.

B. Chemical composition calculated from the modes and optical properties of constituent minerals.

	83	Trachyte [3]	680	265	Analcime-rock [4]	477A	477NEA
SiO_2	59.33	61.07	59.15	62.76	66.56	59.0	61.0
TiO_2	0.67	0.69	0.69	0.46	0.11	0.5	0.3
Al_2O_3	18.21	19.47	19.37	18.42	15.77	19.7	16.6
Fe_2O_3	0.28	2.50	0.29	0.19	0.91	1.5	2.0
FeO	5.33	0.71	5.54	3.66	0.28	4.5	5.5
MgO	1.90	0.46	1.97	1.30	0.28	1.5	2.3
CaO	1.56	1.45	1.41	0.85	1.36	1.7	1.6
Na_2O	3.96	4.84	4.89	4.41	4.87	5.6	2.6
K_2O	7.22	7.07	5.69	7.30	4.26	5.3	7.7
H_2O	0.96	1.38	1.00	0.65	4.45	0.7	0.4
P_2O_5	0.59	0.04	—	—	—	—	+
F	0.04	—	—	—	0.60	—	—
Total	100.00	99.68	100.02	100.00	100.21	100.00	100.00

[3] Trachyte or ponzite, Sardinia (Johannsen, 1939).

[4] Analcime-rock or tuffaceous sandstone, Tuva, U.S.S.R. (Bur'yanova, 1954; 1960, cited in Coombs, 1965).

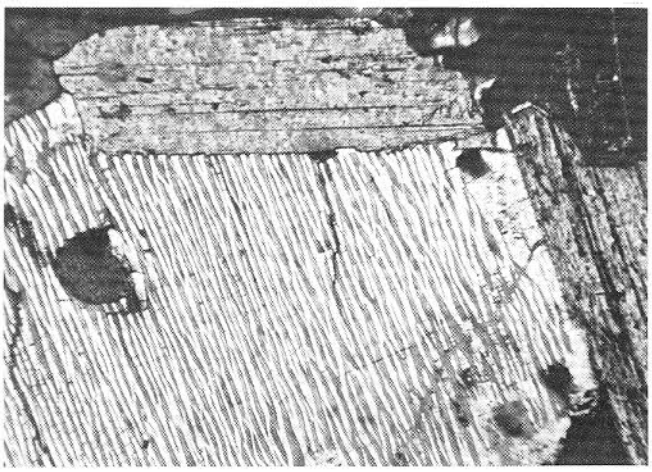

FIGURE 15. Biotite and mesoperthite in biotite-mesoperthite gneiss. Exsolution lamellae are K-feldspar (black strips) in albite-oligoclase (white strips) in almost equal amounts. Lamellae average 10 microns in width. Sample 265. Crossed nicols. Biotite grain is 0.7 mm. in length.

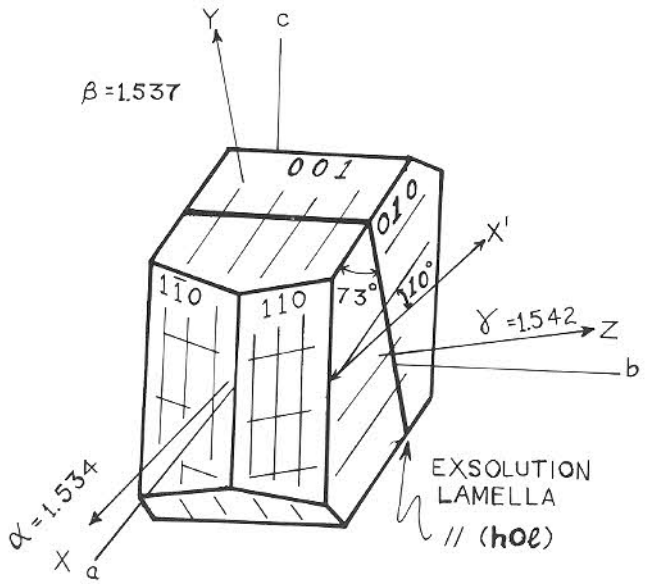

FIGURE 16. Optic orientation diagram of mesoperthite showing albite-oligoclase (An_{13}) host with exsolution lamellae of K-feldspar parallel to (*h0l*).

scope. In plane polarized light, the biotites are commonly pleochroic in orange or pale red-brown, a function of their titanium content. Many of the biotites contain minute almond-shaped zircons and coarser anhedral monazite, both of which produce intense pleochroic haloes. The biotites are set in a sugary mosaic of striped mesoperthite which under crossed nicols suggests the name, "zebra-rock" (fig. 15). The mesoperthite is made up of sharply bounded, wormy, and tapering lamellae of K-feldspar (40 percent) alternating with albite-oligoclase, An_{13}, (60 percent). Sodic plagioclase is invariably the host, and the lamellae range in width from 1 to 10 microns, averaging less than 5 microns in many specimens. A more detailed microscopic study of the mesoperthite shows that the lamellae lie with the (*h0l*) of K-feldspar parallel to the (*h0l*) of the host albite-oligoclase (fig. 16). When viewed on (*010*), the exsolution plane (*h0l*) makes an angle of 73° with the (*001*) cleavage traces, (*001*) $X' = 10$–$12°$ $\alpha = 1.534$–5, and $2V \cong 85°$ (+) for a host with An_{13-15}. The lamellae are length-slow

in all orientations, and when viewed on (*010*), Y′ albite-oligoclase lamellae = 7–8°, and Y′ K-feldspar lamellae = 14–16°.

In appearance, width of lamellae, and bulk feldspar composition, $Ab_{52}An_8Or_{40}$ (fig. 9), mesoperthite appears to be strikingly similar to one from the syenite of the Kiglapait layered intrusion in Labrador (Morse, 1968). Morse, in experiments at the Geophysical Laboratory, determined that the solvus crest and beginning of melting of this mesoperthite occurs at 925° C. at P_{H_2O} = 500 bars. He notes that if the magma had been saturated with water at the pressure of formation, perhaps 5 kilobars, a two-feldspar rock rather than a hypersolvus rock would have resulted. As many of the mesoperthitic rocks in the Monroe quadrangle contain about 8 or more percent quartz, the temperature of crystallization would have been considerably lower than 925° C., but with an An_{18} component in the plagioclase, the temperature of crystallization of this hypersolvus rock must have been on the order of 800° C. Because these rocks were wet, carrying 25 percent biotite, as compared with dry fayalite syenite of Kiglapait, the total pressure and depth of crystallization must have been low.

Biotites in Belt 3 have Fe/(Fe + Mg) ratios ranging from 37–50 as determined from gamma indices of refraction. Because of their titanium content, which would materially raise the index of refraction, the cited Fe ratios are probably too high. In Belts 15 and 21, biotites with Fe/(Fe + Mg) = 60 — 70 are associated with hypersthene and K-feldspar which have formed from the typical high temperature granulite facies reaction:

$$K(Fe,Mg)_3(Al,Si_3O_{10})(OH)_2 + 3SiO_2 \rightarrow KAlSi_3O_8 + 3(Mg,Fe)SiO_3 + H_2O$$

biotite + quartz → K-feldspar + hypersthene + water. An excellent outcrop showing these relations occurs on the south side of Seven Lakes Drive, in the first roadcut east of the bridge over the New York State Thruway. It is just south of the letter N in New York State Thruway. Here biotite-mesoperthite gneiss with magnesian biotite (γ = 1.634, 100Fe/(Fe+Mg) = 44), sample 477A, table 10, does not carry any hypersthene. About 50 feet to the east in the same exposure, sample 477NEA, table 10, carries 7 percent of ferrohypersthene (γ = 1.727, 100Fe/(Fe+Mg) = 51) associated with ferroan biotite (γ = 1.650, 100Fe/(Fe +Mg) = 60). In thin section, bands of biotite-oligoclase-quartz (with no K-feldspar) alternate with layers of hypersthene - microperthite - quartz - plagioclase and minor biotite. Hypersthene is in contact with microperthite and the reactants, biotite and quartz, and can be seen growing around and replacing biotite (fig. 17). All of the minerals in the rock are fresh and there is no evidence of retrograding to produce the reverse reaction. Clearly, the ferroan biotite has broken down, reacting with quartz to yield hypersthene + K-feldspar, whereas the magnesian biotite on the same outcrop has not reacted. Ferromagnesian minerals rich in iron will decompose at lower temperatures than their magnesian counterparts. Sample 757, from the Echo Mountain waterfalls in the Popolopen quadrangle to the east, on strike with Belt 21, contains biotite (γ = 1.655, Fe_{34}) associated with hypersthene (γ = 1.721, Fe_{40}), values very close to those just cited for sample 477NEA of Belt 15. Plagioclase in 757 has an anorthite content of 28 as compared with 22 for sample 477NEA. Both of these values are higher than the average (An_{10}) for this map unit and an increase in Fe with an increase in the anorthite content of plagioclase is opposite from the expected trend for rocks of igneous parentage. This is clearly shown by the biotite-mesoperthite gneiss of Belt 3 where low An contents in plagioclase are associated with relatively high Mg contents in biotite. This suggests that this unit did not originate from an unaltered igneous rock such as a trachyte. The precursor may have been a bentonitic shale diagenetically enriched in Na and Mg or perhaps a sedimentary analcime-rich rock. This latter

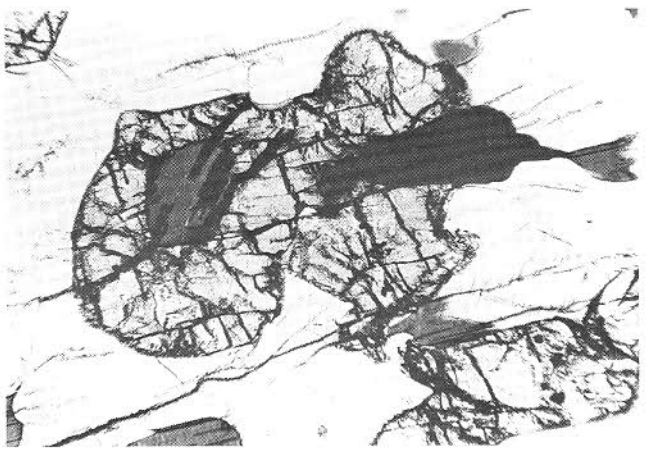

FIGURE 17. Biotite-hypersthene-K-feldspar-quartz-plagioclase gneiss (charnockite). Biotite (dark gray-black) enclosed in hypersthene (large light gray grain with high relief) and in contact with microperthite (white). Biotite has broken down in the presence of quartz to yield the hypersthene + K-feldspar to produce charnockite. Hypersthene grain is 1 mm. in length. Sample 477NEA. Plane polarized light.

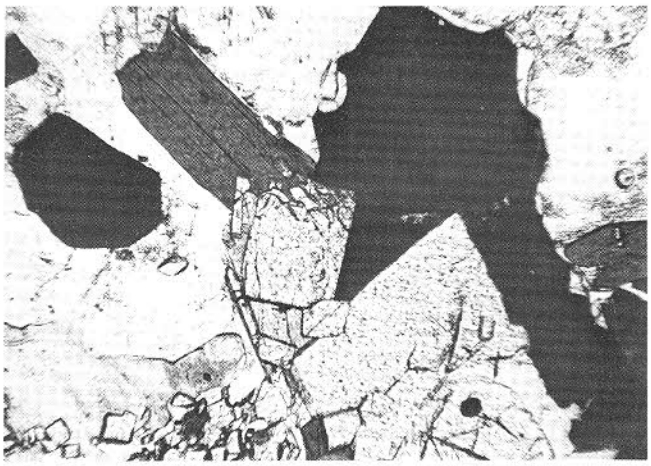

FIGURE 18. End sections of tourmaline (black grain at left center) and sillimanite (diamond-shaped grains) with biotite (gray), magnetite (black grain at right center) in quartz and plagioclase (anhedral, colorless). Thin section is nearly normal to fold axis. Sample 303, cordierite-sillimanite-almandine-biotite-quartz-feldspar gneiss. Plane polarized light. Length of photograph is 1 mm.

paragenesis has been suggested by Coombs (1965) as representing an isochemical parent for soda-rich gneisses and schists.

Here it is worth summarizing that charnockitic gneisses in the Monroe quadrangle have had two important parageneses. Hypersthene in the biotite-mesoperthite gneiss unit has formed from the breakdown of ferroan biotite + quartz to yield this orthopyroxene + K-feldspar, whereas, in the amphibolites, the tschermakitic molecule of hornblende has reacted with plagioclase to yield hypersthene + clinopyroxene + more calcic plagioclase + water.

Sillimanite-cordierite-almandine-biotite-quartz-feldspar gneiss (pelitic paragneiss)

This map unit occupies the tightly-folded anticlinal complex of Belt 7 and is stratigraphically equivalent to the biotite-mesoperthite gneiss. The sillimanite-cordierite-almandine-biotite-quartz-feldspar gneiss is a fine-grained, crenulated, gray and black micaceous to schistose gneiss that is everywhere interleaved with coarse, pink potassic granite pegmatite. It is clearly a venitic migmatite. In several outcrops, black prismatic tourmaline, and relatively coarse needles of white sillimanite can be identified with the unaided eye or with a hand lens. These minerals everywhere lie with their longer c-axes parallel to the fold axes (fig. 18). Garnet and tourmaline commonly occur at contacts of the biotitic gneiss and pegmatitic layers but also occur within the biotite gneiss proper. The garnet occurs in dark red, poikiloblastic grains up to 6 cm in maximum diameter and is commonly wrapped in biotite. The occurrence of this gneiss is restricted to Belt 7 in the Monroe quadrangle although similar rocks have been described by Dodd (1965) from the Popolopen Lake quadrangle to the east, and, on strike with the Belt 7, to the south by Hotz (1953). Although not rusty, it shows mineralogical affinities with the rusty biotite-quartz-feldspar gneiss of Dodd (1965) and is equivalent to the garnetiferous quartz-biotite gneiss of Hotz (1953). The unit is apparently also the equivalent of the biotite-quartz-feldspar gneiss of Sims (1953) in the Dover, New Jersey magnetite district which is on strike with the Sterling-Ringwood magnetite district immediately to the south of the Monroe quadrangle.

Infolded layers of amphibolite, pyroxene granulite, and pockets of associated magnetite and undeformed granite pegmatite are distributed throughout the map unit.

In thin section the sillimanite-cordierite-almandine-biotite-quartz-feldspar gneiss consists of fine-grained (0.3–0.5 mm.), anhedral quartz, intermediate plagioclase, orthoclase or microcline-microperthite, oriented red-brown titanian biotite. Pink, poikiloblastic almandine garnet occurs in either euhedral or anhedral elongated grains in some specimens, (table 11). Compositional layering is apparent in several specimens with some layers being very rich in quartz, others richer in plagioclase + quartz, and still others rich in K-feldspar + quartz + plagioclase, with biotite occurring in all of the layers. Sillimanite, tourmaline, and cordierite tend to favor those rocks richest in quartz and poor in plagioclase, while almandine is more abundant in the specimens richest in K-feldspar, (table 11). Coarse granitic or pegmatitic layers consisting of poorly twinned microcline microperthite and quartz (1–10 mm.) are abundantly interleaved with the finer grained layers. Coarse garnet and biotite occur at the interface between fine and coarse layers and these are of the same Fe/(Fe + Mg) ratio in both layers. Qualitative spectroscopic analysis of the garnets shows them to consist of major amounts of Si, Al, Fe, and Mg, minor amounts of Mn, and very minor or trace amounts of calcium, titanium, and vanadium. Indices of refraction and unit cell dimensions determined from X-ray powder diffraction measurements give values of $n = 1.784 - 1.793$ and $a_o = 11.50 - 11.52$A, respectively, for specimens

TABLE 11. Composition of sillimanite-cordierite-almandine-biotite-quartz-feldspar gneiss (pelitic paragneiss) (sgb).

A. Modes

	Belt 7							Synthetic gneiss	
Sample No.*	125	129	222	225	511	303	WI	Wld[1]				
Quartz	35.1		24.1		7.0		7.7		16.6	35.9	36	28
K-feldspar [2]	25.1		20.7		36.5		41.0		13.2	24.5	9	9
Plagioclase [3]	9.7		19.4		23.2		8.3		34.1	4.6	33	44
Sillimanite	1.8		+		—		—		—	2.2	3	—
Cordierite [7] / Pinite [4]	6.5		—		—		—		—	13.2	12	4
Sericite	+		+		+		+		+	+	—	—
Biotite [5]	8.1		30.9		33.3		38.5		28.3	9.5	3	10
Almandine [6]	—		4.8		—		4.5		7.8	0.3	—	—
Tourmaline	8.3		0.1		—		—		—	7.1	—	—
Magnetite	5.4		+		+		+		+	2.5	4	4
Apatite	+		+		+		+		+	+	—	—
Sphene	+		—		—		—		—	0.1	—	—
Zircon	+		+		+		+		+	0.1	—	—
Epidote	—		—		—		—		+	—	—	—
Mol. % An	52		69		31		44		34	49	19	40
Color Index	22		36		33		43		36	20	7	14
Avg. grain (mm)	0.4		0.5		0.5		0.4		0.5	0.3	—	—
100Fe/(Fe+Mg)	50		52		66		54		75	50	—	—
% Almandine	—		—		—		—		72	63	—	—
100Fe/(Fe+Mg)	—		—		—		—		—	25	—	—

* Sample locations in appendix.

[1] Synthetic paragneisses produced from experimental metamorphism of graywackes (Winkler, 1967).

[2] Orthoclase or microcline microperthite.

[3] Mol. % An / Color Index / Avg. grain (mm)

[4] Sericite+chlorite+miscellaneous alteration products of cordierite.

[5] 100Fe/(Fe+Mg)

[6] % Almandine

[7] 100Fe/(Fe+Mg)

B. Chemical compositions calculated from the modes and the optical properties of constituent minerals.

	129	222	225	511	303	Ogsh [8]	Graywacke [9]
SiO_2	58.60	55.54	52.95	57.03	64.90	56.29	64.7
TiO_2	0.84	0.93	1.05	0.76	0.33	0.64	0.5
Al_2O_3	17.65	19.32	18.85	18.92	16.08	19.22	14.8
Fe_2O_3	0.36	0.39	0.44	0.32	0.17	4.39	1.5
FeO	8.37	7.42	9.89	8.67	3.52		4.0
MgO	3.33	2.64	3.83	3.62	2.53	1.65	2.2
CaO	2.67	1.51	0.72	2.31	0.53	0.09	3.1
Na_2O	0.96	2.13	0.90	2.71	0.69	0.19	3.1
K_2O	6.02	8.89	9.87	4.58	4.76	10.85	1.9
H_2O	1.20	1.33	1.50	1.08	0.89	5.58	3.1
B_2O_3	+	—	—	—	0.81	—	—
ZrO_2	—	—	—	—	0.11	—	—
P_2O_5	—	—	—	—	—	—	0.2
SO_3	—	—	—	—	—	0.72	—
Total	100.00	100.00	100.00	100.00	100.00	99.62	99.1

[8] Potash-rich Glenwood shale, Ordovician of Minnesota (Gruner and Thiel, 1937).

[9] Average of 23 graywackes (Pettijohn, 1957).

in the most magnesian assemblages and correspond to an approximate composition of almandine$_{63}$pyrope$_{35}$-spessartine$_2$ (Winchell, 1958), the calcium content having been established to be low. More iron-rich specimens carry garnet with n = 1.807 and a_o = 11.53A corresponding to approximate compositions of almandine$_{72}$-pyrope$_{23}$-spessartine$_5$. Cordierite, until recently, has gone unnoticed in the pelitic paragneisses of the Hudson Highlands. This mineral is the Achilles' heel of most petrographers because it is commonly misidentified as either plagioclase, when polysynthetically twinned, or as quartz when untwinned. Within the last year, Dodd (personal communication) told the authors that he had definitely identified cordierite in rusty biotite-quartz-feldspar gneiss from near Queensborough Circle in the Popolopen Lake quadrangle. After these discussions and a careful study of the pelitic paragneiss from the Monroe quadrangle, it became apparent that cordierite was indeed present in this unit. The cordierite in these rocks is either untwinned or polysynthetically twinned (fig. 19), and rarely sector-twinned. About half of it is peripherally altered to pinite, a mixture of sericite, yellow-brown chlorite and other unidentified fine-grained alteration products. Yellow pleochroic haloes that are peculiarly characteristic for this mineral are present, but they are much feebler in color than in cordierite-bearing rocks from other areas (Robinson and Jaffe, 1969). Its presence in the Highlands rocks is significant because it verifies other data, suggesting that metamorphism took place under relatively low pressures.

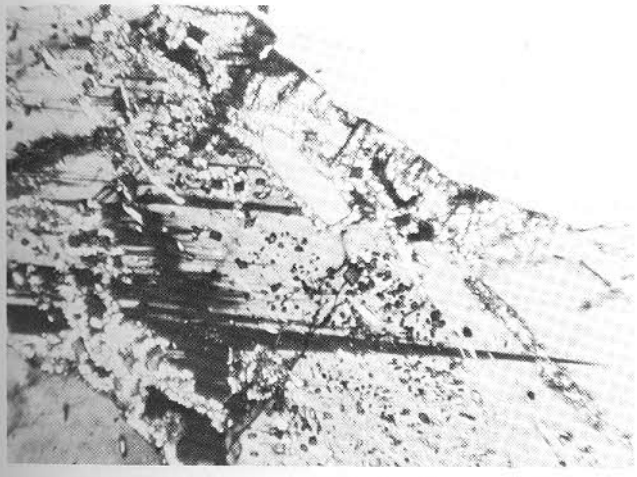

FIGURE 19. Polysynthetic twinning in cordierite grain showing marginal pinitization. Fine black equant inclusions and white needles are sillimanite. Sample 303, cordierite-sillimanite-almandine-biotite-quartz-feldspar gneiss. Crossed nicols. Length of photograph is 1.6 mm.

Cordierite with α = 1.542 — 1.543, β = 1.546, γ = 1.550, corresponding to 100Fe/(Fe+Mg) = 25, sillimanite, and the most magnesian biotite, γ = 1.640, 100Fe/(Fe+Mg) = 50, occur with the most magnesian almandine as would be expected. These assemblages are plotted in figure 20, an AFM diagram projected from K-feldspar after Thompson (1957) and Barker (1961). The four-phase field, sillimanite-cordierite-almandine-biotite, found in sample 303 (table 11) and plotted in figure 20, may represent a disequilibrium assemblage, or an extra component with Mn-zoning in the garnet, or a transitional metamorphic facies. This four-phase assemblage is identical to that reported by Wynne-Edwards and Hay (1963) for a transitional amphibolite-granulite facies in southern Ontario. They noted that incidence of cordierite was favored by a high Mg/Fe ratio and a low Ca content for the bulk composition of the rock. This is exactly that shown in table 11, where it is apparent that cordierite occurs only in those rocks low in plagioclase (the only Ca-bearing mineral) and high in Mg/Fe ratio. Sillimanite also favors the same rocks because a high Ca content would tie up Al in added plagioclase preventing the formation of sillimanite. In a similar way, a bulk composition richer in Fe tends to allow the formation of almandine to tie up excess Al again restricting the formation of sillimanite.

Assuming that the metamorphism was essentially isochemical, these gneisses would have originated from pelitic rocks, perhaps potash-rich shales (table 11) or

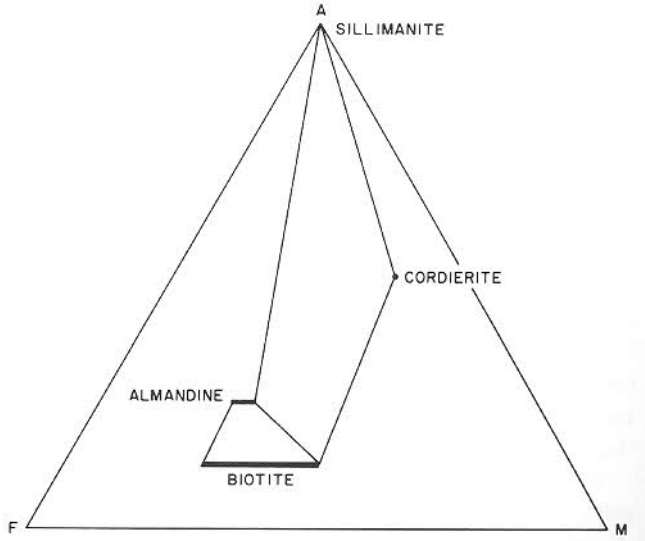

FIGURE 20. AFM diagram, projected from K-feldspar, showing assemblages in pelitic paragneisses from the Monroe quadrangle. Additional phases are quartz, K-feldspar, intermediate plagioclase, and tourmaline.

graywacke uncommonly rich in matrix content. Where the calcite content of the original or parent shale was low, high grade regional metamorphism would lead to the formation of sillimanite according to the reaction:

$$KAl_2(Si_3Al0_{10})(OH)_2 + SiO_2 \rightarrow KAlSi_3O_8 + Al_2SiO_5 + H_2O$$

muscovite + quartz → K-feldspar + sillimanite + water

Muscovite is virtually absent from the gneisses of the Monroe quadrangle, occurring only rarely as a retrograde mineral in Belts 1 and 6.

At still higher temperatures of metamorphism, at low to moderate (but not high) water pressure, cordierite may form in rocks of appropriate bulk composition from the following reaction, modified from Schreyer and Seifert (1969):

$$2\ K(Mg,Fe)_3(Si_3A10_{10})(OH)_2 + 6\ Al_2SiO_5 + 9\ SiO_2 \rightarrow$$

2 biotite + 6 sillimanite + 9 quartz

$$3\ Al_3(Mg,Fe)_2(Si_5A10_{18})\cdot O.5H_2O + 2\ KAlSi_3O_8 + 0.5H_2O$$

3 cordierite + 2 K-feldspar + 0.5 water

This reaction was proposed by Hietanen (1947), Schreyer and Yoder (1961), von Platen (1965), and Schreyer and Seifert (1969) as the important process of cordierite formation in high grade regional metamorphic rocks. Schreyer and Seifert (1969) show an invariant point for the latter reaction at 695° C. and 5 kilobars water pressure, where **phlogopite** rather than biotite is involved. They emphasize, however, that the addition of ferrous iron to the mica will permit the reaction to go at lower pressures, and result in the appearance of an additional phase such as almandine. Further, Richardson (1968) has shown that the reaction: almandine + sillimanite + quartz → Fe cordierite takes place at water pressures as low as 2–3½ kb (kilobars). Because the cordierite in sample 303 (table 11) is relatively iron-rich, Fe_{25}, it is possible to use these data to estimate a maximum pressure of kb for the formation of these gneisses; perhaps even less than 3 kb would be a reasonable value.

Winkler and von Platen (1961) were able to produce synthetic sillimanite-cordierite-biotite-quartz-feldspar gneisses from the experimental metamorphism of graywacke and shale. Modes of two of these from Winkler (1967) are presented in table 11 for comparison with the rocks from the Monroe area. Winkler found that melting of these gneisses began at temperatures of 685–715° C., and a water pressure = 2 kb, depending upon the An content of the plagioclase and presumably upon the Fe/Mg ratios of the mafic minerals. At temperatures of 750–770° C., and 2 kb water pressure, metamorphism of the initial graywacke resulted in the formation of 40–67 percent of anatectic granitic melt and a crystalline residue containing quartz, cordierite, and opaque minerals, with or without biotite, sillimanite, and plagioclase with an increased anorthite content. Winkler and von Platen, by these experiments, have thus produced venitic migmatites, from parent graywackes and shales, which are mineralogically strikingly similar to the migmatitic sillimanite-cordierite-almandine-biotite-quartz-feldspar gneiss of the Monroe quadrangle. The T and P_{H_2O} used by Winkler and von Platen in these experiments, 750° C. and 2 kb, are reasonable estimates for the metamorphism in the Highlands and are in general agreement with estimates from other mineral systems discussed in this report.

Microcline alaskite (leucogranite)

Microcline alaskite and granite pegmatite occur throughout the Monroe quadrangle as small lenses and pods forming the granitic component of migmatitic gneisses and as more extensive, coherent bodies which form mappable units. The most extensive occurrence of these rocks is in Belts 9 and 10, the southern part of Belt 3, and in a narrow zone forming the western border of Belt 7. The alaskite (or leucogranite) is a pink, medium- to coarse-grained, rarely fine-grained, equigranular to indistinctly foliated rock. It is everywhere leucocratic with a color index consistently less than 5. A rude foliation produced by elongated quartz grains may be observed in some outcrops with the aid of a hand lens. The large, bold outcrops of alaskite in the southern part of the quadrangle, along Bramertown Road, although mineralogically homogeneous, often show a stratiform appearance, presumably due to textural inhomogeneity. The alaskite weathers light buff.

In thin-section the alaskite consists of equigranular, well-twinned, fresh microcline, about 50 percent, moderately to heavily sericitized albite-oligoclase, about 20 percent, and elongated tongues of quartz, about 30 percent (table 12). Biotite, which may be slightly chloritized, is the only mafic mineral and is present in amounts up to 2 percent. Accessory minerals include the usual apatite, red zircon, sphene, and less commonly, muscovite, and garnet. An occasional specimen contains microcline microperthite in place of microcline. The alaskite appears to have crystallized from a melt under relatively low-temperature subsolvus condi-

TABLE 12. Modes of microcline alaskite(leucogranite)(al) and magnetite-garnet-andesine microperthite leucogneiss(mag).

	Microcline alaskite					Magnetite-garnet-andesine microperthite leucogneiss				
Belt	7	7	9	9	1	7	7	8	8	8
Sample No.*	7	43	80	292	264	196	417	379	395	396
Quartz	28.7	32.2	25.7	32.1	37.0	31.2	26.1	31.0	30.3	42.6
Microcline	49.3	42.4	64.2	39.9	56.5					
Microperthite						36.8	34.8	42.2	50.3	22.4
Plagioclase [1]	20.1	23.2	10.1	27.8	6.4	26.4	34.2	24.1	6.0	28.8
Biotite	1.8	2.2	+	0.1	+	1.8	1.5	0.4	0.7	+
Magnetite	+	+	+	0.1	+	3.8	3.4	2.2	1.0	1.8
Garnet	—	—	—	—	—	—	—	—	11.7	4.4
Epidote	+	+	—	—	—	—	—	0.1	—	—
Others [2]	+	+	+	+	0.1	+	+	+	+	+
[1] Mol. % An	9	13	3	4	12	33	32	36	31	31
Color Index	2	2	0	0	0	6	5	3	12	6
Avg. grain (mm)	1.0	0.8	1.5	1.2	3.0	2.5	1.8	1.5	2.5	2.0

[2] Includes apatite, zircon, muscovite, garnet, and chlorite in the alaskites and apatite, zircon, chlorite, and sphene in the leucogneiss.

* Sample locations in appendix.

tions. A spectacular outcrop showing blocks of amphibolite, 1 to 2 feet in length, rotated at all angles in microcline-albite alaskite occurs south of Walton Lake in Belt 1. The exposure is located about 1,800 feet east of the O in Lake Road at the 900 foot contour. Contacts of the included blocks of amphibolite with alaskite are sharp. Samples of the alaskite taken near included amphibolite contain a small amount of hornblende.

Magnetite-garnet-andesine-microperthite leucogneiss

Magnetite-garnet-andesine-microperthite leucogneiss occupies most of Belt 8 and forms the major part of Buchanan Mountain. It is on strike with and immediately underlies the sillimanite-cordierite-almandine-biotite-quartz-feldspar gneiss of Belt 7. To the south, it is cut off by a cross-fault from the microcline alaskite of Belt 10. The leucogneiss is a pinkish white to buff, medium-grained (1–5 mm.) rock that resembles alaskite in many outcrops. It is distinguished from alaskite by its higher color index (=3–12), abundant accessory magnetite, and often abundant garnet content. Many outcrops show a definite stratified appearance produced by compositional and textural layering. Concordant lenses of biotite-quartz-feldspar gneiss, amphibolite, and pyroxene granulite occur throughout.

In thin section, the gneiss is distinguished from alaskite primarily by the presence of microperthite and andesine as contrasted with microcline and albite-oligoclase of the latter (table 12). Parallel trains of granular grains of magnetite (1–5 percent) are present in almost all specimens. Texturally, most specimens show fine-grained (0.2 mm.) plagioclase-quartz-mafic mineral-rich lenses being crowded out by medium-coarse (1–10 mm.) K-feldspar and quartz. The potassic feldspar may be orthoclase, microcline, or microcline microperthite in different specimens. Presumably all of these crystallized as orthoclase or microperthite and represent different stages of unmixing. Although the composition of the garnet was not determined, its resemblance to garnet of the pelitic paragneiss to the north suggests that it is an almandine.

The composition, textural, layering and stratigraphic position suggest that this rock originated as a sediment. As it underlies the pelitic paragneiss in the lowest part of the stratigraphic section, the magnetite-garnet-andesine leucogneiss may represent a more advanced stage of anatexis and migmatization of the type described for the former unit. As such it may be considered a nebulite whereas the pelitic paragneiss is a venite.

Pyroxene and hornblende granulite

Rocks composed almost entirely of clinopyroxene, clinopyroxene + orthopyroxene, both pyroxenes + hornblende and quartz occur as thin lenses or layers infolded in either the sillimanite-garnet-biotite-quartz-feldspar gneiss, amphibolite, and in the magnetite-garnet-andesine leucogneiss. They are here classed as

pyroxene or hornblende granulite rather than assigning the name skarn which Hotz, (1953), applied to similar rocks in the area directly to the south.

Modes of pyroxene and hornblende granulite are presented in table 13 along with optical properties of the constituent minerals. Although these rocks are usually in proximity to small bodies of magnetite ore, their clinopyroxenes are not necessarily enriched in iron. Contrast, for example, clinopyroxenes from samples 223 and 228 (table 13), both in the vicinity of magnetite deposits, yet containing large and small amounts of iron, respectively.

TABLE 13. Modes of pyroxene and hornblende granulite.

Belt	2	7	7	2
Sample No.*	681	223	228	799
Quartz	—	14.8	—	—
Plagioclase	5.0[1]	—	—	—
Clinopyroxene	95.0[2]	50.1[3]	100.0[6]	12.5[7]
Orthopyroxene	—	30.0[4]	—	—
Hornblende	—	5.1[5]	—	83.3
Magnetite	+	—	—	—
Pyrrhotite	—	—	—	5.2

[1] $=1.542$; An_{27}.
[2] $=1.681$, $\beta=1.687$, $=1.710$; $100Fe/(Fe+Mg)=25$.
[3] $=1.720$; $100Fe/(Fe+Mg)=38$.
[4] $=1.729$; $100Fe/(Fe+Mg)=52$.
[5] This is the only blue-green hornblende found in the entire map area. $=1.671$; $100Fe/(Fe+Mg)=65$.
[6] $=1.672$, $\beta=1.6785$, $=1.699$; $100Fe/(Fe+Mg)=8$.
[7] $=1.727$; $100Fe/(Fe+Mg)=42$.
* Sample locations in appendix.

Those clinopyroxenes richest in iron contain the most abundant exsolution lamellae of another clinopyroxene oriented in as many as three different directions (figs. 5, 21, and 22). In sample 223, exsolution lamellae in augite, $100Fe/(Fe+Mg)=38$, are oriented as follows: parallel to (*100*) of the host; parallel to a second direction making an angle of 116° with (*100*) of the host (hence not parallel to (*001*) of fig. 22); and parallel to a third (*h0l*) direction making an angle of 6° with (*100*) of the host and 122° with the second direction. All three sets of lamellae are tentatively identified as clinohypersthene and/or pigeonite on the basis of distinctly inclined extinction angles. Lamellae in the first and second sets are about 1μ in width and those in the third set, about 0.1–0.5μ in width. The first set, parallel to (*100*) of the host is commonly the least abundant (fig. 21) although abundance relations vary in different grains.

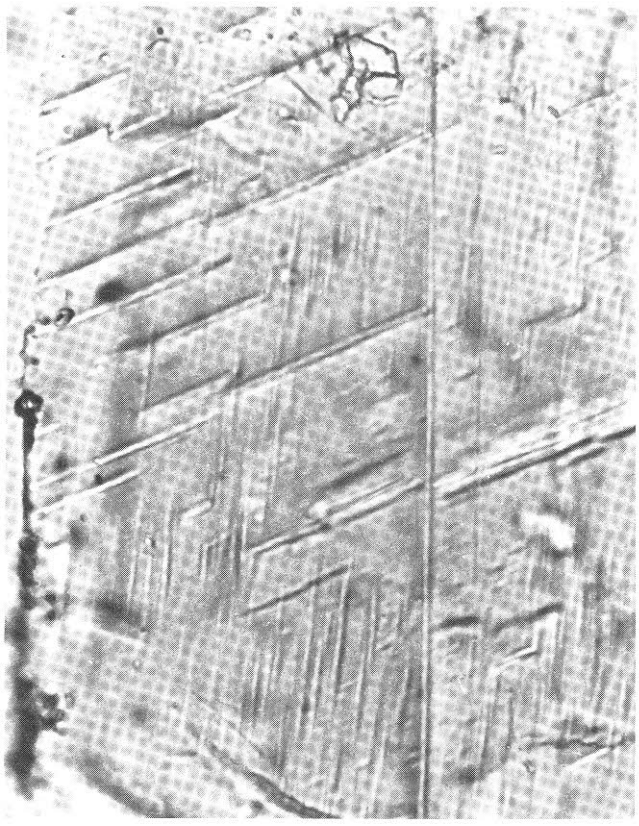

FIGURE 21. Augite ($Ca_{42}Mg_{36}Fe_{22}$) host grain containing three sets of exsolution lamellae of clinopyroxene (pigeonite and/or clinohypersthene). Compare with figure 22. Lamellae are parallel to (*100*), (*h0l*), and to a direction that makes an angle of 116° rather than 105° ($<\beta$) with the c-crystallographic axis. Sample 223. Plane polarized light. Exsolution lamellae are 0.5–1.0μ in width.

In sample 223, the coexisting orthopyroxene is ferrohypersthene, $100Fe/(Fe+Mg)=52$. It contains exsolution lamellae parallel to (*100*) and these are clinopyroxene as indicated by Hess (1960). The lamellae range up to 1μ in width, and under crossed nicols alternate sets extinguish on opposite sides of the parallel extinction position of the host ferrohypersthene. This indicates that the lamellae are polysynthetically twinned on (*100*), a feature common to pigeonites of terrestrial rocks and clinohypersthenes of meteorites (Mason, 1968). Recently, Boyd and Brown (1968, 1969) have verified the presence of clinohypersthene lamellae in host augite, $100Fe/(Fe+Mg)=31$, and augite lamellae in coexisting hypersthene, $100Fe/(Fe+Mg)=38$ from gabbro of the Bushveld intrusion. These

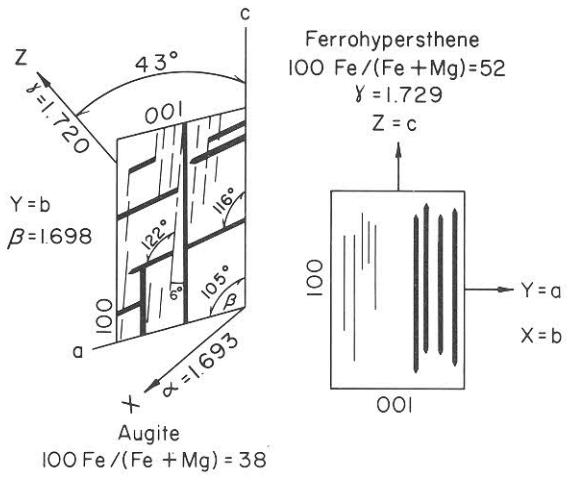

FIGURE 22. Exsolution lamellae in and optic orientation diagram for coexisting augite (Fe_{38}) and ferrohypersthene (Fe_{52}). Sample 223, pyroxene granulite.

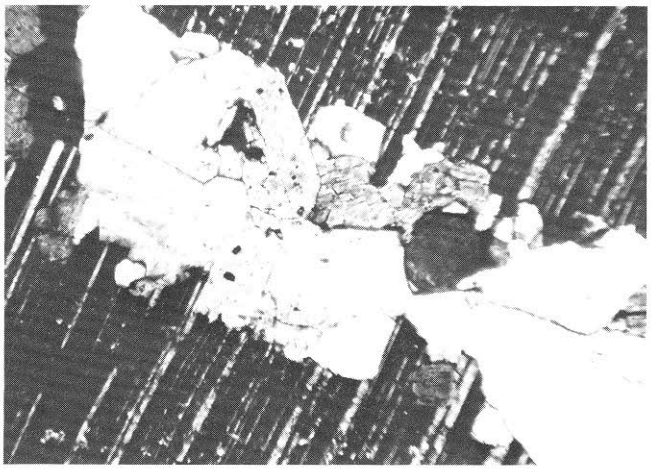

FIGURE 23. Prehnite in vein crosscutting albite in retrograded calc-silicate gneiss from near the east contact of Goose Pond Mountain klippe. Sample 529. Crossed nicols. Prehnite vein is 0.4–0.5 mm. wide.

appear to be similar to the lamellae in coexisting pyroxenes of the Monroe granulites.

Thus, in both igneous and metamorphic parageneses, mutual solid solution in coexisting pyroxenes increases with increasing iron content, as would be predicted from the inferred shape of the pyroxene solvus (Poldervaart and Hess, 1951). The same trend has been reported by Jaffe, Robinson, and Klein (1968) for coexisting hornblende and cummingtonite from sillimanite zone rocks from New Hampshire, each containing exsolution lamellae of the other.

If, as these data indicate, initial crystallization, prior to exsolution, took place above the pigeonite-orthopyroxene inversion temperature, the exsolution textures may be difficult to explain for those who propose a low-temperature hydrothermal or metasomatic origin for both "skarn" and the associated magnetite deposits (Hotz, 1953; Sims, 1953). Although ferric iron, sodium, and other minor constituents may lower the solvus temperature, this effect should not be large when contrasted with relatively low temperatures usually associated with hydrothermal ore solutions.

ALLOCHTHONOUS PRECAMBRIAN GNEISSES

Belts 23, 24, 25, and 26 consist of allochthonous Precambrian gneiss blocks that have become detached from their root zones and thrust over Cambrian and Ordovician rocks. They are here interpreted to be synclinal saucers or klippen that perhaps formed one continuous overthrust nappe outlying the western border of Schunemunk Mountain. Because the gneisses are lithologically, mineralogically, and texturally distinct from those in the Monroe and Ramapo blocks, they will be described separately.

Belt 23 Goose Pond Mountain Klippe

The major part of Goose Pond Mountain allochthon is exposed in the Goshen quadrangle mapped by Offield (1967). The northeastern edge of this mass projects into the western part of the Monroe quadrangle where it is very well exposed. The gneisses of this klippe are extensively retrograded along their eastern and western contacts with the underlying Paleozoic rocks and generally less altered to unaltered towards the center of the block. This suggests that the klippe is a saucer with its presently exposed center lying at a further distance from the sole of the thrust.

An east-west section across Goose Pond allochthon shows three lithologic units. These are, from east to west: calc-silicate and amphibolite; amphibolite and albite leucogneiss, and graphitic calc-silicate gneiss and quartzite. Representative modes of rocks from each of these lithologies are given in table 14. The plagioclase of this and most of the other allochthonous gneisses, particularly border facies, is usually albite. The albite in many of these rocks is believed to be a retrograded plagioclase originally richer in anorthite content. Another unique feature of this and the Museum Village

TABLE 14. Modes of allochthonous gneisses from Goose Pond Mountain and Museum Village klippen (gcs, alg, and acs).

	Belt 23 Goose Pond Mountain klippe				Belt 24 Museum Village klippe			
	East	Center		West	East	Center		West
Sample No.*	529	788	20	527	36	769As	769N	769W
Quartz	16.8	5.0	29.0	81.7	22.2	2.0	35.1	21.5
Microperthite	—	10.0	42.2	2.6	49.5	37.0	22.5	68.8
Plagioclase [1]	65.6	49.0	27.7	—	20.2	36.0	32.4	3.3
Sericite	7.2	—	0.8	—	0.7	—	0.3	—
Biotite	—	2.5	—	—	—	8.0	6.0	—
Chlorite	1.7	—	—	0.3	5.8	—	—	2.5
Diopside	1.3	+	—	8.0	—	—	—	—
Actinolite	0.2	—	—	3.0	—	—	—	—
Hornblende	0.2	33.0	—	—	—	—	—	—
Garnet	—	—	—	—	0.1	2.0	—	—
Graphite	—	—	+	4.2	—	3.0	—	—
Sillimanite	—	—	—	—	—	12.0	3.7	—
Tourmaline	—	—	—	—	—	+	+	—
Calcite	—	—	—	—	+	—	—	3.4
Apatite	+	0.3	0.1	+	0.7	+	+	+
Zircon	+	+	+	+	0.1	—	—	+
Ilmenite	—	0.2	0.2	—	0.7	+	+	+
Pyrite	—	—	—	—	+	+	—	0.5
Sphene	—	—	—	0.2	+	—	—	+
Prehnite	7.0	—	—	—	—	—	—	—
[1] Mol. % An	0	20	4	—	3	32	32	—
Color index	3	36	0	16	7	13	6	3

* Sample locations in appendix.

klippe of Belt 24, is the absence of magnetite. The gneisses are generally depleted in opaque minerals and the small amounts found are consistently ilmenite. A sample along the east edge of Goose Pond Mountain (529, table 14) contains the unusual assemblage diopside-albite-quartz. The rock is shattered and transected by veinlets of prehnite (fig. 23) which cut the rock at a variety of angles. Albite is moderately to heavily sericitized. Amphibolite lying to the west of this gneiss contains labradorite, An_{54}, diopside, hornblende, biotite, and sericite. Towards the center of the allochthon, amphibolite (788, table 14) interlayered with leucogneiss carries quartz and microperthite. A typical white leucogneiss (20, table 14) consists of microperthite, albite, and quartz, with only traces of dark minerals (fig. 24). From here, towards the western contact, the rocks become increasingly graphitic. Most of these are graphitic quartzite with quartz grains and pebbles stretched into thin corrugated tongues showing elongations of up to 20:1, parallel to the a- and b-fabric axes. Many of the quartzites are calcareous as well as

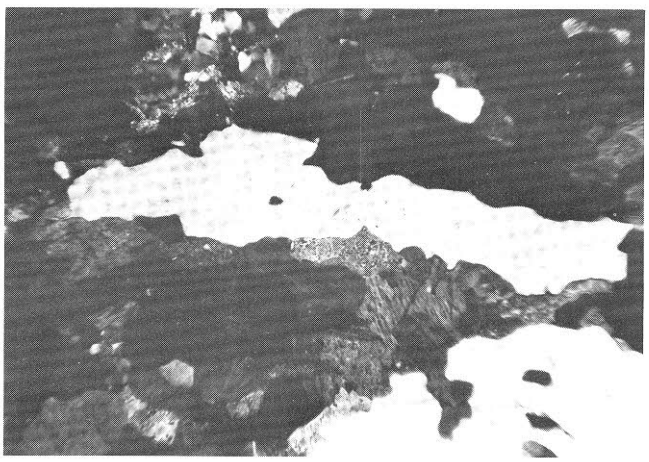

FIGURE 24. Albite-leucogneiss, Goose Pond Mountain klippe, showing marked elongation of quartz grains. Sample 20. Crossed nicols. Quartz grain in center of photo is 1.2 mm. in length.

graphitic (527, table 14) and carry diopside and actinolite in addition to graphite and quartz. Yellow and green, " limonitized " fault breccia occurs in places along the western contact and some of these rocks carry an abundance of megascopic dark red zircon. Occasional pelitic beds found in the western zone carry abundant K-feldspar, biotite, and some chloritized garnet.

Belt 24 Museum Village Klippe

Museum Village klippe is another saucer-shaped slice consisting exclusively of gray-white, albite leucogneiss in the eastern part of the block and graphitic and pelitic gneisses toward the western part. Representative modes of these gneisses are given in table 14. The albite leucogneiss (36, table 14) is very similar to that found in Goose Pond allochthon. In outcrop it is heavily shattered and slickensided with lineations often running in three different directions at a given place. Quartz again occurs as elongated tongues showing 15 to 20:1 elongations. Over most outcrops, biotite and garnet are extensively retrograded to chlorite and abundant veinlets of calcite cross the rocks at all angles.

Towards the central and western part of the body, there occur occasional thin layers rich in fresh biotite, Fe_{50}, and uncommonly coarse laths (not needles) of fresh blue-gray sillimanite that have survived the complex orogenic history of multifolding and thrusting. As none of the Cambrian-Ordovician or younger rocks in the area show any metamorphic grade higher than low chlorite zone metamorphism, the sillimanite is assumed to be Precambrian in age, and its preservation in large fresh laths in an otherwise extensively retrograded slice of gneiss is remarkable.

The original sedimentary record of Precambrian deposition is preserved in graphite-rich quartzitic layers, the pelitic beds or shales that gave rise to the sillimanite, and in microscopic placer layers rich in apatite, zircon, sphene, and ilmenite.

Belts 25 and 26 Bull Mine Mountain and Merriewold Klippen

No detailed petrographic studies were made of these two klippen. Bull Mine Mountain, once mined for its minor magnetite deposits, consists largely of shattered albite leucogneiss, brecciated and " limonitized " granitic rocks, and albite amphibolites. The granitic gneisses carry albite, An_3, quartz, microperthite or mesoperthite, and " limonite," and manganese oxides as fracture-fillings. Amphibolite occurs in rotated blocks in the albite — K-feldspar leucogneiss all over the mountain. One specimen of amphibolite, near a mined out magnetite lens, consists of green hornblende and albite, An_5, uncommonly sodic for such an occurrence, again suggestive of retrograding in a fault zone.

METAMORPHIC HISTORY

Mineral assemblages and metamorphic facies

The principal prograde metamorphic mineral assemblages characteristic of the gneisses of the Monroe quadrangle are delineated on an ACF diagram (fig. 14) and an AFM diagram (fig. 20). Because diagrams of this type and metamorphic facies classifications usually represent oversimplifications, the more important mineral assemblages of the Monroe gneisses are listed below for clarification. The assemblage numbers correspond to those on the ACF diagram (fig. 14).

Pelitic:

1. sillimanite-cordierite-almandine-plagioclase-biotite-quartz-K-feldspar
2. almandine-plagioclase-biotite-quartz-K-feldspar
   2a. plagioclase-biotite-quartz-K-feldspar

Intermediate:

3. hypersthene-antiperthitic plagioclase (An_{31})-biotite-quartz
   3a. hypersthene-microperthite-plagioclase-biotite-quartz

Basic:

4. hornblende-plagioclase-biotite
5. hypersthene-hornblende-plagioclase-biotite
6. clinopyroxene-hornblende-plagioclase-biotite (quartz)
7. clinopyroxene-hypersthene-plagioclase (hornblende, biotite, quartz)
8. clinopyroxene-hypersthene-hornblende-quartz
9. clinopyroxene-hypersthene

Calc-silicate

10. salite-calcic plagioclase-sphene-microcline-quartz
11. salite-calcic plagioclase-sphene-scapolite-microcline-quartz (epidote)
12. ferrosalite-andradite-scapolite-sphene-quartz (epidote)
13. diopside ($Ca_{50}Mg_{46}Fe_4$)

The following assemblages for which vacant fields are shown on the ACF diagram are absent in the Monroe but present in adjoining quadrangles:

calcite - diopside - andradite (Sloatsburg quadrangle, Hotz, 1953)

garnet-eulite (Fs_{83})-quartz (clinopyroxene), (Popolopen Lake quadrangle, Dodd, 1963).

Most of the mafic assemblages (various combinations of hypersthene, clinopyroxene, and hornblende with plagioclase) are representative of metamorphosed basaltic rocks classed as mafic granulites from Precambrian terranes which include the Broken Hill area of New Zealand (Binns, 1965), the Adirondack area of New York (Buddington, 1963; de Waard, 1965), Madras, India (Howie, 1965), the Central Highlands of Ceylon (Cooray, 1962), and the Highlands of Scotland (O'Hara, 1961), to mention a few. Noteworthy is the absence of almandine garnet from the basic assemblages of the Monroe quadrangle. Buddington (1965) suggests that the absence of garnet and its presence in amphibolites of similar composition in the Adirondacks is indicative of disequilibrium. In the Monroe quadrangle, there is no such anomaly, as garnet is totally absent from amphibolite and pyribolite assemblages. This may result either from an inappropriate bulk composition, low pressure, or perhaps a low oxygen fugacity. Ernst (1966) has noted that, in synthetic systems a high oxygen fugacity favors the formation of garnet, whereas a low oxygen fugacity favors the formation of amphibole.

The intermediate assemblages, 3 and 3a, are typical of rocks from these same areas that are classed as charnockite or charnockitic gneiss by some of these authors. Here it is important to reemphasize that the hypersthene-microperthite-bearing assemblage, 3a has resulted from the breakdown of ferroan biotite in the presence of quartz to yield a charnockitic gneiss, *sensu stricto*; by contrast, the hypersthene-clinopyroxene-plagioclase-quartz assemblage, 7, has resulted from the breakdown of hornblende in the presence of plagioclase, to yield an intermediate charnockite or enderbite. The same reaction has produced the hypersthene in the quartz-free amphibolites and pyribolites, yielding the basic charnockites of some authors. Distinction between two modes of formation of hypersthene can be made on the basis of the presence or absence of major amounts of K-feldspar. The breakdown of biotite must produce a large amount of K-feldspar whereas the breakdown of hornblende will produce none or only trace amounts. From the standpoint of metamorphic grade, or isograd location, the biotite reaction is a higher temperature reaction than the hornblende reaction as evidenced by the persistence of biotite in the Oslo hornfelses (Goldschmidt, 1911) and other high-grade contact metamorphic rocks. Hornblende, by contrast, is absent from rocks of the pyroxene hornfels facies. This distinction is used here to show that the hypersthene K-feldspar (charnockitic) gneiss of Belts 15 and 20 places the Ramapo block in a higher metamorphic grade than the Monroe block. In the latter block, biotites with $100Fe/(Fe+Mg)=80$–100, in the presence of abundant quartz (hornblende granite gneiss unit) have not broken down to yield any hypersthene. Although hornblende granite gneiss in Belts 17 and 19 of the Ramapo block does not contain any hypersthene, it carries a more magnesian biotite, with $100Fe/(Fe+Mg)=60$–70 which would require a still greater temperature increase to cause its breakdown.

According to Fyfe, Turner, and Verhoogen (1958) and Winkler (1967), grossularite-andradite is alien to and unstable in calc-silicate assemblages of the granulite facies. On the other hand, de Waard (1965) shows it as a stable phase in some granulite facies rocks. The authors believe that the andradite-grossularite found in assemblage 12 is indeed a stable prograde mineral. It may have resulted from the instability of epidote according to the following reaction proposed by Holdaway (1966):

4 clinozoisite + quartz → 5 anorthite + grossularite + 2 water. According to data of Holdaway, the anorthite-grossularite assemblage thus produced would be stable at the high temperature and moderate to high pressure associated with granulite facies formation. In some publications, scapolite is incorrectly located on ACF diagrams, being placed in the anorthite position. When it is located in its correct position, which is the same location as for epidote, the calc-silicate assemblages, 10, 11, and 12, make much more sense on an ACF diagram (fig. 14). Most, if not all, of the scapolite is considered to be a prograde mineral and not a retrograde phase replacing plagioclase.

The presence of cordierite in almandine-biotite gneisses of pelitic parentage again suggests that these rocks originated at a lower pressure than most granulites. This would again imply a transition towards the pyroxene hornfels facies of Fyfe, Turner, and Verhoogen (1958), now renamed by Winkler (1967), the K-feldspar-cordierite hornfels of shallow contact metamorphism.

Thus, prograde mineral assemblages of the Monroe quadrangle, although granulites as defined by the characteristic hypersthene-clinopyroxene-plagioclase assemblages of the basic gneisses, still contain abundant, fresh hornblende, biotite, grossularite-andradite, and cordierite. Here is the dilemma of the metamorphic facies concept. It is usually resolved by erecting either a new facies, a new subfacies of the already large and growing

list, or by redefining and extending the "boundaries" or limits of existing facies. Eskola (1939) expanded his original list from 5 to 8 facies, Turner (1968) expanded the list to 11, and Winkler (1967) has come up with 13. In addition, these authors list several subfacies, and new additions have been supplied by de Waard (1965, 1966) and others. Evidently the boundaries used to delimit metamorphic facies and subfacies are much like those used to pigeonhole the igneous rocks, and are subject to much the same problems.

If the rocks of the Monroe quadrangle must be assigned a facies status, they are classed as belonging to the newly erected biotite-cordierite-almandine subfacies of the hornblende granulite facies of de Waard (1966). Note, however, that the hornblende granulite facies itself was erected by Fyfe, Turner, and Verhoogen (1958) to explain the transitional nature of the almandine amphibolite facies with the granulite facies, *sensu stricto,* of Eskola, now renamed the pyroxene granulite facies. If nothing else, the prograde assemblages in the Monroe quadrangle emphasize the transitional nature or overlapping of the metamorphic facies.

Temperature, pressure, and chemically active fluids

The following reactions, previously discussed in the text, have been used in arriving at an estimate of the intensive parameters governing the conditions of formation of the Monroe gneiss terrane.

1) muscovite + quartz → sillimanite + K-feldspar + H_2O

Using the new data of Richardson, Gilbert, and Bell (1969) for the aluminum silicate triple point, 622°C and 5.5 kb, the conditions of formation of the pelitic paragneiss are estimated to be 690°–760°C at 4–2 kb fluid pressure. The total absence of prograde muscovite, and any vestiges of andalusite or kyanite suggest the high temperature and low to moderate pressure range delineated in figure 25.

2) 2 biotite + 6 sillimanite + 9 quartz → 3 cordierite + 2 K-feldspar + 0.5 water

The iron-rich nature of the cordierite, 100Fe/(Fe+Mg)=25, and data of Schreyer and Seifert (1969) for pure Mg-cordierite and by Richardson (1968) for pure iron cordierite, suggest an estimate of 3–4 kb as the maximum water pressure at which the pelitic gneisses were formed.

3) The experimental data of Winkler and von Platen (1961) demonstrating the formation of 43–67 percent of anatectic granitic melt and a residual sillimanite-biotite-cordierite-intermediate to calcic plagioclase-quartz-K-feldspar gneiss from a graywacke parent, at T = 740–770C and P_{H_2O} = 2000 bars, suggest similar conditions for the formation of the pelitic gneisses of the Monroe quadrangle. The similarity in mineralogy of the migmatitic pelitic gneiss of Monroe with the experimentally-derived migmatite can hardly be coincidental.

4) Ferroan biotite + K-feldspar + magnetite + vapor

The presence of this equilibrium assemblage in hornblende granite gneiss where biotites show ratios, 100 Fe/(Fe+Mg)=80–100, is consistent with conditions of formation of 710–750°C, 2070 bars P_{H_2O}, and an oxygen fugacity defined by the fayalite-quartz-magnetite buffer (Wones and Eugster, 1965).

5) 2 tschermakitic hornblende + 5 oligoclase → 6 hypersthene + 2 clinopyroxene + 7 andesine + $2H_2O$

This is similar to the reaction suggested by Binns (1965) and implies that the reaction of the tschermakitic component will produce a residual hornblende richer in edenitic component, in addition to the phases shown above. The general absence of hornblende from pyroxene hornfels facies rocks suggests temperatures on the order of 700°C at low water pressure, or more likely, at conditions where P_{H_2O} may have been less than P_s.

6) Ferroan biotite + 3 quartz → 3 hypersthene + K-feldspar + H_2O

This reaction leading to the production of charnockitic gneiss requires temperatures on the order of 700°–800°C according to Miyashiro (1961). In addition, a similar temperature range is suggested by the data of Yoder and Eugster (1954) for the stability limits of phlogopite. The products shown above will also contain magnetite if the original biotite contained ferric iron. This is probably the principal reaction leading to the formation of charnockite, *sensu stricto*. The parent of a charnockite need not have been igneous so long as it was rich in biotite and quartz.

7) Mesoperthite, $Or_{40}Ab_{52}An_8$

The presence of mesoperthite of this composition in a hypersolvus biotite mesoperthite gneiss of quartz syenitic composition (8 percent quartz) suggests a temperature of formation on the order of 800°C, at low water pressure. If water pressure was high, a two-feldspar subsolvus rock rather than a hypersolvus rock would have formed. As the tight folding of these rocks and other indicators imply pressures of 2–4 kb, it is likely that the water pressure was lower than the total pressure of formation of these gneisses.

8) Exsolution lamellae in coexisting pyroxenes

Exsolution lamellae of pigeonite and/or clinohypersthene in augite and of clinopyroxene in coexisting

hypersthene both increase with increasing iron content. As the host pyroxenes are of intermediate iron content, the exsolution lamellae imply that crystallization took place above the pigeonite-orthopyroxene inversion temperature. According to Brown (1968) this might involve temperatures on the order of 990° C which appears to be unreasonably high for this terrane based upon other criteria. Perhaps the presence of sodium and ferric iron, along with other impurities, would lower the inversion temperature to a value more consistent with the other geologic thermometers.

Summing up these data, it appears that regional metamorphism in the Monroe area of the Hudson Highlands took place at temperatures in the range of 700°–800°C and pressures of 2–4 kb (fig. 25). In many parts of the terrane, it is assumed that water pressure was less than the total pressure acting on the rocks.

Retrograde metamorphism

The Precambrian crystalline rocks of the Monroe quadrangle exclusive of the allochthonous outliers are remarkably free of obvious effects of any large scale retrograde metamorphism. Local, small-scale retrograding of plagioclase to sericite, and hypersthene to either talc + magnetite, serpentine or chlorite can be found in many specimens in proximity to Phanerozoic faults. Biotite, normally a sensitive indicator of retrograde metamorphism, is consistently fresh rather than chloritized. Retrograding appears to be largely related to faulting rather than to a regional reheating as evidenced by its spotty development and the proximity of alteration zones to faults. The most retrograded unit in the Monroe block is the calc-silicate gneiss, which is the most brittle, and also the richest in calcic plagioclase. Perhaps along with hypersthene it is the mineral most susceptible to hydrothermal alteration. On the other hand, some specimens of this unit contain fresh bytownite and anorthite and many of the amphibolites carry labradorite.

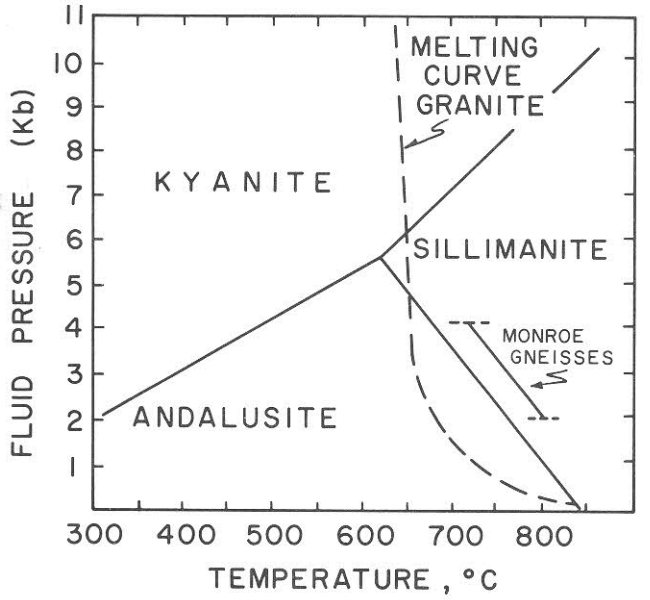

FIGURE 25. Diagram showing the estimated T and P of formation of the gneisses of the Monroe quadrangle with reference to the new aluminum silicate triple point of Richardson, Gilbert, and Bell (1969) and the minimum melting curve for granite (Or-Ab-Q-H_2O).

One example of retrograding of an unusually complete nature was found in an amphibolite bank a few inches wide in the northeast-trending fault that runs along the contact of Belts 6 and 7, and passes into Mombasha Lake. The sample is located 500 feet east of East Mombasha Road at a point 900 feet south of the 8 in elevation 803 near the Precambrian-Paleozoic contact. Here, complete pseudomorphous alteration has converted all of the plagioclase to paragonite, hornblende to pargasite, hypersthene to serpentine, diopside to tremolite, and magnetite to goethite. A modal analysis of this unusual specimen and the optical properties of the pargasite are given in table 15. Inches away, the amphibolite is so completely fresh that it is difficult to locate the alteration zone. Microcline alaskite along this same fault, and in the same vicinity, contains moderately sericitized oligoclase along with fresh microcline. A short distance to the north, microcline and oligoclase detrital grains in the Cambrian Poughquag arkosic conglomerate beds do not show any alteration of this kind. This suggests that most of the retrograding just described is of Precambrian age and may have occurred in the waning stages of the major metamorphic episode that produced these rocks. Although the effects of retrograding are interesting to observe in the microscope, it is the relative lack, rather than the presence of such alteration that is remarkable in rocks as old as these.

TABLE 15. Mode of totally retrograded amphibolite.

	162A *	
Paragonite	46.1	(after plagioclase)
Pargasite [1]	35.1	(after hornblende)
Serpentine	15.3	(after hypersthene)
Tremolite	3.5	(after diopside)
Goethite	+	(after magnetite)

* Sample locations in appendix.

[1] =1.646, β=1.655, =1.665, 2V=85°(+), Z c=18; 100Fe/(Fe+Mg)=25.

An additional example of alteration will be described in the section of this report dealing with post-Wappinger lamprophyre dikes. These have been extensively altered by deuteric processes. Precambrian and Paleozoic rocks of varying lithology intruded by these dikes show none of the effects of this alteration.

A study of thin sections of the Ordovician Bushkill shales and the Middle Devonian Bellvale graywackes suggests that large grains or flakes of chlorite and muscovite in otherwise very fine-grained rocks may be of low-grade metamorphic origin (table 19). This cannot be easily proved, but if true, the entire region was subjected to a mild reheating during either the Acadian or Alleghanian Orogeny responsible for the last major period of folding. Effects of such a reheating on the Precambrian crystalline rocks are not apparent, or perhaps cannot be readily identified. The moderately reduced Precambrian ages reported for gneisses west of the Hudson River by Long and Kulp (1962) using the K-Ar method, may result from such a reheating.

Extensive cataclasis and retrograding is apparent throughout the small, allochthonous Precambrian slices of Belts 23–26, and is described in the section dealing with these. In the degree of shattering and retrograding, these rocks stand in marked contrast to the fresh gneisses of the Monroe block.

Retrograding of the Precambrian and younger rocks also occurred in association with the Triassic block faulting. Narrow shatter veinlets and associated calcitic, sericitic, and chloritic alteration can be observed in specimens collected along the Thruway fault zone. This fault-related alteration is local and specimens collected within 60–90 meters of the fault zone may show shatter- and alteration-veinlets only a fraction of a millimeter in width.

In conclusion, it may be stated that the Precambrian gneisses of the Monroe and Ramapo blocks show the effects of a limited amount of fault-related retrograde alterations. These can be recognized as having occurred in the Precambrian and again in Triassic time. By contrast the small Precambrian klippen in the northwest part of the quadrangle were extensively shattered and altered, presumably during their emplacement in the Taconian Orogeny of Medial and Late Ordovician time. Retrograde overprinting by either the Acadian or Alleghanian Orogeny cannot be identified in the gneisses. Isotopic studies may be required to determine their extent.

TABLE 16. Mode of Lower Cambrian Poughquag conglomeratic arkose.

Specimen No. 466 *

Microcline	47.4
Microcline microperthite	+
Quartz	48.6
Albite-oligoclase	+
Muscovite	+
Rutile, Anatase, Tourmaline (green and brown)	0.5
Zircon	0.5
Hematite, Mn oxides	3.0

* Sample locations in appendix.

Paleozoic Rocks

CAMBRIAN SYSTEM

Poughquag quartzite, conglomerate, and arkose

The Poughquag Quartzite is the oldest Paleozoic formation in the Monroe quadrangle. Although no fossils have yet been found in the Monroe outcrops, similar rocks from elsewhere in New York carry Early Cambrian olenellid trilobites (Gordon, 1911).† Olenellid trilobites are also found in the equivalent Lower Cambrian Hardyston Quartzite of New Jersey (Offield, 1967) which occurs sparingly in the Goshen quadrangle at the base of Mt. Eve where it rests unconformably on Precambrian rocks. He reports it to be shaly and feldspathic towards the base grading upwards into evenly bedded quartzitic sandstone and conglomerate, and ultimately into blue-gray dolostone in the upper part.

The Poughquag Quartzite occurs at only one area in the Monroe quadrangle where a 3 meter section provides the best of several exposures. It is located near the center of the quadrangle where the Monroe village boundary line intersects the Orange Turnpike about 300 meters south of the E in Turnpike. Here it is exposed in low-lying roadcuts of blue-gray feldspathic quartzite on both sides of the Orange Turnpike. The best exposure lies about 250 meters due west of the road at this point and over a hilltop where it forms the cliff of flat-lying red and gray ferruginous quartzite and quartz conglomerate. The section consists of alternating 5 to 60 cm. thick beds of ferruginous quartzite, conglomerate, and arkose striking N 75° W and dipping 8° or less to the north. Just to the south of this exposure the Precambrian gneisses strike about N 30° E and have vertical dip. Although the contact is concealed, from the very marked contrast of the attitudes of foliation of the gneiss and bedding of the quartzite, the two may be separated by a marked angular unconformity. The feldspathic nature of several of the beds is a feature uncommon to the Poughquag of the Poughkeepsie quadrangle (Gordon,' 1911). One such bed at the Monroe section is a conglomeratic arkose which is a true high rank arkose in the sense of Krynine (1948). A remarkable textural feature of this rock is the abundance of authigenic feldspar (microcline?) which is the principal cementing material in sample 466 for which a mode is given in table 16. The specimen consists of 1–2 mm. pebbles of quartz and microcline or microcline microperthite (all very round) lying in a matrix of 0.2 mm. grains of microcline and much less quartz (fig. 26). The microcline grains, each with a dirty peripheral stain of Fe and Mn oxides appear to float in the matrix of authigenic feldspar cement which is clear in appearance. Some sawtooth or hacksaw terminations on detrital microcline cores (Edelman and Doeglas, 1931) indicate that interstratal solution has taken place after deposition, presumably *in situ*. The authigenic overgrowths show only weak twinning when grown around detrital cores showing strongly developed microcline grid twinning. The mineralogical composition of the Poughquag at Monroe leaves little doubt that it was derived from erosion of the granitic gneisses it overlies.

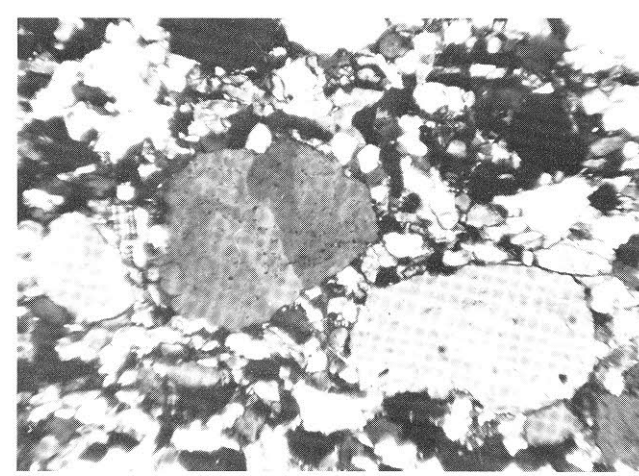

FIGURE 26. Poughquag conglomerate, Lower Cambrian. Subrounded, strained pebbles of quartz and a small twinned microcline in a quartzo-feldspathic matrix. Sample 466, Monroe Block. Crossed nicols. Strained quartz pebble is 1 mm. in length.

† Olenellid trilobites have recently been collected from the uppermost Poughquag by Donald W. Fisher along Interstate 84 near Honness Mountain on the Hopewell Junction quadrangle—Ed.

Several very good examples of camptonite dikes intrude the Poughquag at different locations along the top of this hill (plate 1).

CAMBRIAN-ORDOVICIAN SYSTEM

Wappinger Group

The Poughquag Quartzite at the locality in the Monroe quadrangle, just described, is conformably overlain by fine-grained, dense blue-gray Wappinger dolostone. At another locality, near the northeast corner of Mine and Rye Hill Roads, the Wappinger is a thin-bedded, light gray, argillaceous dolostone or marlstone. Most of the scattered small outcrops on the geologic map are represented by the blue-gray, fine-grained dolostone. Outcrops in Harriman, in roadcuts along N.Y. 32, consist of the blue-gray dolostone with small, elongate (to 5 cm.) fragments of dark gray chert. At 0.3 km. east of the New York State Thruway, where the Woodbury-Tuxedo town line takes a sharp angular bend to the southeast, the Wappinger dolostone is exposed in a quarry. Here a steep vertical wall of Precambrian gneiss is the plane of the major northeast-trending Triassic fault that parallels the Thruway. At the quarry entrance, beds of highly sheared black shale are interlayered in the dolostone. This outcrop, which is part of the down-dropped Thruway graben of dolostone, may lie near the upper part of the Wappinger as evidenced by the black shale members.

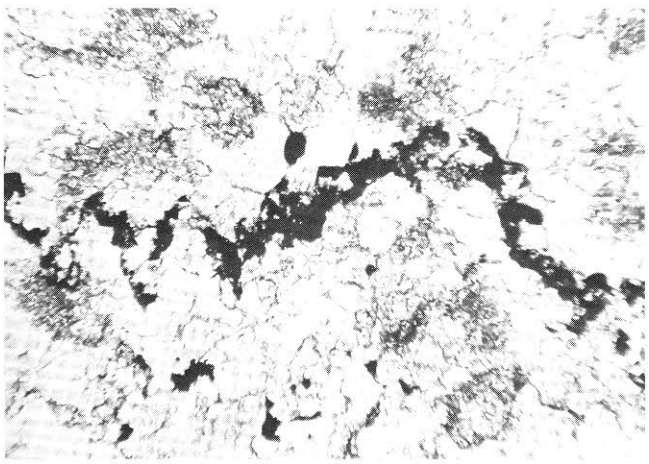

FIGURE 27. Wappinger dolostone, Cambrian-Ordovician. Stylolites of manganese oxide in fine-grained dolomite. Sample 44. Plane polarized light. Length of photograph is 1.3 mm.

No modal analyses were made of the Wappinger, which is a fine-grained pure granular dolostone over virtually all of the Monroe area. Vague clots of relict intraclasts (?) suggest that the Wappinger formation originated as a limestone and was metasomatically dolomitized perhaps during diagenesis. Some samples show well preserved black stylolites outlined by manganese oxides (fig. 27).

No fossils have yet been found in the Wappinger outcrops around Monroe. Offield's observation that the upper part of the Poughquag Quartzite grades into blue-gray dolostone (Stissing) suggests that the Wappinger dolomite of the Monroe quadrangle is the equivalent formation. Assignment of the Stissing formation as Lower Cambrian is based upon the occurrence of *Hyolithellus micans* (Knopf, 1946, 1956). On the basis of lithologic similarity with the Stissing and the gradational relations with Poughquag Quartzite, the Wappinger dolostone of the Monroe quadrangle may be of Early Cambrian age.

Post-Wappinger Dikes

General Statement

Dikes in the Monroe quadrangle fall into three general categories of broad classification: 1) lamprophyres, 2) diabase, and 3) leucophyres. Lamprophyres are dark, dense, porphyritic rocks occurring principally or exclusively as dikes. The name is from λαμπρος, shining, with reference to the glistening flakes of biotite found in such rocks as minettes which do not occur in the Monroe area. Rosenbusch (1887) extended von Gümbel's (1879) original definition, and provided us with the many colorful names: camptonite, kersantite, spessartite, and others.

In the field, many lamprophyres are difficult to distinguish from the diabase dikes with which they are commonly associated. In place of the familiar ophitic or diabasic texture of the diabases, lamprophyres show a pronounced panidiomorphic-granular (sugary, euhedral) texture in which euhedral, seriate phenocrysts of mafic minerals (often zoned) occur in a fine-grained alkalic groundmass. Interspersed among the phenocrysts in many lamprophyres are spherical amygdules similar to those described by Campbell and Schenk (1950) from Boulder Dam, by Jaffe (1953) from the Adirondacks, and by Hudson and Cushing (1931) from the Lake Champlain area camptonites. Similar oblate vesicles or ocelli are described by Vincent (1953) from the Skaergaard camptonites. These are often filled with calcite, chlorite, epidote, and other deuteric minerals.

Lamprophyres are silica-undersaturated or saturated rocks (25–53% SiO_2), often alkalic and ultramafic, remarkably enriched in Ti, P, CO_2, F, and other fugitive constituents of the magma, and often stewed in their own juice by late magmatic or deuteric alteration.

Lamprophyre dikes may originate by fractionation of an alkaline-rich differentiate of an olivine basaltic magma aided by filter-pressing when the magma was injected into narrow tension fractures (Vincent, 1953). Discontinuous reactions: olivine-titanaugite-kaersutite, resorption, high volatile content and extensive deuteric alteration characterize these rocks (Jaffe, 1953). Other theories include differentiation from an ultramafic magma, resorption of hornblende by basaltic magma (Bowen, 1928), melting of ultramafic crystal accumulations, resorption of olivine by granitic magma, assimilation of limestone by basalt, and metasomatic alteration of basalt.

Lamprophyres, especially camptonitic types, occupy northeast- or northwest-trending tension fractures or joints in New York, Vermont, Quebec, and the Skaergaard peninsula of Greenland. The albite-camptonites of the Monroe quadrangle, and the leucophyres as well, occupy only northwest-trending transverse tension joints prevalent in the Precambrian gneisses, the Lower Cambrian Poughquag quartzite, and the Cambrian-Ordovician Wappinger dolostone. They have not been observed, or reported, to cut any younger strata although Middle Ordovician, Silurian, and extensive Middle Devonian rock sections are exposed in the area. The general absence of northwest joints in the Devonian (fig. 40) provides further evidence that the dikes are older. Lamprophyres are known to range in age from Silurian to Pleistocene or Holocene (Campbell and Schenk, 1950). Zartman (1967) has determined K-Ar and Rb-Sr ages on such rocks ranging from Late Ordovician (435 m.y.) for alkalic rocks near Beemerville, New Jersey to Jurassic-Cretaceous (120–150 m.y.) for lamprophyres from Vermont, New York, and Virginia. The results of a potassium-argon age determination on kaersutite from a Monroe lamprophyre dike, recently completed by Zartman (private communication, 1969), are summarized in table 18. According to Zartman, the date, 398±17 m.y., represents either the Siluro-Devonian (the accepted boundary is at 400 m.y.) age of emplacement of the dike or an older emplacement age reduced by a subsequent regional reheating. In the Highlands, K-Ar ages on hornblendes are 910 m.y. on Storm King hornblende granite (Hart, 1961), and 900 and 1,000 m.y. on amphibolites from the Popolopen Lake quadrangle (Hart and Dodd, 1962) as contrasted with a moderately older, essentially concordant set of isotopic Pb-U and Th dates (1140, 1150, 1170, 1030 m.y.) on zircon from Canada Hill quartz-plagioclase gneiss. For this reason and because of the compelling geologic evidence for a pre-Martinsburg age cited in this report (see under Structural Geology-joints and dikes), the authors believe that the age, 398 m.y., may represent a modestly reduced (~ 10 percent) Middle Ordovician age of emplacement of perhaps 450 m.y.

Diabase dikes

Diabase dikes are rare in the Monroe quadrangle although many lamprophyres are misidentified as diabase. Only one diabase dike has been found, and it cuts the amphibolite-granodiorite unit of Belt 14 on the west side of N.Y. 17-M in the fault zone that parallels this road. It is the only dike in the quadrangle with a northeasterly strike. In thin section, it is a heavily sericitized ophitic diabase devoid of phenocrysts. Unlike the lamprophyres, it carries an intermediate plagioclase. The only other true diabase in the vicinity occurs cutting the hornblende granite unit at a waterfalls in the Warwick quadrangle, just west of the limits of the Monroe quadrangle, and reported here because it does not appear on Offield's (1967) map. The dike is near the western boundary of the crystallines with the powerline group (Oriskany or Esopus?) of Offield. It is a large dike, 12 meters wide, and strikes N 40° W, and is exposed for some 60 meters upstream from the waterfalls. In thin section it is a normal, nonporphyritic, ophitic diabase.

LAMPROPHYRE DIKES

Camptonite

At least 30 lamprophyre dikes have been recorded in the Monroe quadrangle (plate 1). These range from inches up to about 10 meters in width and all occupy the northwest-trending transverse joints. Most of these are a variant of camptonite, which Johannsen (1939) classifies as an alkalic rock (his Code—3216H) containing phenocrysts of titanaugite and the titaniferous, alkali-rich, oxy-amphibole, kaersutite, and sometimes olivine, in a dense matrix consisting largely of andesine. Although nepheline is not usually observed in camptonites, Johannsen notes that the rock has alkalic tendencies as indicated by the presence of the alkalic amphibole. The validity of this assignment is shown by the persistent occurrence of normative nepheline in these rocks (table 17, C). The Monroe camptonites are

TABLE 17. Composition of camptonitic lamprophyre dikes.

A. Modes

	Albite mela-camptonite				Albite meso-camptonite			
Sample No.*	523	51	50	218	715	240	184	46
Quartz	—	—	—	—	2.0	0.8	2.0	1.2
Orthoclase	—	—	—	—	—	—	—	0.4
Albite [1]	22.8	26.7	23.6	36.6	35.6	44.8	41.3	53.3
Kaersutite	39.2	37.0	46.6[4]	42.4	39.6	24.8[5]	27.6	21.5
Titanaugite	8.0	13.1	6.0	5.9	—	—	—	—
Epidote	0.3	5.2	7.9	2.1	—	12.8	14.3	12.6
Chlorite	13.3	9.0	8.4	3.7	10.7	11.2	10.0	7.3
Magnetite [6]	4.2	4.0	4.9	3.8	3.3	0.8	2.7	3.2
Apatite	5.2	1.6	1.8	4.0	2.0	0.8	1.3	0.1
Biotite [2]	—	1.6	0.2	—	—	—	0.8	—
Andradite	1.0	0.4	0.2	0.4[3]	—	—	—	—
Calcite	4.3	—	0.2	—	3.3	0.8	—	0.4
Prehnite	—	—	0.2	—	—	—	—	—
Pyrite	—	1.4	—	—	—	—	—	—
Sphene	1.7	—	—	1.1	3.5	3.2	—	—
[1] Mol. % An	4	4	4	5				4
Color index	77	73	76	63	62	42	57	45

[2] Dark green absorption associated with ferric varieties.
[3] a_0=12.088, n=1.89, evidently a titanian andradite.
[4] =1.679, β=1.690, =1.706, Z c=12°, 2V=78°(—) (calc.) Also see chem. anal.
[5] =1.673, β=1.683, =1.699 $2V_{(calc.)}$=76°(—)
[6] Magnetite is very titanian.
* Sample locations in appendix.

B. Chemical compositions calculated from the modes and optical properties of constituent minerals

	523	51	50	218	715	184	46
SiO_2	38.33	42.29	41.46	45.13	44.30	47.65	50.91
TiO_2	3.38	2.72	3.98	4.11	4.93	1.71	1.34
Al_2O_3	12.10	13.12	14.23	13.74	13.87	16.96	17.30
Fe_2O_3	7.53	8.73	7.51	5.62	4.86	6.79	6.82
FeO	8.83	8.44	8.39	6.48	7.10	5.92	5.03
MgO	8.39	8.55	8.44	7.55	6.93	5.24	4.07
CaO	11.91	8.88	9.55	9.41	9.01	7.94	6.36
Na_2O	3.20	3.51	3.40	4.70	4.59	4.95	6.13
K_2O	0.71	0.78	0.85	0.77	0.74	0.59	0.48
P_2O_5	2.22	0.68	0.76	1.74	0.89	0.58	0.04
H_2O	1.56	1.12	1.18	0.51	1.29	1.55	1.18
CO_2	1.63	tr	0.07	—	1.30	—	0.16
F	0.37	0.22	0.27	0.35	0.26	0.17	0.10
S	—	1.18	—	—	—	—	—
Total	100.16	100.22	100.09	100.12	100.07	100.05	99.92

C. CIPW Norms

or	4.45	4.45	5.01	4.45	4.45	3.34	2.78
ab	20.45	25.17	20.97	35.13	32.51	38.27	49.28
an	16.41	17.80	21.14	15.02	14.19	22.25	18.36
ne	3.69	2.56	4.26	1.99	3.98	1.99	1.42
wo	6.97	8.48	8.01	5.92	8.01	5.46	4.41
en	5.22	7.23	6.32	4.92	6.83	4.12	3.71
fs	1.06	0.13	0.79	0.26	0.13	0.79	0.13
fo	10.98	9.85	10.16	8.65	8.37	6.25	4.50
fa	2.65	1.02	1.43	0.51	0.30	1.28	0.91
mt	10.88	12.73	10.88	6.95	8.10	9.72	9.96
il	6.37	5.16	7.59	9.45	7.74	3.19	2.58
ap	5.38	1.68	1.68	2.02	4.04	1.35	—
cc	3.70	—	0.20	3.00	—	—	—
fr	0.32	0.43	0.47	0.47	0.63	0.31	0.20
pr	—	2.22	—	—	—	—	—

TABLE 18. Electron microprobe analysis, optical properties, and K-Ar age determination of kaersutite from camptonite dike (Sample No. J-50 *)
Probe analysis by Brian Mason

Analysis		Ionic ratios					
		Cations per 23 O			Cations per 24[O, (OH)] [1]		
SiO_2	40.7	Si	5.919	8.000	Si	6.061	8.000
TiO_2	5.5	Al	2.081		Al	1.939	
Al_2O_3	13.5	Al	.233	5.000	Al	.430	5.000
FeO	11.3	Ti^{+4}	.601		Ti^{+4}	.616	
MnO	0.16	Mg	3.034		Mg	3.107	
MgO	14.0	Fe^{+2}	1.132		Fe^{+2}	.847	
CaO	10.5	Fe^{+2}	.243	2.000	Fe^{+2}	.561	2.000
Na_2O	2.3	Mn^{+2}	.020		Mn^{+2}	.021	
K_2O	1.1	Ca	1.636		Ca	1.418	
Total	99.1	Na	.101		Ca	.257	
		Na	.547	0.752	Na	.664	1.130
		K	.205		K	.209	
					H	.893	0.893

[1] Assuming 0.9% H_2O, by difference.

Optical properties: (by the authors)
α=1.706 Z=deep red-brown Z c=12°
β=1.690 Y=deep red-brown Y=b
γ=1.679 X=very pale brown
$\gamma-\alpha$=0.027
$2V_{(calc.)}$=78°, r < v=strong.

K-Ar age determination by R. E. Zartman, R. F. Marvin, and V. Merritt, courtesy of Isotope Geology Branch, U.S. Geological Survey.

K_2O%	% Radiogenic Argon	Ar^{40}/K^{40}	Age (m.y.)
1.05_5	97	0.0259	398±17

* Sample locations in appendix.

unique in that they carry almost a pure albite as their plagioclase (table 17, A). They are otherwise texturally, mineralogically, and compositionally identical to camptonites from other localities. Rather than introduce an entirely new name for these dikes, as was the vogue in the past, the authors prefer to classify them as albite mela-camptonite (color index > about 60 and quartz-free), and albite meso-camptonite (color index < about 60 and carrying small amounts of interstitial quartz). In plane polarized light, these dikes show seriate-porphyritic textures characterized by abundant phenocrysts of purplish-tan titanaugite and deep red-brown, strongly pleochroic kaersutite (table 18 and fig. 28). Both of these are strongly zoned, and lie in a matrix of albite laths containing included grains of epidote. As is typical of these rocks, only the dark silicates form phenocrysts, and these minerals generally occur as a second generation in the groundmass, as well. The titanaugite and kaersutite are commonly partly altered to chlorite. Oblate vesicles or ocelli are abundant in some specimens and these are filled with calcite and epidote. Apatite in well developed, long crystals, is remarkably abundant, and may make up as much as 5 or more percent of the rock. Along with magnetite, it is an essential constituent. Small amounts of green ferric biotite, andradite, sphene, pyrite, and prehnite are present in many specimens. The garnet has

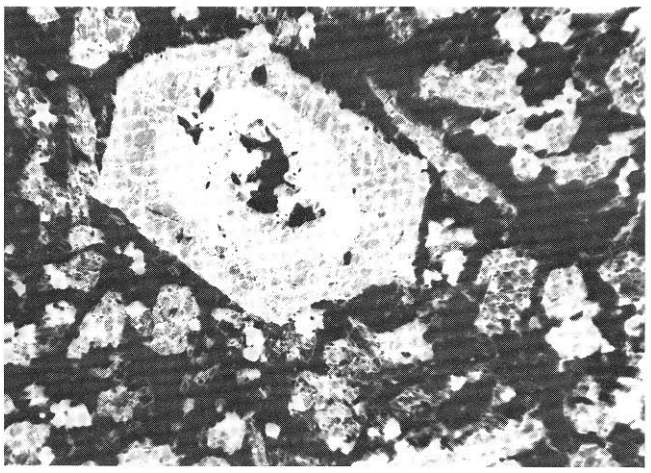

FIGURE 28. Negative reproduction showing zoned kaersutite phenocryst and smaller kaersutite grains (light) in albite groundmass (black) in albite-mela-camptonite dike. Sample J-50. This mineral, for which a probe analysis is given in table 18, yielded a K-Ar age of 398 m.y. Plane polarized light. The zoned kaersutite phenocryst is 1.6 X 1.0 mm. in size.

a unit cell dimension of 12.088 A., larger than that of pure andradite, 12.048 A. (Skinner, 1956). The large unit cell may result from the presence of titanium in an octahedral or tetrahedral site. It could not be due to the presence of $(OH)_4$ substituting for SiO_4 because this would lower the index of refraction markedly. The andradite has an index of refraction of 1.89, close to that of pure andradite, 1.887 (Skinner, 1956).

In the vicinity of the calcitic alteration in the ocelli, half of a phenocryst of red-brown kaersutite may be leached of its iron and titanium, leaving an amphibole that is half-kaersutite and half, colorless tremolite. Elsewhere, titanaugite may be replaced by chlorite, minute grains of pink, isotropic andradite, and minor sphene. Kaersutites are characterized by high titanium contents, high Mg:Fe ratios, and low Fe^{+3} and (OH) contents. These are shown by the electron probe analysis (table 18) excepting the oxidation state of the iron which cannot be determined on the probe. In the absence of a water determination, and a ferric iron determination, the 99.1 percent analytical summation is high. As Fe^{+3} would raise the summation, neither it nor water would appear to be present in appreciable quantity, assuming the analysis to be otherwise accurate. The formula calculated on a water-free basis of 23 oxygens is slightly better than that on a basis of [24 O, (OH)] where water is taken by difference. Determination of ferric iron and water, along with fluorine would be required to arrive at a more precise formula.

The alteration of these dikes is believed to be largely of deuteric origin. The abundance of CO_2, water, and other volatiles, along with richness of ferric iron in the alteration minerals, and the total absence of any alteration in the host rocks intruded by these dikes suggest a deuteric origin for the andradite, epidote, calcite, prehnite, ferric biotite, pyrite, and perhaps, sphene. An alternative suggestion is that the dikes were altered by a slight reheating to which the area may have been subjected during one of the later Paleozoic orogenies.

The chemical compositions calculated from the modes and the norms calculated from these (table 17) are very similar to those for similar dike rocks from other localities. All of the rocks, including those that show modal quartz, carry normative nepheline as a consequence of the abundance of the low-silica, high alkali amphibole.

Kersantite

Kersantite is a lamprophyre containing biotite phenocrysts in a sodic plagioclase groundmass. One such dike was found in the Ramapo block cutting amphibolite of

Belt 16, figure 3. Although the host-rock amphibolite is unaltered, the kersantite contains pseudomorphs of actinolite after euhedral pyroxene. Surprisingly, biotite phenocrysts are fresh, although fine groundmass biotite and kaersutite are altered.

LEUCOPHYRE DIKES

A 5 meter wide leucophyre dike of granodioritic composition cuts amphibolite in Belt 11, near the T in East Mombasha Road in a fine roadcut along the western side of this road. It strikes N 68° W and contains a wedge-shaped keystone of amphibolite in its central part. Except for another identical dike located slightly to the west of this occurrence, no other leucophyres have been found in the quadrangle although Dodd (1965) reports late granodiorite intrusives in the Popolopen Lake quadrangle. The Monroe leucophyre is composed of sparse phenocrysts of oligoclase, quartz, less microcline, and rare biotite lying in a matrix which is again porphyritic on a microscopic scale (fig. 29). The second generation of phenocrysts is made up of square to rhombic-shaped, zoned potash feldspar and laths of albite. These lie in a very fine granophyric groundmass made up of feldspar, quartz, mica, chlorite, and ferric and manganese oxides. The oxides form megascopic, crenulated black streaks which give the dike a flow layering in places. A mode was not obtained because of the fine-grained nature of the groundmass. X-ray data show that oligoclase > quartz > microcline, hence the dike is of granodioritic composition.

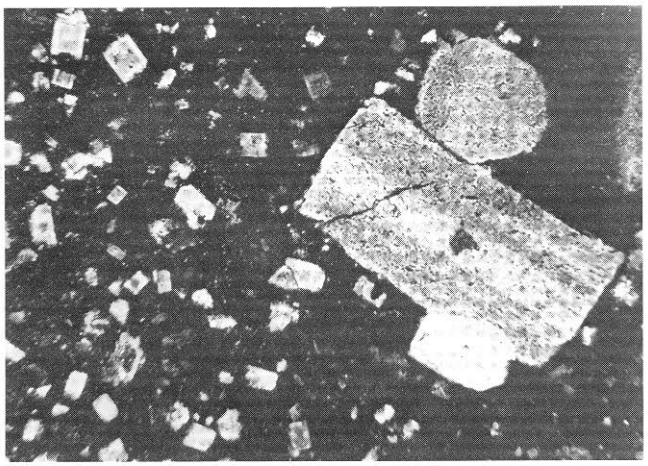

FIGURE 29. Oligoclase phenocrysts and second generation microphenocrysts in fine granophyric groundmass in granodiorite leucophyre dike. Sample 53. Crossed nicols. Largest twinned oligoclase phenocryst is 0.85 X 0.40 mm. in size.

ORDOVICIAN SYSTEM

Martinsburg Formation

Upper member — Penn Argyl Shale, some graywacke, sandstone = Offield's Snake Hill
Middle member — Ramseyburg Graywacke Sandstone = Offield's Austin Glen
Lower member — Bushkill Shale = Offield's Mt. Merino

Bushkill Shale

Offield (1967) has identified the prevalent black shale of this area as Mount Merino. The outcrops of this unit in the Monroe quadrangle are small, discontinuous, and relatively few; the authors have not found any fossils in them. The lithologic description of the Mount Merino by Offield (1967) as typically alternating layers of mudstone and calcareous siltstone, 6 mm. to 15 cm. thick, and the similarity of his outcrops to those in Monroe leave no doubt that the two are equivalent. However, in accordance with currently accepted terminology the authors have identified this black shale unit as Bushkill in the Monroe quadrangle. Although the Bushkill is fine-grained, a modal analysis was made of a typical sample (573) from near Camp La Guardia, and the results are given in table 19. This sample consists of carbonaceous shale intercalated and cross-laminated with dolomitic siltstone. Individual laminae in this specimen are 0.05–0.1 mm., and average grain diameters in these laminae are on the order of 0.01–0.03 mm, and grains are very well sorted. The presence of elongated, sinuous " snakes " of muscovite, and chlorite in strips with dimensions of 0.1–0.2 X 0.01–0.02 mm., suggests that they may be of a low-grade regional metamorphic origin.

TABLE 19. Mode of Bushkill Shale of Middle Ordovician Martinsburg Formation (Ob)

	Sample 573 *	
	Calcareous laminae	Carbonaceous laminae
Detritals+matrix		
Quartz	45	25
Dolomite+calcite	30	5
Plagioclase+microcline	10	+
Sericite, clay, chlorite	15	50
Carbonaceous matter	—	15
Pyrite	—	+
Metamorphic		
Chlorite, muscovite	—	5

* Sample location in appendix.

Ramseyburg calcareous quartzite (subarkose) and shale

The Ramseyburg Formation is well exposed in the Monroe quadrangle. A good section of slabby calcareous, feldspathic quartzite (subarkose) and intercalated calcareous mudstone forms a northeast-trending wedge of sediments bounded on the west by Lazy Hill Road and on the east by the power line on top of Lazy Hill ridge. To the north it is cut off from the Bushkill Shale by the east-west Quickway transverse fault. To the south it barely extends into the Goshen 15′ quadrangle where it pinches out. Offield (1967) apparently missed the edge of this unit and mapped it as Mount Merino. Because the subarkose and shale lithologic units are distinct, the authors mapped both, and this subdivision of the Ramseyburg appears on the map, emphasizing its unconformable contact with the overlying Shawangunk. Modal analyses of two samples of the quartzitic member are given in table 20. The rock is a fine-grained sand (0.3–0.4 mm), not a grit, consisting largely of detrital quartz, oligoclase, microcline, and chert in a calcite cement. There is very little matrix material. Using Pettijohn's sandstone classification (1957), the ratio of quartz : feldspar : rock fragments determined from modes of both specimens shows that they are subarkose. Detritals are sub-rounded, quartz is strained, and plagioclase and microcline show bent and broken twin lamellae. Calcite cement partly replaces quartz and feldspars. The deformation of the feldspar twin lamellae suggests that this is due to a Paleozoic orogeny although it could be argued that this feature was inherited. Replacement of feldspar by calcite cement in areas of broken lamellae however favors the Paleozoic deformation hypothesis (fig. 30).

No modal analyses were attempted on the fine-grained calcareous mudstone interbedded with the subarkose.

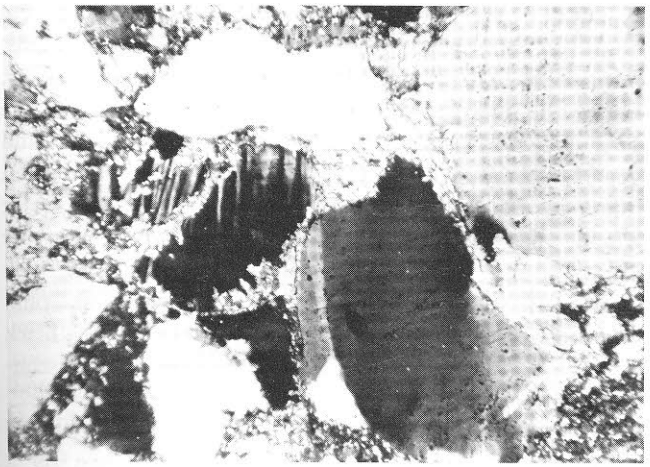

FIGURE 30. Calcareous quartzite (subarkose) unit of Ramseyburg Member of Martinsburg Formation, Middle Ordovician. Strained quartz and twinned microcline grain cracked and veined by calcite. Sample 568. Crossed nicols. Length of photograph is 1.1 mm.

TABLE 20. Modes of Ramseyburg Member of Middle Ordovician Martinsburg Formation (Org).

	568 *	576 *
Quartz	59.2	76.4
Oligoclase	5.4	11.0
Microcline	+	+
Chert	2.4	1.6
Calcite	21.4	5.8
Chlorite	11.6	5.2
Sericite		
MnO_2	+	+
Tourmaline	+	+
Zircon	+	+
Avg. grain (mm)	0.3	0.4

* Sample location in appendix.

SILURIAN SYSTEM

Shawangunk conglomerate and orthoquartzite

Shawangunk conglomerate and orthoquartzite (Early to Medial Silurian age) outcrops extend northeastward along the western edge of the Schunemunk Mountain syncline. Excellent outcrops of the orthoquartzite occur in the west-central part of the quadrangle about 300 meters west of the intersection of the powerline cut with Dug Road, near elevation 527. Several additional small outcrops of the orthoquartzite occur in lenses (channels?) to the northeast. The principal exposures of the coarse vein quartz pebble conglomerate and interbedded orthoquartzite occur on the eastern part of Lazy Hill. Here the steep, southeast-facing escarpment of Lazy Hill consists of about 75 percent of white to buff conglomerate intercalated with 25 percent of fine-grained green-gray to white orthoquartzite. The conglomerate consists of coarse white pebbles of milky vein quartz (averaging 15–50 mm. in length) in a matrix of finer pebbles and grains of rounded quartz, all cemented by secondary silica and less commonly by buff-orange-red ferric oxides. Occasional pebbles of white orthoclase are present, increasing toward the eastern edge of the scarp. A 10 meter section of steeply dipping Shawangunk ex-

posed across the top of Lazy Hill, shows from west-east; about 1 meter of gray-buff orthoquartzite, 2.5 meters of coarse white pebble conglomerate, 4.5 meters of white orthoquartzite with ripple marks on bedding planes, and 1.25 meters of finer white quartz pebble conglomerate. Quartz pebbles are strongly elongated and range up to 10 cm. in length. Toward the eastern edge of Lazy Hill scarp, the conglomerate carries some coarse orthoclase pebbles and the unit grades into a red arkosic conglomerate below the ridgetop. Deformation also increases in this direction and both quartz and orthoclase pebbles are considerably stretched, and often heavily shattered and veined. Pebble elongation is 3–4:1. A large exposure of thin-bedded, pink, buff, and white orthoquartzite occurs at the north end of Lazy Hill on the Durland property on Bull Mill Road just south of N.Y. 17-M. A thin section of the orthoquartzite from this locality (552) is given in table 21.

TABLE 21. Modes of Shawangunk orthoquartzite (Silurian) (Ssk) and Bellvale graywacke (Devonian) (Dbv).

	Shawangunk Orthoquartzite 552 *	Bellvale Graywacke 622 *
Detritals:		
Quartz	93	20
Oligoclase	—	2
Shale	—	44
Phyllite	—	
Siltstone	—	
Chert	5	15
Greenstone	—	1
Zircon	+	—
Tourmaline	+	—
Matrix:		
Clay, sericite, chlorite	2	14
Mn-oxide	—	1
Metamorphic:		
Chlorite	—	2
Muscovite	—	1

* Sample location in appendix.

In thin section, the quartz grains are well rounded, moderately elongated, well sorted (average diameter = 0.75 mm.), and very tightly cemented. Each grain of quartz is cemented to another by authigenic quartz overgrown in optical continuity with the detrital cores (fig. 31). Undulatory extinction due to deformation passes through both the core and overgrowth of each grain. Small slabs of red argillaceous sandstone were found at localities near the base of the eastern edge of the Lazy Hill scarp and suggest a gradation to the Longwood Shale. The prominent valley between Lazy Hill and Durland Hill is filled with thick glacial deposits and is devoid of outcrop. There is room in this valley for Longwood Shale (Silurian) and the Helderberg limestones (Lower Devonian), neither of which outcrops in the Monroe quadrangle. Durland Hill consists largely of Devonian rocks, Bellvale Graywacke, Cornwall Shale, and a solitary outcrop of Connelly Conglomerate at the western edge.

The Shawangunk white pebble conglomerate is also well exposed on a small knoll south of Spring Glen Golf Range. This outcrop lies about 600 meters north of Orange and Rockland Lakes and 185 meters west of N.Y. 208 (fig. 39), and is very similar to the vein quartz pebble conglomerate of Lazy Hill but contains, in addition, occasional black pebbles resembling chert. However, microscopic examination revealed they were rock fragments consisting of green tourmaline and quartz. Similar tourmaline-quartz pebbles have been found in the Clough Conglomerate of New Hampshire which may be stratigraphically equivalent to the Shawangunk. At the Spring Glen outcrop, the weathered surface of the outcrop varies from pink (hematite) to yellow-brown (goethite) to black (manganese oxide dendrites) with some greens contributed by lichens.

The pebbles, obviously well rounded when deposited on the Ordovician erosion surface, have taken on a

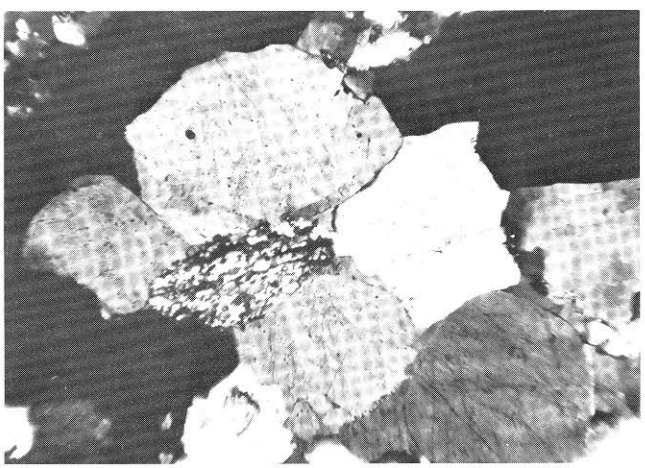

FIGURE 31. Shawangunk orthoquartzite, Lower to Middle Silurian. Rounded quartz detritals with optically continuous, angular authigenic overgrowth; the elliptical grain is chert. Sample 552. Crossed nicols. Length of photograph is 3.0 mm.

secondary angularity and elongation due to stretching, crowding, rotation, and slippage in bedding planes produced during Paleozoic orogenies. Most of the pebbles show a maximum elongation parallel to the fold direction (b-fabric direction) and modest elongation parallel to the dip of the bedding (a-fabric axis). Many of the pebbles have been corrugated and a large number are cracked and sliced parallel to the b-c fabric plane. Bedding surfaces are slickensided, fluted, and warped parallel to the a-axis (down-dip). A fine-grained, gray-green interbedded quartzite is composed of quartz and minor amounts of orthoclase cemented by authigenic quartz, muscovite, chlorite, and ferric oxides.

The size, degree of elongation, and shattering of the pebbles here and at Lazy Hill greatly exceeds that in pebble beds in Lower and Middle Devonian rocks (Connelly Conglomerate and Bellvale Graywacke, respectively).

The lithology of the Shawangunk Formation in the Monroe quadrangle closely resembles that of the Shawangunk Formation in the Shawangunk Mountains near Accord, New York. It is less similar to the presumed equivalent and geographically nearer Green Pond conglomerate and quartzite at Pine Hill in the western part of the Popolopen Lake quadrangle. The latter rocks are characteristically red rather than white or buff. Although they are less deformed and far less metamorphosed than the New Hampshire rocks the lithology of the Shawangunk Conglomerate at Monroe does resemble that of the Clough Formation.

DEVONIAN SYSTEM

Although the Helderberg limestone is exposed in the Popolopen Lake quadrangle, east of the New York State Thruway (Boucot, 1959), it does not occur in the Monroe quadrangle. Boucot shows a north-south fault cutting it out at Highland Mills. In a similar fashion, the Shawangunk and Longwood Formations at Highland Mills (Boucot, 1959) do not continue on strike into the Monroe quadrangle. No Shawangunk is exposed on the eastern side of the Bellvale syncline in the Monroe area. However, there is room in the covered interval between the Wappinger and Esopus, east of the Bellvale syncline, to accommodate these stratigraphic units.

Connelly Conglomerate

The Lower Devonian Connelly Conglomerate (equivalent to Oriskany) is the lowermost Devonian unit in the Monroe quadrangle; only two or three very small outcrops have been found. The best exposure underlies the Esopus directly behind the Monroe Bowl-O-Fun near N.Y. 17-M in Monroe. Here the red and white pebble conglomerate consists of weathered, yellow "limonitic" conglomerate (1 meter or more) succeeded by white to buff, pebble-bearing orthoquartzite (1.5 meters), which is, in turn, overlain by bright red hematitic quartzite (3 meters). The pebbles in the Connelly are white, round to slightly elongated quartz, averaging 1–2 mm. in maximum dimension. Their shape, size, and degree of elongation as well as the overall lithology is distinct from that of the Shawangunk Conglomerate with which it has often been confused in this region.

Darton (1894) reported finding fragments of Helderberg fossils in float down-dip from a small quartzitic outcrop near what is now the north end of Orange and Rockland Lakes, and on this evidence mapped all the exposures of quartzitic and conglomeratic rock on the west side of Schunemunk Mountain as Oriskany. Ries (1895) accepted Darton's identification and also mapped the exposures of Shawangunk as Oriskany. A small outcrop of "limonitic" quartz conglomerate exposed in a field south of a small road north of the Orange and Rockland Lakes, does, in fact, resemble the Connelly Conglomerate more than it does Shawangunk, and has here been mapped tenuously as Connelly.

A third very small outcrop tentatively identified as Connelly Conglomerate occurs below the west edge of Durland Hill near a small stream crossing Museum Village Road along the western edge of the hill. The exposure is about 60 meters downstream from the road, at about the 560 foot contour. It consists of heavily shattered and slickensided quartz conglomerate and quartzite; none of the pebbles are large. No rock is exposed between this outcrop and the Shawangunk of Lazy Hill ¼ mile across the valley.

Esopus shale, siltstone, and quartzite

The Lower Devonian Esopus shales, siltstones, and quartzites in this region were described and subdivided by Boucot (1959) from study of large exposures along the New York Thruway and in railroad cuts at Highland Mills. These were also studied by Kothe (1960), and again by Southard (1960). Boucot subdivided the Esopus into three members consisting of a lower siltstone and sandstone, designated the Highland Mills member; a black shale designated the Middle member; and an uppermost medium-fine-grained sandstone, in places feldspathic, which he designated the Woodbury

Creek member. According to Boucot, the lower part of the Woodbury Creek member is of Esopus age and the upper part of Onondaga age. Southard (1960 unpublished) further subdivided the Esopus Formation into five divisions, recognizing additional shale members. To the best of the author's knowledge this has not been published, although it represents an excellent piece of work.* Southard divided the Esopus Formation as follows: 1) lowermost or Mountainville Member, 2) Lower Black Mudstone member, 3) Highland Mills Member of Boucot (1959), 4) Upper Black Mudstone member, and 5) Woodbury Creek Member of Boucot. This division of the Esopus appears to be logical and consistent with observations made by the authors in this area. Southard's division of the Esopus is followed in the descriptive part of this report. No attempt was made to delineate the separate members of the Esopus on the geologic map.

The Connelly Conglomerate exposure at the rear of the Monroe Bowl-O-Fun in Monroe has already been described. Here, the Connelly underlies the lowermost member of the Esopus Formation. The attitude of both the Connelly and the Mountainville member of the Esopus at their contact is N 68° E, 45° N. A heavily slickensided fault surface, trending N 53° E, 60° SE cuts across the Connelly beds and presumably also cuts the overlying Esopus beds.

The lowermost member (Mountainville) of the Esopus, at its base, consists of fissile, blue-gray siltstones which weather brown to orange on cleavage surfaces. Many bedding planes are marked with *Taonurus cauda-galli*. At this outcrop the authors have collected a remarkable fauna including a giant trilobite, *Coronura myrmecophorus,* not previously reported from the Esopus horizon (fig. 32). According to D. W. Fisher, New York State Paleontologist, who identified the specimen, it has previously been reported from the Schoharie and Onondaga formations. The specimen was donated to the New York State Museum. The Mountainville member is also relatively rich in conulariids, none of which has yet been identified. Brachiopods include *Leptocoelia flabellites, Schuchertella* sp., *Acrospirifer macrothyris,* as well as some chonetids and orbiculoids. Platyostomid and loxonemid gastropods, rugose corals, and a dalmanitid trilobite were also collected.

The Mountainville Member grades into a black, poorly fossiliferous mudstone member, Lower Mudstone member, which in turn grades into a purple sandstone at the north end of the 110 meter exposure. The sandstone is presumably the lower part of the Highland Mills member of Boucot (1959).

At the north end of Bald Hill, due east of Monroe Village the Highland Mills member and the underlying Lower Mudstone member are exposed. The former is represented by fine-grained (0.05–0.08 mm.) red and gray quartzite or siltstone, here dubbed the "ringing quartzite" because of the sound it produces when hit with the geologic hammer. The unit contains spiriferoid brachiopods and unidentified pelecypods. The spirifers are either *Histerolites perimele* or *Spirifer macra*. The siltstone consists of quartz and muscovite cemented by hematite; small amounts of tourmaline and zircon are present. The underlying shale is a dark gray, fissile shale containing fossil fragments which form the nucleii of mud-ball concretions. These along with knots of pyrite are characteristic of this unit at Bald Hill.

A gray, ferruginous quartzite or siltstone on Bakertown Road about 0.6 kilometers beyond its intersection with N.Y. 208 to Highland Mills, contains abundant fossils on yellow to orange ferric oxide-stained bedding planes. The authors have collected the following brachi-

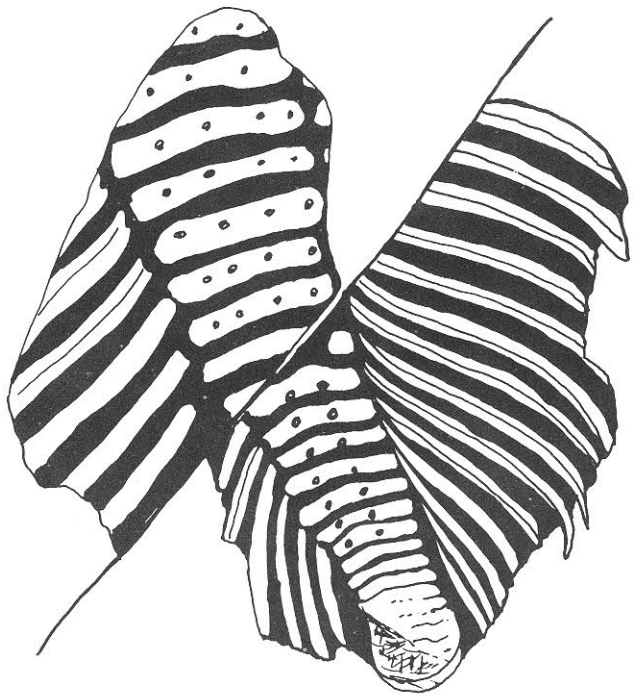

FIGURE 32. *Coronura myrmecophorus* from basal Esopus beds at Monroe Bowl-O-Fun. X 1.

* This has since appeared as "Silurian and Lower Devonian brachiopods, structure and stratigraphy of the Green Pond Outlier in southeastern New York." by A. J. Boucot, K. L. Gauri, and John Southard.
Palaeontographica, Band 135, Abt. A, (1970)....D.W.F.

opods: *Leptocoelia flabellites, Cyrtina rostrata, Platyorthis planoconvexa, Hysterolites perimele, Prionothyris diobolarus, Eodevonaria* sp., *Spirifer macra* (?); the unit is also rich in pelecypods. Here, the Highland Mills Member is also underlain by the Lower Mudstone Member, and possibly by the Mountainville Member as well.

Additional outcrops of Esopus shale and siltstone occur all along the western part of Adria Hill and along Acre Road. These have not been studied sufficiently to ascertain their position in the Esopus.

Bellvale graywacke, shale, and conglomerate

In the Monroe quadrangle, the large down-dropped synclinal block of Schunemunk Mountain and its southeasterly extension to Bellvale Mountain is composed largely of the Bellvale graywacke and interbedded blue-gray-green shale with minor amounts of conglomerate and red beds. The Bellvale Formation is assigned to the Hamilton Group of Medial Devonian age.

Excellent sections of Bellvale are well exposed in the Monroe quadrangle. Exposures in the cloverleaf interchange to N.Y. 17 (4 lane highway) to the east of Orange and Rockland Lakes are among the best. A typical exposure occurs on Oreco Terrace, above the intersection of N.Y. 208 and Oxford Road, near the southern tip of Orange and Rockland Lakes. Here a 68 meter thick section of Bellvale consists of 6–12 meter beds of dark blue-gray, green-gray, or gray, fine- to medium-grained (0.08–0.25 mm.) lithic arenite or graywacke, rhythmically interbedded with dark green-gray to blue-gray shale. A representative mode of the graywacke is given in table 21. Texturally, the rock consists of angular, elongated slivers of detrital quartz and predominantly phyllitic rock fragments (0.08–0.25 mm.) set in a fine matrix of sericitic muscovite, clay, and chlorite (fig. 33). It is often difficult to distinguish smeared-out phyllitic fragments from balled-up micaceous matrix, both of which frequently blend or flow together. Depending upon the uncertainty of the matrix content, or the classification used, the Bellvale is either a low-rank graywacke (Krynine, 1948), a subgraywacke or lithic graywacke (Pettijohn, 1957), or a graywacke (Folk, 1954). Larger, bent grains of chlorite and muscovite in the matrix are common, and are here interpreted to have grown from fine matrix material, marking the beginning of the chlorite zone-greenschist facies of regional metamorphism, imprinted in either the Acadian or Alleghenian Orogeny.

In general, the Bellvale graywackes tend to show rhythmic interbedding with shale, with graded bedding low in the section and strong current cross-bedding higher in the section. Occasional brachiopods are found low in the section whereas plant fossils are found higher up. Both features suggest a gradation from marine to nonmarine environment. The provenance was a low-rank metamorphic or sedimentary terrane. Plant fossils may be found along Seven Springs Road south of the Mountain House.

The thickness of the Bellvale section in the Schunemunk Mountain area was estimated to be 400 meters by Colony (1933).

Along the western edge of Durland Hill, a gray, highly deformed, fissile shale grades uphill to the east into sandy, cross-bedded graywackes typical of the Bellvale Formation. Although this may be the Cornwall Shale which underlies the Bellvale graywackes to the northeast of the map area, it was not mapped as a separate unit here because of its gradational nature and uncertain assignment. The Cornwall Shale occurs near an old railroad overpass on the west edge of the Albany Turnpike, N.Y. 32 to Newburgh. This is a black shale carrying plant fossils and does not resemble the shale at Durland Hill.

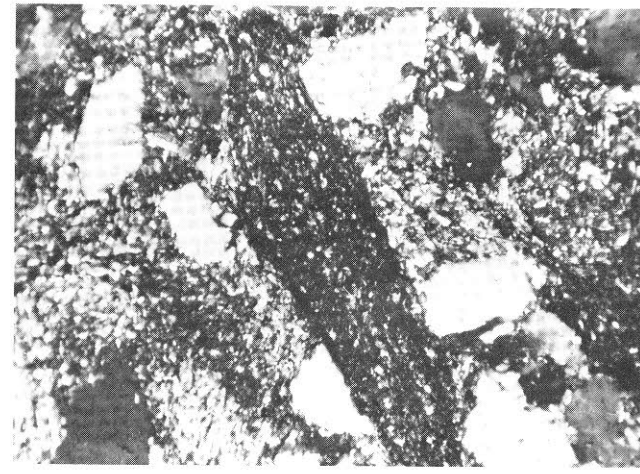

FIGURE 33. Bellvale Graywacke, Middle Devonian. Large phyllitic rock fragment and small angular quartz grains in argillaceous matrix. Sample 622. Crossed nicols. Angular quartz grains are 0.25 mm. in length.

Structural Geology

INTRODUCTION

The Monroe quadrangle has had a long and complex structural history. Because block-faulting has been the most recent event in this history, juxtaposing rocks of widely differing ages and characteristics, it seems best to discuss the structure in terms of the faulted blocks (delineated in fig. 34). Block 1, the Ramapo massif, consists entirely of Precambrian metamorphic rocks. Block 2, the Monroe massif, is also Precambrian for the most part. At its north end, however, it is veneered with early Paleozoic strata. The metamorphic rocks of the Ramapo massif are of slightly higher grade than those of the Monroe massif. Block 3, the Thruway graben, downfaults Wappinger dolostone between the upthrown Precambrian massifs. Block 4, the Bellvale syncline, is a graben containing folded Devonian rocks.

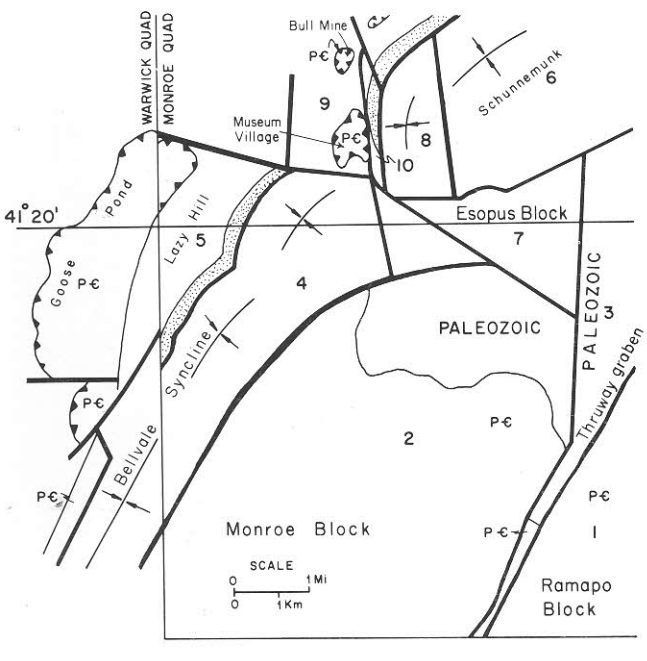

FIGURE 34. Principal fault blocks of the Monroe quadrangle, and their extension in the Warwick quadrangle (geology of the Warwick quadrangle after Offield, 1967). Stippled area is the Shawangunk.

Block 6, the main mass of Schunemunk Mountain, is its downthrown northern continuation, and block 8 is a rotated and downthrown nose of the same structure. Block 7, the Esopus block, was detached from block 2 along a NW-SE fault, probably during the downfaulting of block 6. Block 5, the Lazy Hill-Goose Pond block, was downthrown in pre-Silurian time along a N 75° W fault the (the Quickway fault). Blocks 8, 9, and 10 were rotated counterclockwise at some time after the formation of the Schunemunk-Bellvale Syncline.

Although block faulting is characteristic of the Triassic in this area, the block faulting in the Monroe quadrangle is demonstrably not all Triassic, as will be shown in the following discussion.

PRECAMBRIAN ROCKS

Ramapo Block (Block 1).

The Precambrian rocks of the Ramapo massif form the east wall of the Thruway graben. Except where their attitude is disturbed by faults, the ancient rocks strike uniformly about N 45° E and dip steeply to the east; they are stretched out in monotonous bands along strike in the Monroe quadrangle, and the nature of their folding cannot therefore be deduced from their outcrop pattern. As in the Popolopen Lake quadrangle (Dodd, 1965), all lineations plunge gently north.

The fault bordering the Thruway graben on the east is exposed in a small dolostone quarry on the Harriman estate, about one mile (1.6 kilometers) north of Arden and east of the Thruway. The back wall of the quarry is nearly vertical and made up of biotite gneiss which dips steeply east. About 0.4 km. east of Arden a complex of faults branches to the east, cutting off several blocks of rock and either tilting them or thrusting them up as horsts. These faults may be fairly late, because the rock is more shattered and crushed than chemically altered in contrast to some faults in the Monroe block.

Monroe Block (Block 2).

The Monroe massif is bounded on the east by the Thruway graben, to the west by a steep essentially vertical fault which separates it from the Bellvale syncline, and is covered to the north by a thin veneer of gently dipping Cambrian Poughquag conglomerate and Cambrian-Ordovician Wappinger dolostone. Under this thin sedimentary cover the Precambrian massif probably continues to its fault boundary against the Esopus block (block 7): evidence for this is that the positive magnetic anomaly shown over almost all the Precambrian of the Monroe and Maybrook quadrangles (Henderson et al., 1962) continues this far north, and then weakens abruptly along the presumed fault line.

Fold axes and other lineations in the Monroe massif show a broad maximum spreading from N18°E to N35°E, plunging about 15°N, and two subordinate maxima at S27°W and S35°W plunging 5°S (fig. 35 A-D). Foliations in all the Precambrian gneisses strike predominantly N15°–35°E; their dip is vertical to about 20°E; about 5 percent dip steeply west (fig. 35 A-D). Folding is, with a few exceptions, isoclinal and overturned to the west. Because of this, the many faults along and across the strike, and the widespread melting

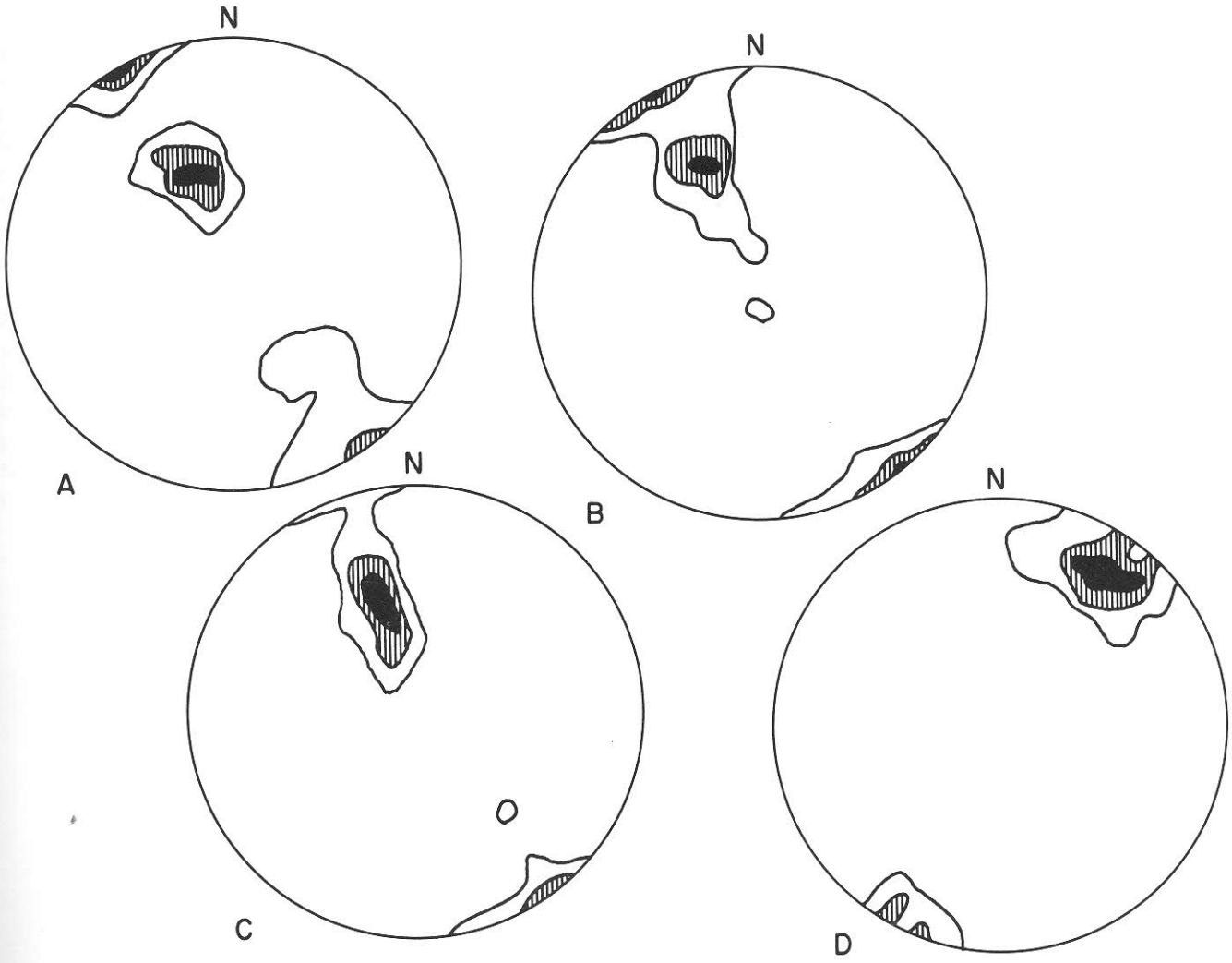

FIGURE 35. Fold axes and poles of foliation of Precambrian gneisses, plotted on equal-area projections, lower hemisphere. A. Poles of 130 amphibolite foliations. B. Poles of 137 hornblende granite foliations. C. Poles of 258 foliations of sillimanite-cordierite-almandine-biotite-quartz-feldspar gneiss, hypersthene-quartz-plagioclase gneiss, biotite mesoperthite gneiss, amphibolite-granodiorite gneiss. D. 104 axes of minor folds and mineral lineations.

and recrystallization, elucidation of the structure of the Monroe massif has been an interesting and complex task.

Although the hornblende granite gneiss (Belts 1, 5, 13) is believed to be the youngest of the Precambrian formations, it will be discussed first because its structure in Belts 5 and 13 has been the key to the stratigraphy of the Precambrian in the Monroe block. In most of Belt 13, the hornblende granite gneiss strikes NE and dips west: however, at Indian Hill in the southern part of Belt 13 it opens out into a clearly defined syncline, whose axis lies in the narrow valley atop the hill, and whose axial plane dips steeply east. In Belt 5, at its intersection with the Appalachian Trail, the hornblende granite gneiss lies horizontally on flat-lying amphibolite of Belt 6 and forms the mountain top. It is here interpreted as a remnant of the bottom of another syncline. This is borne out by the geologic map of the Sloatsburg quadrangle (Hotz, 1953), where the extension of Belt 5 is mapped as a complex refolded syncline. If, then, Belts 13 and 5, as well as the petrographically similar Belt 1, are the downfolded remnants of one sheet, the formations underlying the hornblende granite gneiss are stratigraphically equivalent, and must form complex anticlines between these major synclines.

Because the thick granite gneiss masses discussed above probably tended to behave more rigidly during folding than the thinner-bedded, hence less competent underlying strata, the anticlinal folds are extremely discontinuous and difficult to interpret. Strike faults in the amphibolite and hypersthene-quartz-plagioclase gneiss further complicate the picture, as does the melting which has produced the cross-cutting alaskites. Precambrian block-faulting which post-dates the metamorphism (evidence presented later) poses more problems. Although most folds in the Highlands plunge gently to the northeast, in the Monroe Quadrangle fold axes tend to be arranged in belts across the strike, plunging alternately north and south (fig. 35E). Thus, outcrop pattern alone is not a reliable guide to the anticlinal or synclinal nature of a particular fold. The porpoising of fold axes shown in figure 35E seems to imply a late folding or

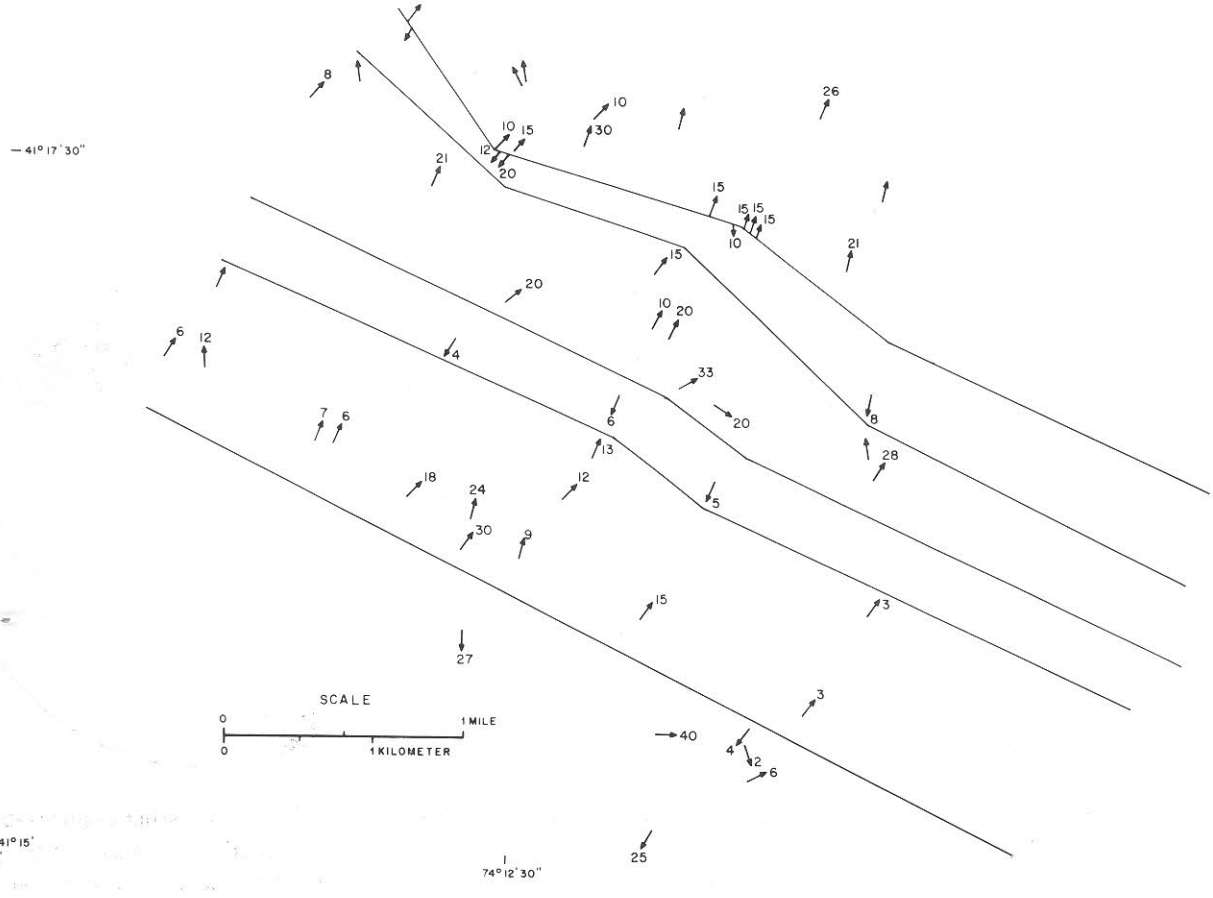

FIGURE 35E. North and south plunges of fold axes aligned in northwest-trending belts.

warping about a northwest axis. However, our data are insufficient to support such a conclusion.

East of Mombasha Lake, structures are generally strongly overturned to the west; the dip of the foliation is relatively shallow. The calc-silicate gneisses of Belt 12, figure 3, and the pelitic and other gneisses of Belts 7 and 8 are interpreted to be folded back on themselves in overturned anticlines. This kind of folding can be seen in minor structures within these belts but can be shown only diagrammatically in cross section.

West of Mombasha Lake, foliations are for the most part vertical or very steep east or west. The biotite mesoperthite gneiss and associated granodioritic rocks which are interpreted to form the core of the anticline between Belts 1 and 5 form complex folds with and melt across the overlying amphibolite-granodiorite gneiss.

Within Belt 6 is another anticlinal fold which has been ruptured at its crest by a strike fault. The anticlinal core was completely melted to alaskite (Belt 9). The east limb of this anticline is shallow in dip: the west limb is nearly vertical. To the east of this fold, all the structures are overturned to the west; west of it, most structures are vertical, a few are overturned to the east. Figure 36 shows a small structure that reflects what we believe to be the style of this larger anticline. This sketch shows an amphibolite anticline whose nose is cut across by mobilized hypersthene-quartz-plagioclase gneiss, in much the same way that the larger anticlinal belt of quartz-plagioclase gneiss is cut by the more mobile alaskite.

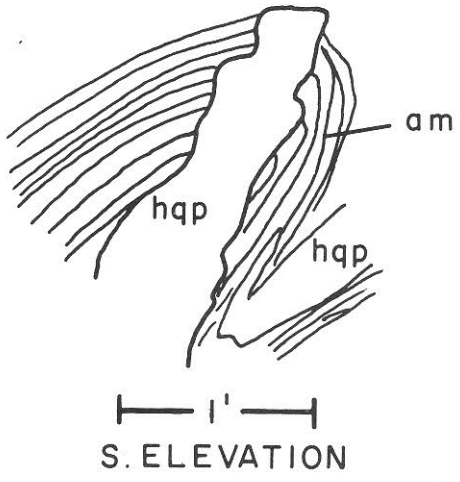

FIGURE 36. Fold in amphibolite (am) and hypersthene-quartz-plagioclase gneiss showing rupture of fold nose and local mobilization of hypersthene-quartz-plagioclase gneiss which is cross cutting the amphibolite.

In a highly metamorphosed area such as the Precambrian of the Monroe massif, the study of structure must take into account the relative competence of rock types toward metamorphism and anatexis. In general, the more granitic gneisses are less resistant and more readily mobilized than are the more basic rocks which tend to fail by rupture rather than by flowage, and are often left as disoriented remnants which have been floated around to all angles within the more plastic matrix that surrounds them. The alaskite is, of course, the extreme example of this kind of anatexis: *sensu stricto,* it rarely has foliation of its own, but remnant shreds of partly digested inclusions may supply one. The quartz plagioclase gneiss, though relatively basic, is also fairly easily mobilized owing to its high content of quartz: it also may form a massive matrix with disoriented, finely-foliated shreds at all angles. There is a fine example of this on the Appalachian Trail west of East Mombasha road, and another at the circular drive on the west shore of Mombasha Lake. At the latter locality, the quartz-plagioclase gneiss matrix is extremely coarse and massive, and most certainly has been locally molten.

Faults within the Monroe block strike northeast, parallel to the foliation and the Triassic border fault; slightly west of north; and across the foliation at angles near 90°. The faults approximately parallel to West Mombasha Road and Bramertown Road along with the fault between Belts 11 and 12 delimit a block which the authors believe, from the apparent displacement and from petrographic considerations, to have been uplifted with respect to the rest of the Monroe block: uplift may have been greatest to the south and west. The major movement along all of these faults must have been post-metamorphic but Precambrian because the feldspars of the Poughquag conglomerate immediately overlying the metamorphic gneisses have fresh authigenic rims, and are not sericitized, while just to the south both amphibolite and alaskite have heavily sericitized plagioclase feldspars due to retrograde metamorphism along the fault. This reasoning does not, of course, rule out minor movement along these faults in subsequent episodes, but only movement intense enough to produce retrograde metamorphism.

Klippen

Four Precambrian klippen west of the main massif are a special problem in themselves. They are petrographically distinct from the Precambrian of the Monroe and Ramapo blocks in the Monroe quadrangle. Poles of foliations within the klippen show no well-defined maximum, but seem to delineate a saucer tipped gently toward the east. Their petrography has already been

described as resulting from extreme cataclasis. The Goose Pond klippe rests on the west on northward overturned Ordovician shale. The Museum Village klippe's southwest corner rests in overthrust contact on Cambrian-Ordovician Wappinger dolostone (fig. 37). All the klippen of the Monroe, Maybrook, and Warwick quadrangles lie within a narrow belt, with the exception of Goose Pond and Museum Village klippen: the former is much broader and apparently displaced to the west from the general trend; the latter is also somewhat broad, and is not only displaced to the east but rotated to a north-south trend. Bull Mine Mountain, to the north of Museum Village klippe, also shows a similar but lesser rotation. The significance and explanation of these displacements will be elucidated in the section on Structural History.

PALEOZOIC ROCKS

Poughquag Quartzite

This lowest Cambrian formation occurs only in one area of Block 2 (fig. 34), where it unconformably overlies the Precambrian gneisses of Belts 5 and 6 (fig. 3). The contact is everywhere covered. Foliation in the gneiss is nearly vertical or steeply dipping east, whereas the Poughquag dips about 5–10° to the north, northeast, and northwest, apparently following the Cambrian shoreline. Because the outcrops are discontinuous and the bottom is not exposed, no estimate of thickness has been made.

Wappinger Group

In Block 2 the Wappinger Dolostone overlies the Poughquag Quartzite, or, in its absence, may overlie the Precambrian gneisses. The contact is covered; outcrops are sparse. In this block the dolostone dips 5–10° north, northeast, and northwest, again probably following the ancient shoreline. It does not outcrop to the north of the fault that separates Blocks 2 and 7 but may lie under the Pleistocene and Recent cover up to this fault.

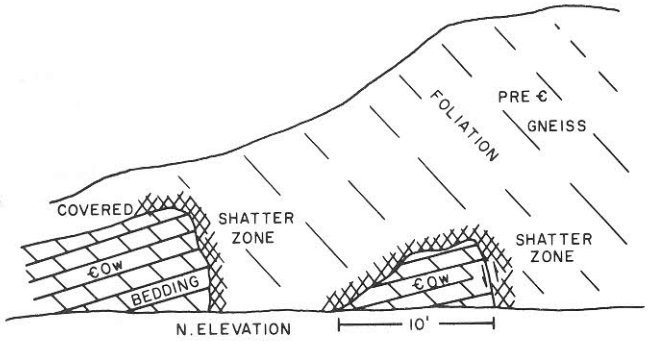

FIGURE 37. Exposure on the north side of N.Y.-17 Quickway, about 220 meters west of Museum Village overpass, showing Precambrian gneiss of Museum Village klippe thrust over Cambrian-Ordovician Wappinger dolostone.

In Block 3, the Thruway graben, the Wappinger Dolostone is downfaulted between the Ramapo massif on the east and the Monroe massif on the west. The dolostone probably extends as far as Arden. The dolostone is much crumpled and its folding probably reflects the movement along the boundary faults, which was greater along the east side than along the west side. In the quarry 1.6 km. north of Arden on the east side, the dolostone is nearly vertical, while directly across the graben on its west side, the dolostone dips gently east, forming a syncline between the Precambrian blocks. Along the stream which cuts Dunderberg Road south of Central Valley, the dolostone is thrown into relatively tight folds on itself.

In Block 5, the dolostone dips gently west, toward the Goose Pond klippe. Its possibly unconformable contact with the overlying Ramseyburg shale and subarkose is covered as is its contact with the klippe.

The only other occurrence of Wappinger dolostone in the Monroe quadrangle is in Block 9, where it underlies the Museum Village klippe. It is here exposed from N.Y. 17 M to the north side of the Quickway at Museum Village where it is well exposed underlying the sole of the thrust (fig. 37). About 15 meters to the west of this sketch, the dolostone is broken into blocks by steep faults, the blocks being surrounded by shattered dolostone. The dolostone in these fault blocks dips 10–15° west. Isolated outcrops of dolostone on the east side of Block 9 dip vertically or steeply to the east, and may indicate that the klippe came to rest on the crest of an old anticline: however it is more likely that the attitude of the dolostone was disturbed during the emplacement of the klippe.

Bushkill Shale

The Bushkill Shale does not outcrop east of the Devonian syncline. It occurs around the klippen, whose emplacement has evidently influenced its attitude. There is a small anticline in the shale between Bull Mine klippe and Merriewold klippe. Northwest of Goose Pond klippe along N.Y. 17 M just over the border of the Warwick quadrangle, the shale is overturned to the north.

No systematic study was made of the attitudes of the Bushkill Shale away from the klippen because out-

crops were too few. Bedding generally strikes NE–SW along the regional strike, and dips are gentle east and west. This would indicate the same sort of broad open folding Offield (1967) found in the Goshen 15-minute quadrangle.

Ramseyburg calcareous quartzite (subarkose) and shale

The Ramseyburg outcrops only in Block 5, where it forms the major part of Lazy Hill. It is here tightly folded, with strike faults along the crests of folds (fig. 38), and may be overturned to the east. Owing to the scarcity of outcrops, few readings were obtained, but the mode of east dips is 60–65°, of west dips 35°. Offield (1967, p. 64) notes that the Paleozoic syncline between his middle block and west block of Precambrian, and the Paleozoic anticline around his west block, have an asymmetry which is "the reverse of the usual asymmetry of Allegheny Valley and Ridge folds," which he ascribes to the rotation of Precambrian blocks during a general rise of the basement. However, it is difficult to see how this could have affected the Ramseyburg in Lazy Hill, unless there were a general compressive force from the west during its folding. That there may have been such a force is indicated by the similar asymmetry of the folding in the Monroe block, which is generally gently dipping east, east of Mombasha Lake, and vertical or steeply dipping west, west of Mombasha Lake.

Because of few outcrops, no attempt was made to detail the folding of the two members of the Ramseyburg; it is probably more complex than is indicated on cross section B–B′, Plate 1. That the Ramseyburg of Lazy Hill is overlain unconformably by the Shawangunk Conglomerate is indicated by the fact that both the 'grit' and the shale member are in contact with the Shawangunk. There was a period of folding (Taconian) before the deposition of the Shawangunk.

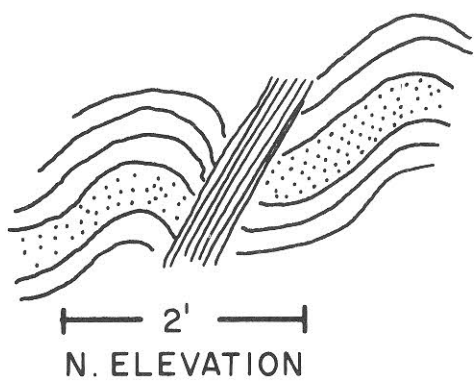

FIGURE 38. Fold in Ramseyburg shale just below the powerline on Booth Road, on Lazy Hill, Block 5. Closely spaced diagonal lines indicate a zone of faulting.

Shawangunk conglomerate and orthoquartzite

The Shawangunk conglomerate outcrops both in Block 5, Lazy Hill, where it overlies the Ramseyburg grit and shale, and in Block 10, where it has had a rather special structural history and it has been found in the Maybrook quadrangle between Schunemunk Mountain and the line of klippen.

In Block 5, the Shawangunk forms a dip slope to the east along the side of Lazy Hill, were it has protected the less resistant Ramseyburg shales from erosion. Both its upper and lower contacts are covered, and there is a broad valley between the top of the Shawangunk and the bottom of the Devonian syncline. Because of marked downdip pebble-stretching, fluting, and other lineations, the Shawangunk is assumed to have moved during folding and faulting as a series of rigid plates. A normal fault is assumed to be present at its top between Blocks 5 and 4, partly on the basis of the down-dip lineations, and because the Devonian syncline must have been considerably downdropped to account for the thickness of rock that outcrops.

Block 10 is an especially interesting case. It apparently once lined up with the Shawangunk of Lazy Hill, and of the Maybrook quadrangle to the north, but has been rotated and crumpled during the rotation of Blocks 8 and 9 between which it lies. Figure 39 is a diagrammatic plan view of strikes, dips, lineation, and a fault in the Shawangunk outcrop of Block 10, which is a narrow, continuous ridge roughly 185 meters in length.

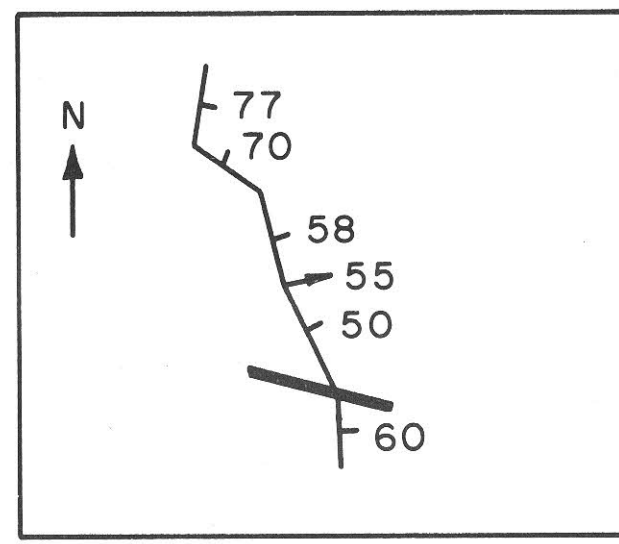

FIGURE 39. Diagrammatic plan view of strikes, dips, lineation, and fault in 185 meter outcrop of Shawangunk quartzite and conglomerate near Spring Glen golf driving range 185 meters west of N.Y. 208 and .5 km. north of Museum Village Road.

Connelly Conglomerate and Esopus Shale

The Esopus Shale occurs in Blocks 4 and 7. The Connelly Conglomerate occurs with the Esopus shale of Block 4, and may also occur in Block 10. Block 10 contains an outcrop of a highly silicified conglomerate with rounded pebbles, so cross bedded that its attitude is extremely puzzling. It would in any case have been involved in the rotation and crumpling of Block 10; this is apparent from a great many silicified fractures. In Block 4, a small outcrop on the west side of the Devonian syncline, just below Museum Village road, is thought to represent Connelly Conglomerate. The Connelly has been identified with certainty only at the Monroe Bowl-O-Fun, where it underlies the Esopus Shale and is separated from it by a fault.

In Block 4, the Esopus Shale is exposed only on the east side of the Devonian syncline. On the west side of Walton Lake, a small pit at the west side of Greenwood Lake Road exposes steeply west-dipping, highly fractured and contorted unfossiliferous shale. At the Monroe Bowl-O'-Fun, at the northeast end of Block 4, there was a large outcrop of fairly fossiliferous shale and siltstone since obliterated to make room for commercial development. This overlay the Connelly Conglomerate, but was separated from it by a fault, trending N65°E, 60°S. Bedding of the Connelly here was N78°E, 65°N, of the Esopus, N80°E, 45°N. A rude bedding-plane cleavage ran N63°E, 53°N, but bedding and bedding-cleavage relationships were obscured by many faults and joints, since the Bowl-O-Fun is located near the intersection of several major faults.

In Block 7, the Esopus outcrops in three small localities. In all, it dips gently to the north (about 25°) and the projected strikes form a broad east-west arc convex to the north. In contrast to the outcrop at the Bowl-O-Fun, the Block 7 outcrops show little evidence of stress or cataclasis. They are believed to have broken off the north end of Block 2, the Monroe massif, which had served to buffer them against the major faulting, during the folding of the Devonian syncline. This break, which would explain their dips which are somewhat steeper than those of the perfectly protected Poughquag and Wappinger of Block 2, probably occurred after the folding of the Devonian syncline and during the downdropping of Block 6 possibly as late as the Triassic. This sinking downwarped Block 7 and caused the rotation of Blocks 8, 9, and 10.

Bellvale Graywacke

The Bellvale Graywacke occurs in Blocks 4, 6, and 8, in a fairly broad, open syncline which is a continuation of Schunemunk Mountain to the north and the Green Pond syncline to the south. Its synclinal axis follows the regional trend with the single exception of Block 8; the syncline is overturned to the west, the average of west dips being 49° and the average of east dips being 34°. The graywacke is extensively cross-bedded, and it is often difficult to determine the true bedding.

The continuity of the Bellvale syncline is broken at the north end of Block 4 by faults trending E-W and N-S. Outcrops at this end of the syncline strike aberrantly NW and dip NE; many fault surfaces with heavy vertical slickensides are apparent. In the rest of Block 4 bedding slopes gently in to the synclinal axis.

In Block 6, strata on the north side of the syncline dip regularly east, but on the south side irregular dips and strikes may reflect the multiple character of the fold. Outcrops in the Monroe quadrangle are, however, too sparse to clarify these relationships.

In Block 8, the synclinal axis is rotated counterclockwise to N-S. Vertical slickensides are apparent on most outcrops, especially those to the south and west of the block. It is the author's contention that at some time after the folding of the syncline, Block 6 was dropped down with respect to Block 4, and Block 8 was broken off and rotated about 47° during the sinking of Block 6.

FRACTURES

Joints and Dikes

Figure 40A shows the principal maxima of the joints in all the pre-Devonian rocks. The single NNE joint set is approximately perpendicular to the regional compression. The conjugate joint set striking NW-SE, with the stronger component perpendicular to the regional strike, may represent shear joints in response to the same stress or tension joints in response to slightly different directions of stress.

Figure 40B shows the principal maxima of joints for Devonian rocks only. The joint set perpendicular to the regional compression is relatively weak. There is a conjugate joint set at about 90° to that of the pre-Devonian rocks, and there is an additional strong set of almost E-W joints. Such a pattern might result from a counterclockwise couple acting parallel to the E-W joint (or approximately parallel to the Quickway Fault). Movement of this sort might have caused the counterclockwise rotation of Blocks 8, 9, and 10; this

rotation would have relieved the strain caused by such movement, so that it penetrated no further east to disturb Blocks 7, 3, and 1.

Figure 40C shows poles of 33 dikes in the Monroe quadrangle. It is immediately obvious from the joint patterns that these dikes must be pre-Devonian, and indeed, they are found only in the Precambrian and immediately overlying Poughquag and Wappinger. Further, they do not occur outside the Monroe and Ramapo blocks. However, Offield (1967, p. 30) reports a dike which is "a series of sheared, broken and disconnected pieces at the crest of the hill...[on]...the east side of Sugarloaf Mountain" which is the southwestward extension of Goose Pond klippe. This dike, as described, must have been overthrust with the klippe, and therefore was emplaced before the thrusting. Dodd (1965, p. 31) reports similar dikes but does not show such a clearly bimodal maximum for their poles. His single maximum, however, coincides exactly with the more northerly pole maximum of figure 40C.

Faults

An attempt was made to elucidate the nature of the faulting by plotting the poles of fault planes observed in the field on point diagrams. As the points were literally all over the map, this led nowhere, even when the points were separated out by formations and blocks. It was then decided that the observed faults were subsidiary to the major faults which were obvious from the map pattern; the relative movements of the major fault blocks were then deduced. The Monroe area, and in particular the area between Blocks 4, 8, 9, and 10, has been the focus of intense shattering since the Precambrian, and all the block faulting in the Highlands is not necessarily Triassic.

STRUCTURAL HISTORY

Precambrian

After deposition, a large pile of volcanic and sedimentary rocks were folded along a NE-SW axis and metamorphosed. A period of block faulting ensued, with the faults parallel, perpendicular, and diagonal to the foliation. A large block delimited by faults along West Mombasha and Bramertown roads in Block 2 was tilted to the north. Perhaps shortly after the termination of the folding, a fault roughly parallel to the foliation, and of unknown displacement, separated the rocks with gently dipping foliations east of Mombasha Lake from the rocks with steeply dipping foliations west of it.

Cambrian

At some time before the deposition of the Poughquag Quartzite, the Precambrian rocks were uplifted and denuded. This may have been contemporaneous with the block faulting mentioned above. The Poughquag and at least the basal Wappinger were deposited unconformably on the resulting erosion surface; the former was probably preserved only in sheltered coves.

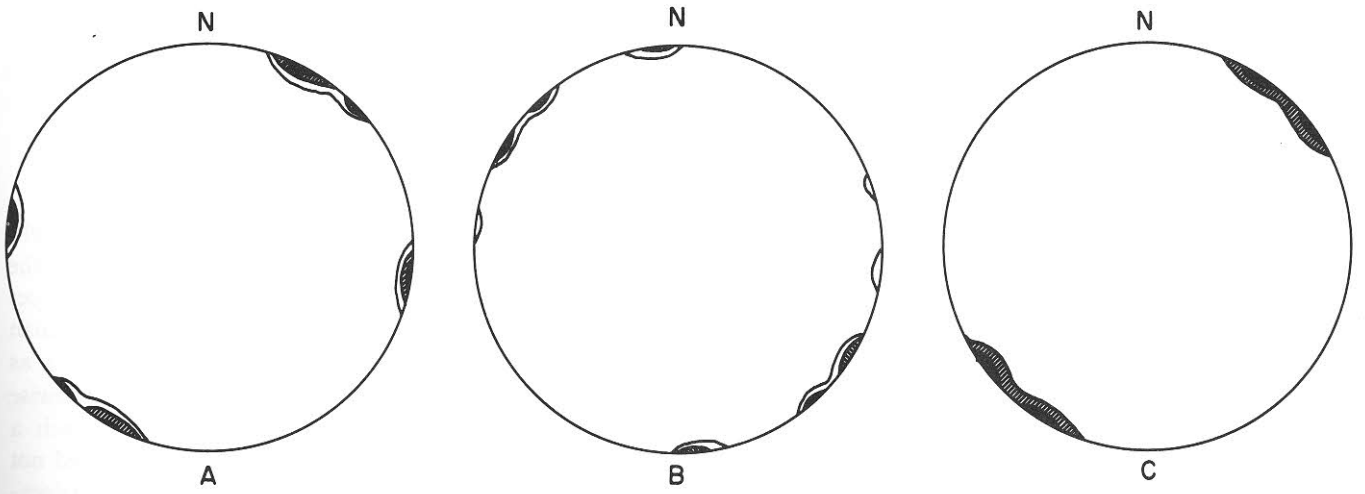

FIGURE 40. Poles of joints and dikes. A. Poles of 164 joints in the Precambrian rocks. > 20%, > 15%, > 10%. B. Poles of 71 joints in Devonian rocks. > 10%, > 5%. C. Poles of 33 dikes. > 20%, > 10%.

Ordovician

Deposition of the Wappinger may have continued into the Ordovician. At some time the same fractures that cut the Precambrian were impressed on the Poughquag and Wappinger, and dikes were intruded into the tension joints. Possibly there was some renewed movement along the Precambrian faults at this time, because the NE-SW fault that goes through the center of Mombasha Lake appears to have shifted the position of the lamprophyre dike that cuts across it just to the south of the Poughquag outcrop. However, curved tension fractions are relatively common and the displacement may only be apparent. Possibly this same fault may cut off the Poughquag outcrop, which ends abruptly at this point, but no evidence of this has been found, and the juxtaposition may be merely coincidental.

The Middle Ordovician Bushkill shale was deposited, and succeeded by the Ramseyburg 'grit' and shale. In Block 5, the Ramseyburg may rest unconformably on the Cambrian-Ordovician Wappinger dolostone where the Bushkill Shale is absent. An unconformity of analogous age has been reported by Hall (1968) in the Manhattan Prong, where Middle Ordovician Manhattan Schist rests unconformably on Cambrian-Ordovician Inwood dolomite marble. During or shortly after the deposition of the Martinsburg Formation in the Monroe area, the Taconic folding occurred, gently warping the shales and the Wappinger. During or shortly after Taconic folding the klippen were probably overthrust, inducing additional folding in the adjacent Bushkill "as though the thin skin of shale above the dolostone had been rumpled above the moving thrust block" (Offield, 1967).

The shales had been deposited over the entire area, providing a slippery surface for the thrusting of the gneiss klippen. These are not akin to any of the other Precambrian gneisses of the Monroe area and must have come from farther east. The dike which Offield reports on the east side of Sugarloaf Mountain, the continuation of Goose Pond klippe, must have been emplaced before thrusting, and traveled with the klippe. During or shortly after emplacement, the klippen were folded along a NE-SW axis, and then eroded to leave a synclinal remnant extending from Balmville, north of Newburgh, to Snake Mountain in the Warwick quadrangle.

This folding and erosion was followed by faulting along the Quickway Fault (N75W), with apparent displacement of the line of klippen to the east (Offield, 1967, postulates a similar fault to account for the displacement of Snake Mountain with respect to Sugar Loaf and Goose Pond Mountains). This displacement could be accounted for either by lateral movement or by uplift of east-dipping klippen. The latter alternative seems to be more germane to the regional style. If uplift is then the answer to the apparent displacement of the klippen, the more easterly klippen should stand higher topographically. This is true in the Monroe quadrangle, where Goose Pond Mountain rises from an elevation of 500 feet, while Museum Village klippe begins at 600 feet and Bull Mine klippe at about 800. In the Warwick quadrangle, Sugar Loaf Mountain's Precambrian rocks are indicated as low as 500 feet, while Snake Mountain's klippe begins at about 600 feet (Offield, 1967, Plate 1).

Silurian

After an erosion interval, the Shawangunk Conglomerate was deposited unconformably on the older rocks.

Devonian

Lower Devonian Connelly and Esopus and Middle Devonian Bellvale sediments were deposited, possibly, as Offield (1967) suggests, between rising basement blocks forming a syn- or very shortly post-depositional syncline. During this folding — which may have been, as Offield suggests, by draping between rising basement blocks, or may instead have been related to the Acadian or Alleghanian folding — the relatively thin and brittle Shawangunk beds broke into detached plates which apparently bore the brunt of the downfaulting. This faulting produced the fluting parallel to the dip of the beds and the marked stretching of the pebbles parallel to both the a and b fabric axes.

Post-Devonian

Following the formation of the Schunemunk-Bellvale-Green Pond syncline, and perhaps as late as the Triassic, further movement of the basement blocks occurred. As has been previously noted, the Devonian rocks have their own distinct set of joints, such as might have been produced by a counterclockwise couple acting parallel to the N75°W fault. Such a couple might be a component of uplift, which need not be strictly vertical. The events of this latest dislocation include:

a. the uplift of Block 1 to form the Ramapo Mountains.

b. the uplift of Block 2, including its overlying Paleozoic sediments.

c. the downfaulting of Block 3, the Thruway graben. Based on the attitude of the Wappinger dolostone within the graben, Block 1 was lifted up higher than Block 2. This is borne out by petrographic evidence, that is, the slightly higher grade of metamorphism in the Ramapo block, which implies deeper burial.

d. Block 4, possibly already downfaulted relative to Blocks 2 and 5, was lifted up relative to Blocks 6 and 8. Anomalous dips at the north end of Block 4 may be the result of drag during faulting.

e. Block 5 may have been further upthrown with respect to Block 4.

f. Block 6, the main mass of Schunemunk Mountain, was downthrown considerably with respect to Block 4, which has a moderate positive geomagnetic anomaly, indicating that basement is not very far down (Henderson et al., 1962).

g. Block 7, in which the Esopus dips about 25° N and under which the basement anomaly is absent, probably was tilted to the north during the uplift of Block 2 and the sinking of Block 4. It is detached from Block 2 by an eastward extension of the Quickway Fault.

h. Block 8, where the synclinal axis of Schunemunk swings to north-south, has been rotated counterclockwise.

i. Block 9, including the Museum Village and Bull Mine klippen, has also been rotated counterclockwise.

j. Block 10, including a sliver of Shawangunk and problematic Connelly, has been ground, thrust, rotated, and crumpled between Blocks 8 and 9. Figure 41 shows the probable prerotation status of Blocks 8, 9, and 10. By rotating the blocks 47° clockwise, the Shawangunk and the synclinal axis of the Bellvale are brought into coincidence with their continuation to the southwest. The Museum Village and Bull Mine klippen line up with Merriewold and Snake Mountain Klippen, but not with the Sugar Loaf-Goose Pond mass. The Wappinger Dolostone also remains apparently displaced.

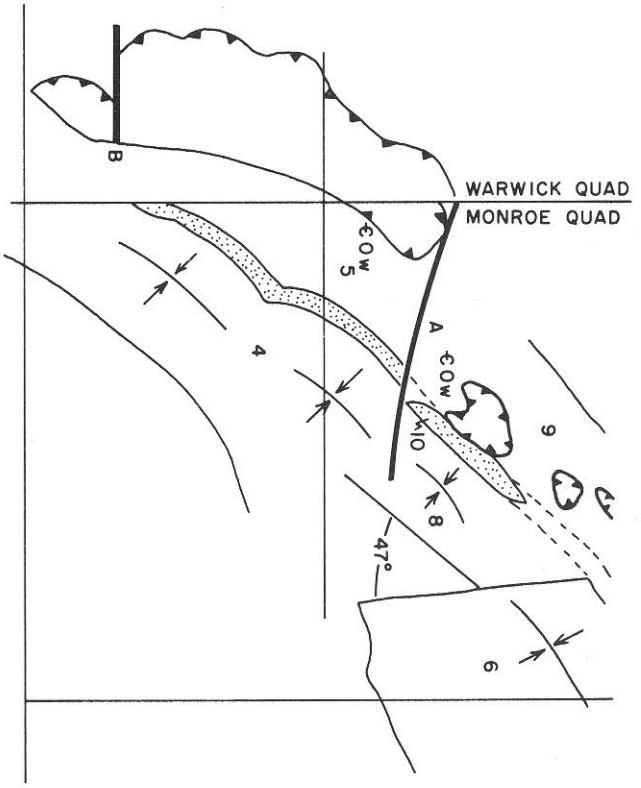

FIGURE 41. Geologic map of parts of the Monroe and Warwick quadrangles as they may have appeared before the rotation of Blocks 8, 9, and 10 (Warwick quadrangle modified after Offield, 1967).

Economic Geology

Except for continuing exploitation of sand and gravel deposits, there has been no significant mining activity in the Monroe quadrangle in recent years. Sand and gravel deposits are exploited in the north-central part of the quadrangle west of the intersection of Mountain Road with N.Y. Route 208, and in the western part of the quadrangle south of Walton Lake. Reserve deposits are abundant in the valleys.

Small magnetite pits, sporadically distributed throughout the quadrangle (plate 1), testify to widespread former mining activity which began in Revolutionary times and continued until late in the nineteenth century. These include Bull Mine, where magnetite occurs in small shoots in amphibolite in Bull Mine klippe of Belt 25. It is evidently a good example of an allochthonous mineral deposit. The O'Neil Mine occurs just south of the Orange Turnpike at the boundary of Belts 7 and 11. Small elongate ore shoots were localized here along the contact of amphibolite with leucogranite. Another deposit on the south side of Mine Road in Belt 2 is associated with a pyroxene-hornblende granulite lens in the amphibolite-granodiorite unit. Clinopyroxene in the granulite contains exsolution lamellae of pigeonite and/or clinohypersthene and evidently crystallized at a high temperature. Additional small, scattered magnetite pits occur, associated with pyroxene granulite in pelitic paragneiss of Belt 7, on von Schott's hill; in the Faber Mine east of Berry Road in Belt 3, and in hypersthene-quartz-plagioclase gneiss west of Cedar Cliff Road in Belt 2. None of these could have constituted relatively large deposits similar to those found farther south in the Sterling-Ringwood and Dover magnetite districts of New York and New Jersey. No studies were made of these small deposits.

Ruins of Greenwood Furnace are located near the intersection of the Orange Turnpike and Bramertown Road in the south-central part of the quadrangle. The chain that was stretched across the Hudson River near West Point to stop the British navy during the Revolution, was reportedly forged at this furnace. Ruins of another furnace, Arden Furnace, are located east of the New York State Thruway near the village of Arden.

Dolomite was once quarried from the Wappinger Formation east of the Thruway in a quarry located at the sharp bend in the Woodbury-Tuxedo town line (plate 1). No additional dolostone quarries have been found, although three small shale pits occur in the northwest corner of the quadrangle (plate 1).

References Cited

Aubouin, Jean.
1965. Geosynclines: Developments in geotectonics 1. Elesevier Publ. Co., Amsterdam. 241–250.

Barker Fred.
1961. Phase relations in cordierite-garnet-bearing Kinsman quartz monzonite and enclosing schist, Lovewell Mountain quadrangle, New Hampshire. Amer. Mineral. 46: 1166–1176.

Berry, W. B. N.
1959. Graptolitic fauna of the northern part of the Taconic area. In Zen, E-an, Stratigraphy and structure of west central Vermont and adjacent New York. Guidebook for the 51st annual meeting of the New England Intercollegiate Geologic Conf.: 61–62.

———
1962. Stratigraphy, zonation, and age of Schaghticoke, Deepkill, and Normanskill shales, eastern New York. Geol. Soc. Amer. Bull. 73: 695–718.

———
1963. On the "Snake Hill Shale." Amer. Jour. Sci. 261: 731–737.

Binns, R. A.
1962. Metamorphic pyroxenes from the Broken Hill district, New South Wales. Mineral. Mag. 33: 320–338.

———
1965. The mineralogy of metamorphosed basic rocks from the Willyama Complex, Broken Hill district, New South Wales. Part I Hornblendes. Mineral. Mag. 35: 306–326.

Boucot, A. J.
1959. Brachiopods of the Lower Devonian rocks at Highland Mills, New York. Jour. Paleont. 33: 727–769.

Bowen, N. L.
1928. The evolution of the igneous rocks. Princeton Univ. Press, Princeton, N.J.

Boyd, F. R. & Brown, G. M.
1968. Electron-probe study of exsolution in pyroxenes. Carnegie Inst. Wash. Yearbook 66: 353–359.

———
1969. Electron-probe study of pyroxene exsolution. Carnegie Inst. Wash. Yearbook 67: 83–86.

Brown, G. M.
1957. Pyroxenes from the early and middle stages of fractionation of the Skaergaard intrusion, East Greenland. Mineral. Mag. 31: 511–543.

———
1968. Experimental studies on inversion relations in natural pigeonites. Carnegie Inst. Wash. Yearbook 66: 347–358.

Buddington, A. F.
1939. Adirondack igneous rocks and their metamorphism. Geol. Soc. Amer. Mem 7.

———
1963. Isograds and the role of H_2O in metamorphic facies of orthogneisses of the northwest Adirondark area, New York. Geol. Soc. Amer. Bull. 74: 1155–1182.

———
1965. The origin of three garnet isograds in Adirondack gneisses. Mineral. Mag. 34:71–81.

——— **& Leonard, B. F.**
1953. Chemical petrology and mineralogy of hornblendes in northwest Adirondack granitic rocks. Amer. Mineral. 38: 891–902.

———
1962. Regional geology of the St. Lawrence County magnetite district, northwest Adirondacks, New York. U.S. Geol. Survey Prof. Paper 376.

Campbell, Ian & Schenk, E. T.
1950. Camptonite dikes near Boulder Dam, Arizona. Amer. Mineral. 35: 671–692.

Chayes, Felix.
1944. Petrographic analysis by fragment counting. Econ. Geol. 39: 489–504.

———
1952. Relations between composition and indices of refraction in natural plagioclase. Amer. Jour. Sci., Bowen Volume: 85–105.

Colony, R. J.
1923. Magnetite deposits of southeastern New York. N.Y. State Mus. Bull. 249–250.

———
1933. Structural geology between New York and Schunemunk Mountain. XVI Intern. Geol. Cong. Guidebook 9: New York Excursions.

Coombs, D. S.
1965. Sedimentary analcime rocks and sodium-rich gneisses. Mineral. Mag. 34: 144–158.

Cooray, P. G.
1962. Charnockites and their associated gneisses in the Pre-Cambrian of Ceylon. Geol. Soc. London Quart. Jour. 118: 239–273.

Darton, N. H.
1894. Geologic relations from Green Pond, New Jersey to Schunemunk Mountain, New York. Geol. Soc. Amer. Bull. 5: 367–394.

Deer, W. A., Howie, R. A. & Zussman, Jack.
1963. Rock-forming minerals, 2, Chain silicates. John Wiley and Sons Inc., New York.

de Waard, Dirk.
1965a. The occurrence of garnet in granulite facies terrane of the Adirondack Highlands. Jour. Petrol. 6: 165–191.

———
1965b. A proposed subdivision of the granulite facies. Amer. Jour. Sci. 263: 455–461.

———
1966. The biotite-cordierite-almandine subfacies of the hornblende granulite facies. Can. Mineral. 8: 481–492.

Dodd, R. T., Jr.
1963. Garnet-pyroxene gneisses at Bear Mountain, New York. Amer. Mineral. 48: 811–820.

———
1965. Precambrian geology of the Popolopen Lake quadrangle. Southeastern New York. Map and Chart Ser. No. 6, N.Y.S. Mus. and Sci. Serv., Albany.

Eckelmann, F. D.
1963. Precambrian events recorded in zircon populations of the Storm King granite and Canada Hill gneiss, Bear Mountain, New York. (Abs.) Program of 44th Annual Mtg., Amer. Geophys. Union: 120.

Edelman, C. H. & Doeglas, D. J.
1931. Reliktstrukturen detritischer Pyroxenen und Amphibolen. Mineral. Petrog. Mitt. 42: 482–490.

Ernst, W. G.
1966. Synthesis and stability relations of ferrotremolite. Amer. Jour. Sci. 264: 37–65.

Eskola, Pentti.
1939. Die metamorphen Gesteine. In Barth, T. F. W., Correns, C. W., and Eskola, P., Die Enstehung der Gesteine, Springer-Verlag, Berlin.

Fisher, D. W., Isachsen, Y. W., Rickard, L. V., Broughton, J. G. & Offield, T. W.
1962. Geologic map of New York, 1961. Map and Chart Ser. 5. N.Y.S. Mus. and Sci. Service, Geol. Surv., Albany.

Folk, R. A.
1954. The distinction between grain size and mineral composition in sedimentary rock nomenclature. Jour. Geol. 62: 344–359.

Fyfe, W. S., Turner, F. J. & Verhoogen, John.
1958. Metamorphic reactions and metamorphic facies. Geol. Soc. Amer. Mem. 73.

Goldschmidt, V. M.
1911. Die Kontaktmetamorphose im Kristianiagebiet. Oslo Vidensk. Skr., I, Mat. Naturv. Kl., 11.

Gordon, C. E.
1911. Geology of the Poughkeepsie quadrangle. New York State Mus. Bull. 492: 39–48.

Gruner, J. W. & Thiel, G. A.
1937. The occurrence of the fine-grained authigenic feldspar in shales and silts. Amer. Mineral. 22: 842–846.

von Gümbel, C. W.
1879. Die paleolithischen Eruptivgesteine des Fichtelbirges. Gotha, 36.

Hall, L. M.
1968. Times of origin and deformation of bedrock in the Manhattan Prong. In Studies of Appalach-

ian Geology, ed. Zen, E-an, White, W. S., Hadley, J. B., and Thompson, J. B., Jr. 117–127.

Hart, S. R.
1961. The use of hornblendes and pyroxenes for K-Ar dating. Jour. Geophys. Res. 66: 2995–3001.

———, & Dodd, R. T., Jr.
1962. Excess radiogenic argon in pyroxenes. Jour. Geophys. Res. 67: 2998–2999.

Henderson, J. R., Smith, F. C. & others
1962. Aeromagnetic map of parts of the Monroe and Maybrook quadrangles, New York. U.S. Geol. Survey, Geophys. Invest. Map GP-339.

Hess, H. H.
1949. Chemical composition and optical properties of common clinopyroxenes. Amer. Mineral. 34: 621–666.

———
1952. Orthopyroxenes of the Bushveld type, ion substitutions and changes in unit cell dimensions. Am. Jour. Sci., Bowen Volume: 173–187

———
1960. Stillwater igneous complex, Montana. Geol. Soc. Amer. Mem. 80.

Hietanen, Anna.
1947. Archean geology in the Turku district in southwestern Finland. Geol. Soc. Amer. Bull. 58: 1019–1084.

Holdaway, M. J.
1966. Hydrothermal stability of clinozoisite plus quartz. Amer. Jour. Sci. 264: 643–667.

Hotz, P. E.
1953. Magnetite deposits of the Sterling Lake, N.Y. — Ringwood, N.J. area. U.S. Geol. Survey Bull. 982-F.

Howie, R. A.
1965. The geochemistry of the charnockite series of Madras, India. Trans. Roy. Soc. Edinburgh 62: part 3, 725–768.

Hubbard, F. H.
1965. Antiperthite and mantled feldspar textures in charnockite (enderbite) from SW. Nigeria. Amer. Mineral. 50: 2040–2051.

Hudson, G. H. & Cushing, H. P.
1931. The dike invasions of the Champlain Valley, New York. New York State Mus. Bull. 286: 81–112.

Jaffe, H. W.
1953. Amygdular camptonite dikes from Mount Jo, Mount Marcy quadrangle, Essex County, New York. Amer. Mineral. 38: 1065–1077.

———, & Jaffe, E. B.
1962. Geology of the Precambrian crystalline rocks and Cambro-Ordovician sediments of the southern part of the Monroe quadrangle. Guidebook for N.Y.S. Geol. Ass'n., 34th ann. mtg., Trip B: B-1 — B-10.

———
1967. Structure and petrology of the Precambrian allochthon and Paleozoic sediments of the Monroe area, New York. Guidebook for N.Y.S. Geol. Assn., 39th ann. mtg., Trip F: F-1 — F-17.

Jaffe, H. W., Robinson, Peter, & Klein, Cornelis, Jr.
1968. Exsolution lamellae and optic orientation of clinoamphiboles. Science 160: 776–778.

Johannsen, Albert.
1939. A descriptive petrography of the igneous rocks; III and IV, Univ. of Chicago Press, Chicago.

Knopf, E. B.
1946. Stratigraphy of the Lower Paleozoic rocks surrounding Stissing Mountain, Dutchess County, New York. (Abs.), Geol. Soc. Amer. Bull. 57: 1211.

———
1956. Stratigraphy and structure of the Stissing area, Dutchess County, New York. (Abs.), Geol. Soc. Amer. Bull. 67: 1817.

Kothe, K. R.
1960. Structural relations of the Schunemunk Mountain area, New York. Unpub. Ph.D. thesis, Cornell Univ.

Kretz, R.
1963. Distribution of magnesium and iron between orthopyroxene and calcic clinopyroxene in natural mineral assemblages. Jour. Geol. 71: 773.

Krutov, G. A.
1936. Dashkessanite — a new chlorine amphibole of the hastingsite group. Acad. Sci. U.R.S.S. Bull. ser. geol.: 341–373 (cited in Mineral. Abs. 1937, 6: 438).

Krynine, P. D.
1948. The megascopic study and field classification of sedimentary rocks: Jour. Geol., 56, 130–165.

Leake, B. E.
1968. A catalog of analysed calciferous and subcalciferous amphiboles together with their nomenclature and associated minerals. Geol. Soc. Amer. Spec. Paper 98.

Long, L. E. & Kulp, J. L.
1962. Isotopic age study of the metamorphic history of the Manhattan and Reading prongs. Geol. Soc. Amer. Bull. 73: 969–996.

Lowe, K. E.
1950. Storm King Granite at Bear Mountain, New York. Geol. Soc. Amer. Bull. 61: 137–190.

Mason, Brian
1968. Pyroxenes in meteorites. Lithos 1: 1–11.

Miyashiro, Akiho.
1961. Evolution of metamorphic belts. Jour. Petrol. 2: 277–311.

Morse, S. A.
1969. Feldspars. Carnegie Inst. Wash. Yearbook 67: 120–130.

Muir, I. D.
1951. The clinopyroxenes of the Skaergaard intrusion, eastern Greenland. Mineral. Mag. 29: 690–714.

Nanz, R. H., Jr.
1954. Genesis of Oligocene sandstone reservoir, Seeligson field, Jim Wells and Kleberg Counties, Texas. Amer. Assn. Petroleum Geol. Bull. 38: 96–117.

Nockolds, S. R.
1954. Average chemical compositions of some igneous rocks. Geol. Soc. Amer. Bull. 66: 1007–1032.

Offield, T. W.
1967. Bedrock geology of the Goshen-Greenwood Lake area, N.Y. Map and chart series 9, N.Y.S. Mus. and Sci. Service, Albany.

O'Hara, M. J.
1961. Zoned ultrabasic and basic gneiss masses in the Early Lewisian metamorphic complex at Scourie, Sutherland. Jour. Petrol. 2: 248–276.

Pettijohn, F. J.
1957. Sedimentary Rocks. 2d Ed., Harper & Bros., N.Y.

von Platen, Hilmar.
1965. Experimental anatexis and genesis of migmatites. In Controls of Metamorphism, ed. Pitcher, W. S., and Flinn, G. W. Oliver and Boyd, Edinburgh: 203–218.

Poldervaart, Arie.
1955. ed. Crust of the earth. Geol. Soc. Amer. Spec. Paper 62: 135–136.

———, & Hess, H. H.
1951. Pyroxenes in the crystallization of basaltic magma. Jour. Geol. 59: 472.

Rankin, D. W.
1968. Volcanism related to tectonism in the Piscataquis volcanic belt, an island arc of Early Devonian age in north-central Maine. In Studies of Appalachian Geology, ed. Zen, E-an, White, W. S., Hadley, J. B., and Thompson, J. B., Jr. 355–369.

Richardson, S. W.
1968. The composition of synthetic Fe-staurolite. Carnegie Inst. Wash. Yearbook 66: 397–402.

———, Gilbert, M. C. & Bell, P. M.
1969. Experimental determination of kyanite-andalusite and andalusite-sillimanite equilibria; the aluminum silicate triple point. Amer. Jour. Sci. 267: 259–272.

Ries, Heinrich.
1895. Geology of Orange County, New York. N.Y. S. Mus. Rep. 49, part 2: 393–475.

Robinson, Peter, & Jaffe, H. W.
1969. Aluminous enclaves in gedrite-cordierite gneiss from southwestern New Hampshire. Amer. Jour. Sci. 267: 389–421.

Rosenbusch, Harry.
1887. Mikroskopische Physiographie. 2d Ed., 328–335.

Schreyer, Werner & Seifert, F.
1969. Compatibility relations of the aluminum silicates in the systems MgO-Al_2O_3-SiO_2-H_2O and K_2O-MgO-Al_2O_3-SiO_2-H_2O at high pressures. Amer. Jour. Sci. 267: 371–388.

———, & Yoder, H. S., Jr.
1961. Petrographic guides to the experimental petrology of cordierite. Carnegie Inst. Wash. Yearbook 60: 147–152.

Sen, S. K.
1959. Potassium content of natural plagioclases and the origin of antiperthites. Jour. Geol. 67: 479–495.

Shand, S. J.
1947. Eruptive Rocks. 3d Ed., Murby and Co., London.

Sims, P. K.
1953. Geology of the Dover magnetite district, Morris County, New Jersey. U.S. Geol. Survey Bull. 982-G: 245–304.

Skinner, B. J.
1956. Physical properties of end-members of the garnet group. Amer. Mineral. 41: 428.

Southard, J. B.
1960. Stratigraphy and structure of the Silurian and Lower Devonian rocks at Highland Mills and Cornwall, New York. Unpub. B.S. thesis, Mass. Inst. Tech. 72 p.

Spencer, A. C., & others
1908. U.S. Geol. Survey Atlas, Franklin Furnace folio, 161.

Thompson, J. B., Jr.
1957. The graphical analysis of mineral assemblages in pelitic schists. Amer. Mineral. 42: 842–858.

Tilton, G. R., Wetherill, G. W., Davis, G. L. & Bass, M. N.
1960. 1,000-million-year-old minerals from the eastern United States and Canada. Jour. Geophys. Res. 65: 4173–4179.

Turner, F. J.
1968. Metamorphic petrology. McGraw-Hill Book Co.

———, & Verhoogen, John.
1960. Igneous and metamorphic petrology. McGraw-Hill Book Co.

Tuttle, O. F. & Bowen, N. L.
1958. Origin of granite in the light of experimental studies in the system $NaAlSi_3O_8$-$KAlSi_3O_8$-SiO_2-H_2O. Geol. Soc. Amer. Mem. 74.

Vincent, E. A.
1953. Hornblende-lamprophyre dykes of basaltic parentage from the Skaergaard area, east Greenland. Quart. Jour. Geol. Soc. 109: 20–29.

Winchell, Horace.
1958. The composition and physical properties of garnet. Amer. Mineral. 43: 595–600.

Winkler, H. G. F.
1967. Petrogenesis of metamorphic rocks. 2d Ed., Springer-Verlag, Berlin-Heidelberg-New York.

———, & von Platen, Hilmar.
1961. Experimentelle Gesteins-metamorphose-V. Experimentelle anatektische Schmelzen und ihre petrogenetische Bedeutung. Geoch. et Cosmoch. Acta 24: 250.

Wones, D. R.
1963. Physical properties of synthetic biotites on the join phlogopite-annite. Amer. Mineral. 48: 1300–1315.

———, and Eugster, H. P.
1965. Stability of biotite: experiment, theory, and application. Amer. Mineral. 50: 1228–1269.

Wynne-Edwards, H. R. & Hay, P. W.
1963. Coexisting cordierite and garnet in regionally metamorphosed rocks from the Westport area, Ontario, Can. Mineral. 7: 453–478.

Yoder, H. S., Jr. & Eugster, H. P.
1954. Phlogopite synthesis and stability range. Geochim. et Cosmochim. Acta 6: 157–185.

Zartman, R. E., Brock, M. R., Heyl, A. V. & Thomas, H. H.
1967. K-Ar and Rb-Sr ages of some alkalic intrusive rocks from central and eastern United States. Amer. Jour. Sci. 265: 848–870.

Appendix

Location of samples cited in text

Table 1 — hornblende granite gneiss

22. Orchard Hill Road 200 feet north of intersection with Sapphire Road
46. 700 foot elevation, west side of intersection of Orange Turnpike with road to N.Y. 17A and 210
356. 1,120 foot elevation on cross trail 0.4 mile north of Appalachian Trail between N.Y. 17 and Orange Turnpike
360. At north tip of 'k' in Lake Sapphire, on small unnamed road
723. Long hill 0.2 miles east of Orchard Hill Road, 0.35 mile south of Pine Tree Road
751. At 'e' in Albany Turnpike, 0.5 mile north of Arden railroad station
263. 0.1 mile west of Cedar Cliff Road, south side of unnamed crossroad (Mine Road), 0.25 mile east of B. M. 717
699. 0.15 mile east of Lakes Road, due east of Round Lake, at brook below bend in 640′ contour
521. On dirt road east of Lakes Road, 0.2 mile east of B.M. 667, east of Round Lake
724. 1000 foot knob 0.4 mile east of Lake Road east of B.M. 622
407. Elevation 1,262 on Appalachian Trail west of West Mombasha Road
745. At 'B' in Arden Brook, east end of small lake
718. North side of road along Arden Brook, due north of 'ro' in Brook
750. West side of road west of Echo Mountain, 0.15 mile west of the 'E' in Echo, at 940 foot elevation

Table 2 — hornblende granite gneiss

46. 700 foot elevation, west side of intersection of Orange Turnpike with road to N.Y. 17A and 210
22. Orchard Hill Road 200 feet north of intersection with Sapphire Road
168. East of Orange Turnpike at northwest tip of U in TUXEDO
723. Long hill 0.2 mile east of Orchard Hill Road, 0.35 mile south of Pine Tree Road
494. Palisades Interstate Park 0.25 mile south of Appalachian Trail, 860 foot elevation, west side of 1,200 foot hill east of N.Y.S. Thruway

Table 3 — hornblende granite gneiss

692. 0.15 mile west of 'd' in Cedar Cliff Road
263. 0.1 mile west of Cedar Cliff Road, south side of unnamed crossroad (Mine Road), 0.25 mile east of B.M. 717
517. 0.15 mile east of Lakes Road, due east of Round Lake, at brook below bend in 640′ contour
281. 920 foot elevation, 0.35 mile east of 'ba' in West Mombasha Road
270. 0.1 mile west of 'S' in Spillway, north end of Mombasha Lake, at 860 foot elevation
499. Center of square formed by loop drive west of settlement on the west shore of Mombasha Lake, at 1,080 foot elevation
46. 700 foot elevation, west of intersection of Orange Turnpike and road to N.Y. 17A and 210
22. Orchard Hill Road 200 feet north of intersection with Sapphire Road
309. Just east of lake on top of Indian Hill, 880 foot elevation
168. East side of Orange Turnpike, east of 'r' in Orange, north of U in TUXEDO
37. 0.15 mile north of 669 elevation, east side of south end of Orange Turnpike
360. At north tip of 'k' in Lake Sapphire, on small unnamed road
320. South end of Blythea Lake opposite house
359. On trail parallel to Appalachian Trail between Orange Turnpike and Arden, 150 feet north of sharp turn north to Lake Sapphire
793. East side of south end of Orange Turnpike, 0.3 mile north of elevation 669
723. Long hill 0.2 mile east of Orchard Hill Road, 0.35 mile south of Pine Tree Road

132. Dirt road above Route 17, 0.35 mile south of 'J' in Newburgh Junction, northeast of 600 foot mark on contour
740. 0.3 mile north of 'B' in Arden Brook, at bend in 1,020 foot contour
768. 0.25 mile north of 'A' in Arden Brook, on 940 foot contour forming rounded hilltop
718. North side of road along Arden Brook, due north of 'ro' in Brook
743. 800 foot elevation, south side of lake along Arden Brook, 0.1 mile east of 'n' in Arden

Table 4 — amphibolite and pyribolite

345. 0.1 mile north of Tuxedo town line, on 980 foot contour, 0.3 mile west of East Mombasha Road
659A. 1.15 miles west of 'b' in Mombasha Lake, on 1,100′ contour, 1.15 miles north of Sterling Mountain
744. 900 foot elevation south of lake along Arden Brook, 0.5 mile west of 'B' in Brook
515A. Summit of 1,035 foot mountain east of East Mombasha Road
437A. Just east of 'R' in Berry Road
437P. Just east of 'R' in Berry Road
700P. School Road 150 feet west of intersection with Cedar Cliff and West Mombasha Roads
372. South shore of Lake Mombasha, just east of outlet of Kloibers Pond
178. West side of West Mombasha Road at 'b' in Mombasha
406. On Appalachian Trail between West Mombasha Road and Lakes Road, 0.1 mile east of elevation 1, 262 at 1,180 foot contour

Table 5 — hypersthene-quartz-plagioclase gneiss

515. Summit of 1,035 foot mountain east of East Mombasha Road
258. 945 foot elevation west of drained swamp west of East Mombasha Road just northeast of Lake Mombasha spillway
297. 0.4 mile south of 'P' in Prospect Mountain, west side of swamp, northeasternmost of two 840 foot knobs
425. 980′ contour west of West Mombasha Road, 0.15 mile south of south end of Kloibers Pond
648. Southeast corner of swamp, 1,040 foot elevation, 0.7 mile east of 'L' in Lakes Road
481. 840 foot elevation at hairpin bend in Palisades Interstate Park road west of Echo and Island Pond Mountains
71. Sloatsburg Quadrangle, north side of N.Y. 210, 1.95 miles west of its intersection with Long Swamp Road
402. Appalachian Trail, 0.2 mile west of West Mombasha Road
713W. 880 foot elevation at bend in contour north of road along Arden Brook, 0.4 mile north of 'o' in Echo Lake

Table 6 — amphibolite and pyribolite

700. North side of School Road 150′ west of intersection with West Mombasha Road
729. East edge of Warwick Quadrangle, 500 feet east of top of waterfall, where Appalachian Trail crosses a stream
143N. East side of Cedar Cliff Road north of large house east of 'f' in Cliff
659. 1,100 foot elevation, 0.4 mile north fo 'n' in Appalachian Trail between West Mombasha and Lakes Roads, 1 mile east of point where Lakes Road leaves the quadrangle
778. 0.35 mile west of 't' in West Mombasha Road, 0.45 mile south of 'l' in School Road, elevation 1,020 feet
148. West of West Mombasha Road, 0.1 mile east of south end of southernmost of two ponds south of School Road
653. 0.45 mile west of 'sh' in West Mombasha Road, 0.65 mile north of elevation 1,262 on Appalachian Trail between West Mombasha and Lakes Road
437A. Just east of 'R' in Berry Road
455. 0.05 mile west of Berry Road at 'B'
150. Berry Road 0.1 mile east of intersection with West Mombasha Road
372. South shore of Lake Mombasha just east of outlet of Kloibers Pond
241S. Appalachian Trail east of Kloibers Pond at 'i' in Kloibers
178. East side of West Mombasha Road, 0.1 mile north of northernmost crossroads in settlement on west shore of Lake Mombasha
406. Appalachian Trail west of West Mombasha Road, at elevation 1,180′, east of elevation 1,262
495. South of road between Orange Turnpike and East Mombasha Road (Bramertown Road), 0.1 mile west of Orange Turnpike, southeast of small pond north of road
127. West of East Mombasha Road, southwest of outlet of Lake Winape

345. 0.1 mile north of town line, 0.3 mile west of East Mombasha Road, elevation 980 feet
515A. Elevation 1,035 east of East Mombasha Road
155. Orange Turnpike, west side, opposite first house on map on east side of Orange Turnpike south of the intersection with East Mombasha Road
232. South of road between East and West Mombasha Roads (Bramertown Road), 0.85 mile due west of Orange Turnpike
53. East Mombasha Road, 0.2 mile south of town line, 800 foot elevation
61. Road between East Mombasha Road and Orange Turnpike (Bramertown Road), north of road, 0.25 mile east of East Mombasha Road
480. Palisades Interstate Park road past Island Pond and Echo Mountains, 820 foot elevation at hairpin bend, east of road
766. East edge of quadrangle at road from Harriman across Thruway
716. North of road along Arden Brook at 'B' in Brook

Table 7 — hypersthene-quartz-plagioclase gneiss

262. 0.1 mile east of Cedar Cliff Road just north of unnamed crossroad (Mine Road)
691. 0.15 mile west of Cedar Cliff Road at 'C' in Cedar
725. 0.6 mile east of Lake Road at 'e' in Lake, 1,010 foot elevation
798. Southeast corner of Kloibers Pond, 1,010 foot elevation
297. 0.4 mile south of 'P' in Prospect Mountain, west side of swamp, northeasternmost of two 840 foot knobs
71. On Route 210, Sloatsburg Quadrangle, 1.95 miles west of intersection with Long Swamp Road
394. Appalachian Trail east of Kloibers Pond, 0.35 mile east of West Mombasha Road
286. Private road ending in loop drive east of West Mombasha Road, in settlement on west shore of Lake Mombasha, at loop of drive
402. Appalachian Trail west of West Mombasha Road, 980 foot elevation east of 1,262 foot elevation
238. West of West Mombasha Road, .05 mile north of Appalachian Trail crossing
258. 945 foot elevation, west of drained swamp west of East Mombasha Road northeast of Lake Mombasha spillway
515. Summit of 1,035 foot mountain east of East Mombasha Road
318W. 760 foot elevation, north side of stream, 0.1 mile west of East Mombasha Road, 0.2 mile north of road connecting East and West Mombasha Roads (Bramertown Road)
41. 0.2 mile south of intersection of Orange Turnpike and East Mombasha Road, west side of Orange Turnpike
479. 1,000 foot elevation, 0.6 mile east of Thruway, 0.15 north of Appalachian Trail and south of road toward Echo Mountain
742. 810 foot elevation south of lake along Arden Brook, 0.35 mile east of edge of quadrangle
481. 840 foot elevation at hairpin bend in Palisades Interstate Park road west of Echo and Island Pond Mountains

Table 8 — amphibole

345. 980 foot elevation 0.1 mile north of town line, 0.3 mile west of East Mombasha Road

Table 9 — calc-silicate gneiss

287. Just east of dead end of first road off Orange Turnpike south of Harriman Heights Road
58. Harriman Heights Road, 0.4 mile east of Orange Turnpike
332A. Top of isolated 900 foot hill 0.25 mile east Orange Turnpike, 0.25 mile west of road past Blythea Lake
324. 920 foot elevation 0.1 mile west of Orange Turnpike, 0.17 mile south of intersection of Orange Turnpike and Harriman Heights Road
204. 0.22 mile west of Orange Turnpike on north side of dead end road 0.5 mile north of town line
328. 0.1 mile west of Orange Turnpike, 0.1 mile north of town line, 780 foot elevation east of south end of large lake
327. 0.1 mile west of Orange Turnpike, 0.15 mile north of town line, 760 foot elevation east of south end of large lake
348. Appalachian Trail, 880 foot elevation at summit of first ridge east of Orange Turnpike
351. Appalachian Trail west of Orange Turnpike, 740 foot elevation, east side of knob on west side of Little Dam Lake
39. East side of Orange Turnpike, 0.97 mile south of Harriman Heights Road
166. 0.2 mile north of south edge of quadrangle at 'l' of 210, 800 foot elevation, 0.05 mile west of road

Table 10 — biotite mesoperthite gneiss and biotite-hypersthene-K feldspar gneiss

83. At 'o' in Berry Road, southwest side of road
438. Berry Road, 880 foot elevation, north side, north of L-shaped lake
640. 0.68 mile east og 'k' in Lakes Road, 1,020 foot elevation, 0.08 mile west of end of dirt road
680. 0.08 mile east of Cedar Cliff Road opposite entrance of dirt road just south of 'C' in Cedar
265. 0.09 mile north of intersection of School Road and West Mombasha Road
40. Private road east off Lake Road 0.85 mile from east edge of quadrangle, 1,060′ elevation opposite house
84. Berry Road 0.5 mile southeast of intersection with Rye Hill Road, 885 foot elevation
441. 0.07 mile south of 'rr' in Berry Road, 930 foot elevation
472. 900 foot elevation on double switchback, 0.16 mile west of east edge of quadrangle, just north of 17′30″
477A. South of overpass of New York State Thruway, east side of Thruway, south of road toward Echo Mountain
477NEA. Location as 477 A above.
673. Northeast bank of Stahahe Brook at trail crossing, Palisades Interstate Park
757. Popolopen Quadrangle, west edge, 250 feet south of road past Echo Mountain at top of waterfall

Table 11 — sillimanite-garnet-biotite gneiss

125. Just east of East Mombasha Road, south end of Lake Winape, opposite entrance to branched side road
129. Just east of East Mombasha Road at fenceline 0.27 mile north of north end of Lake Winape
222. 0.1 mile east of East Mombasha Road at fenceline 0.27 mile north of north end of Lake Winape, 940 foot elevation
225. 0.17 mile east of East Mombasha Road at fenceline 0.27 mile north of the north end of Lake Winape, 940 foot elevation
511. 0.08 mile west of Orange Turnpike, 0.3 mile west of 'S' in St. Patrick's School, south nose of 900 foot hill
303. 0.06 mile west of East Mombasha Road, 0.08 mile north of '6' in 860′ elevation, southernmost settlement on east shore of Lake Mombasha

Table 12 — alaskite and magnetite garnet andesine gneiss

7. Road 0.08 mile northeast of Orange Turnpike intersection with East Mombasha Road, 150 feet west of turnpike, east bank of small stream
43. At east side of intersection of East Mombasha Road and Orange Turnpike
80. 900 foot elevation north of road connecting East and West Mombasha Roads (Bramertown Road), 0.6 mile west of West Mombasha Road
292. South of road connecting East and West Mombasha Roads (Bramertown Road) 150 feet west of last of 3 houses, 0.35 mile west of West Mombasha
264. End of dead end road on east side of Walton Lake
196. 0.1 mile west of East Mombasha Road at fenceline 0.27 mile north of north end of Lake Winape
417. Just east of East Mombasha Road and north of outlet of Lake Winape
379. 0.25 mile east of southeast corner of Lake Mombasha, 970 foot elevation
395. Appalachian Trail east of Kloibers Pond 0.37 mile east of West Mombasha Road, 1,100 foot elevation
396. Appalachian Trail east of Kloibers Pond 0.40 mile east of West Mombasha Road, 1,120 foot elevation

Table 13 — pyroxene and hornblende granulite

681. 20 feet west of Cedar Cliff Road, just south of entrance to road south of 'C' in Cedar
223. 0.15 mile east of East Mombasha Road, top of 940 foot hill, at fenceline 0.27 mile north of north end of Lake Winape
228. 0.27 mile east of East Mombasha Road, tiny pit at 880 foot elevation, 0.25 mile north of 'e' in Lake Winape
799. 0.4 mile east of Cedar Cliff Road at bend in unnamed crossroad (Mine Road), elevation 660 feet

Table 14 — klippen

529. Northeast nose of Goose Pond Mountain, 0.12 mile west of Seely Brook at 'oo', 500 foot elevation
788. 0.17 mile south of '2' in 2 Lane indication south of N.Y. 17, 520 foot elevation, Goose Pond Mountain

20. South of intersection of Route 17M and old road, just west of 4 houses, Goose Pond Mountain
527. 590 foot elevation, 0.08 mile east of edge of quadrangle, north slope of Goose Pond Mountain
36. Tiny 700 foot knob at west end of triangular intersection of Museum Village Road and road to Oxford, just north of overpass over N.Y. 17
769As. 720 foot elevation, 0.15 mile north of 'v' in Smiths Clove, at bend in contour
769N. Just north of 769 As.
769W. Just west of 769 As.

Table 15 — amphibolite

162A. East of East Mombasha Road, 0.35 mile west of 'P' in Private loop road east of Orange Turnpike

Table 16 — Poughquag conglomerate

466. 0.15 mile west of Orange Turnpike, 760 foot elevation at fenceline, 0.17 mile south of village boundary

Table 17 — dikes

523. Just west of village boundary, 0.06 mile east of Cedar Cliff Road, 0.15 mile south of unnamed road (Mine Road)
51. 0.16 mile west of Orange Turnpike, at bend in fenceline, 0.07 mile south of village boundary
50. At fenceline, elevation 780 feet, 0.1 mile west of Orange Turnpike, 0.12 mile south of village boundary
218. North of East Mombasha Road near north end at east end of small pond
715. 900 foot elevation north of road along Arden Brook, 0.1 mile north of 'B'
240. Northeast end of Kloibers Pond, 980 foot elevation
184. At '5' in elevation 745, near intersection of East Mombasha Road and east-west road between East and West Mombasha Roads (Bramertown Road)
46. West of intersection of Orange Turnpike and unnamed road to N.Y. 17A and 210

Table 18 — lamprophyre dike

J-50=50. 0.1 mile west of Orange Turnpike at small pond just south of Monroe Village boundary

Table 19 — Bushkill shale

573. South of northernmost building in Camp LaGuardia complex

Table 20 — Ramseyburg quartzite

568. Just north of intersection of Bull Mill Road and unnamed road across Lazy Hill (Booth Road)
576. West side of Lazy Hill, north of unnamed road across Lazy Hill (Booth Road), 550 foot elevation

Table 21 — orthoquartzite and graywacke

552. Shawangunk orthoquartzite, northeast end of Lazy Hill, 550 foot elevation, tiny knob in V of two fencelines
622. Bellvale graywacke, 100 feet north of intersection of Ridge Road and Seven Springs Road, east side of Ridge Road

NEW YORK STATE MUSEUM AND SCIENCE SERVICE
HUGO JAMNBACK DIRECTOR

THE UNIVERSITY OF THE STATE OF NEW YORK
THE STATE EDUCATION DEPARTMENT

GEOLOGICAL SURVEY
JAMES F. DAVIS STATE GEOLOGIST

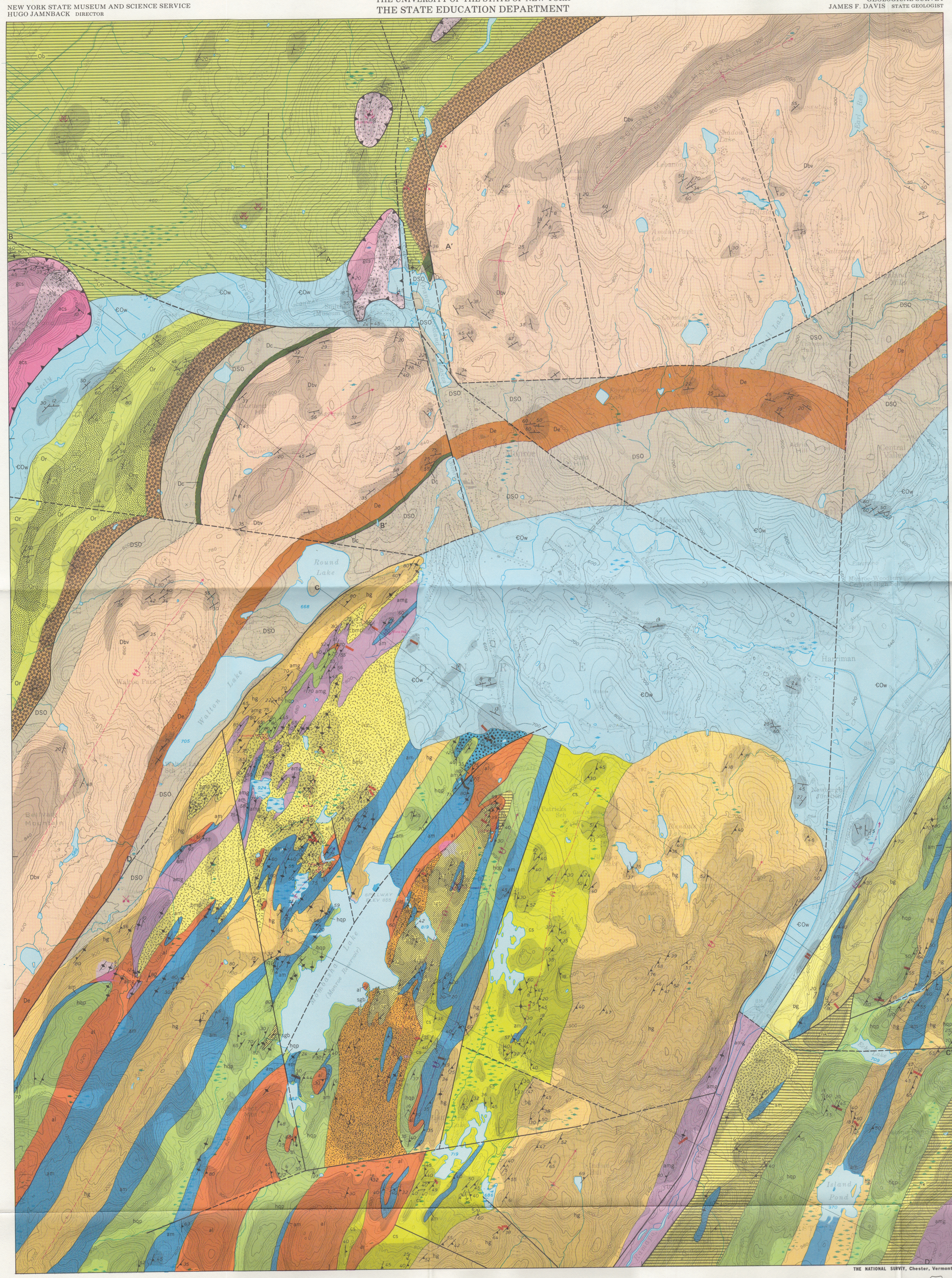

EXPLANATION

PALEOZOIC

Devonian
- DSO — Concealed Devonian, Silurian, Ordovician strata; configuration of units unknown
- Dbv — Bellvale Formation: graywacke, conglomerate
- De — Esopus Formation: siltstone, shale
- Dc — Connelly Conglomerate

Silurian
- Ssk — Shawangunk Formation: quartzite, conglomerate

Ordovician (MARTINSBURG FORMATION)
- Or — Ramseyburg calcareous shale
- Orq — Ramseyburg calcareous quartzite
- Ob — Bushkill Shale

Cambrian-Ordovician
- dikes of lamprophyre, leucophyre, diabase
- €Ow — Wappinger Group: dolostone, minor shale

Cambrian
- €pg — Poughquag Formation: quartzite, arkose, conglomerate

PROTEROZOIC

KLIPPEN: RELATIVE AGES UNKNOWN
- acs — amphibolite, calc-silicate gneiss
- alg — albite leucogranite gneiss
- gcs — graphitic calc-silicate gneiss, graphitic quartzite, graphite-sillimanite gneiss

GNEISSES OF MONROE AND RAMAPO BLOCKS
- hg — hornblende (ferrohasting site) granite gneiss, and pegmatite
- am — amphibolite, pyribolite
- amg — interlayered amphibolite and granodiorite
- cs — calc-silicate gneiss
- hqp — biotite-hypersthene-quartz-plagioclase gneiss
- sgb — sillimanite-cordierite-almandine-biotite-quartz-feldspar gneiss
- bg — biotite gneiss
- bmp — biotite-mesoperthite gneiss and albite-oligoclase leucogranodiorite
- hk — biotite-hypersthene-K-feldspar-quartz-plagioclase gneiss
- mag — magnetite-garnet-andesine gneiss
- al — microcline alaskite (leucogranite); contacts with all other Proterozoic units may be intrusive
- overprint signifies closely spaced outcrops

- Geologic unit contact
- Faults — observed and probable (solid) hypothetical (dashed)
- Trace of overthrust plane: teeth point into thrust block
- 54 Strike and dip of foliation.
- 45 Strike and dip of bedding
- 10 ← Fold axis and plunge
- a ← Mineral lineation and plunge
- Trace of axial plane of anticline and plunge of axis
- Trace of axial plane of syncline and plunge of axis
- Trace of axial plane of overturned syncline
- Trace of axial plane of overturned anticline
- Magnetite mine and prospect
- Shale pit
- Dolostone quarry
- Sand and gravel pit

Mapped, edited, and published by the Geological Survey
Control by U S G S and U S C & G S
Topography from aerial photographs by photogrammetric methods
Aerial photographs taken 1955 and 1956. Field check 1957
Polyconic projection. 1927 North American datum

PLATE 1. BEDROCK GEOLOGY OF THE MONROE QUADRANGLE, NEW YORK

Howard W. Jaffe and Elizabeth B. Jaffe

1973

SCALE 1:24 000

1 MILE
1000 0 1000 2000 3000 4000 5000 6000 7000 FEET
1 KILOMETER

CONTOUR INTERVAL 20 FEET
DATUM IS MEAN SEA LEVEL

MN GN
12° 213 MILS
0°32′ 9 MILS
UTM GRID AND 1957 MAGNETIC NORTH DECLINATION AT CENTER OF SHEET

NEW YORK
QUADRANGLE LOCATION
Geologic Mapping 1967-1970

New York State Museum and Science Service
Geological Survey, Map and Chart Series: No. 20

THE NATIONAL SURVEY, Chester, Vermont

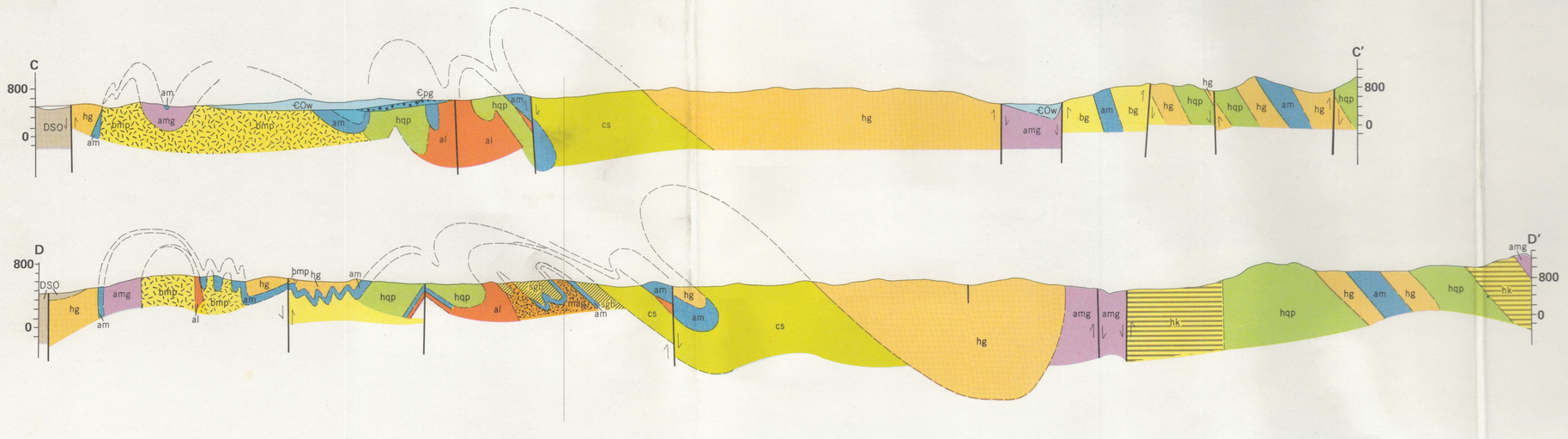

Mapped, edited, and published by the Geological Survey
Control by U S G S and U S C & G S
Topography from aerial photographs by photogrammetric methods
Aerial photographs taken 1955 and 1956. Field check 1957
Polyconic projection. 1927 North American datum

PLATE 2. ANORTHITE CONTENT OF PLAGIOCLASE IN GNEISSES, MONROE QUADRANGLE, NEW YORK

Howard W. Jaffe and Elizabeth B. Jaffe

1972

SCALE 1:24000

1 MILE
7000 FEET
1 KILOMETER

CONTOUR INTERVAL 20 FEET
DATUM IS MEAN SEA LEVEL

THE NATIONAL SURVEY, Chester, Vermont

MN GN
12° 213 MILS
0°32' 9 MILS

UTM GRID AND 1957 MAGNETIC NORTH DECLINATION AT CENTER OF SHEET

NEW YORK
QUADRANGLE LOCATION
Geologic Mapping 1967-1970

New York State Museum and Science Service
Geological Survey, Map and Chart Series: No. 20